

**UPPER ST. LAWRENCE ESTUARY  
CIRCULATION STUDY, 1986  
PRELIMINARY ANALYSIS AND DATA REPORT**

**by**

**P.F. Hamblin**

**NWRI Contribution No. 87-83**

**National Water Research Institute  
Lakes Research Branch  
Canada Centre for Inland Waters  
Burlington, Ontario, Canada L7R 4A6**

**December 1986**

## **MANAGEMENT PERSPECTIVE**

The need to investigate the role played by suspended sediments in the transport and fate of contaminants in the St. Lawrence River Estuary has led to the observation of suspended sediments, salinities and currents along with contaminant chemistry in the Upper Estuary of the St. Lawrence River during the field season of 1986. This report provides a description of the physical data, a review of previous physical studies in the area of interest with special attention to suspended sediments and a preliminary analysis of the physical data collected.

## **PERSPECTIVE-GESTION**

Afin d'étudier le rôle joué par les sédiments en suspension au niveau du transport et du devenir des contaminants dans l'estuaire du fleuve Saint-Laurent, les chercheurs ont dû observer les sédiments en suspension, les salinités et les courants ainsi que la chimie des contaminants dans la partie supérieure du fleuve Saint-Laurent pendant la campagne sur le terrain de 1986. Dans ce rapport on trouve une description des données physiques, une revue des études physiques antérieures dans le domaine d'intérêt, une attention spéciale étant mise sur les sédiments en suspension et une analyse préliminaire des données physiques recueillies.

# **ABSTRACT**

In this report the background physical oceanography of the Upper Estuary of the St. Lawrence River is reviewed, the physical data collected in support of the chemical survey in 1986 is presented and a preliminary analysis of the physical data is given. The estuarine oceanography is complex so that only the tidal water level fluctuation may be simulated with reasonable accuracy. Flow fields and salinity distributions must be measured along with water chemistry if qualitative estimates of chemical transports are required. One of the key physical variables influencing the water chemistry is suspended sediments. A new mechanism for the recycling of sediments and hence contaminants in the Upper Estuary of the St. Lawrence River has been identified. This tidal pumping mechanism is shown by a vertical transport model to be caused primarily by fluctuations in the vertical sediment flux due to mixing variations related to the intrusion of the salt wedge. A possible framework for the interpretation of chemical processes is given.

## RÉSUMÉ

Les auteurs du présent rapport donnent une vue d'ensemble sur l'océanographie physique de la partie supérieure de l'estuaire du fleuve Saint-Laurent, présentent les données physiques recueillies pour appuyer l'étude chimique de 1986 ainsi qu'une analyse préliminaire des données physiques. L'océanographie estuarienne est un sujet complexe de telle sorte que seule la variation du niveau d'eau dû aux marées peut être simulée avec une précision raisonnable. Il faut mesurer des champs de courant et la répartition de la salinité ainsi que les données chimiques de l'eau si des évaluations qualitatives des transports chimiques doivent être effectuées. Les sédiments en suspension constituent l'une des variables physiques clés influant sur les données chimiques de l'eau. Un nouveau mécanisme de recyclage des sédiments et par le fait même des contaminants de la partie supérieure du fleuve Saint-Laurent a été identifié. Ce mécanisme de pompage dû aux marées est illustré par un modèle de transport vertical qui doit être produit par des fluctuations du flux vertical des sédiments causées par des variations de mélange liées à l'arrivée d'un coin salé. Les auteurs indiquent un cadre de travail possible pour l'interprétation des processus chimiques.

## INTRODUCTION

In an overview of the toxic contaminant issue in the St. Lawrence River (Allan and Lum, 1985) have pointed out the need for increased knowledge of the system dynamics for toxic chemicals. To achieve this objective the dynamics of sediment-water partitioning, sedimentation, sediment transport and resuspension and mixing must be determined. One region in the St. Lawrence River where many of the above processes are thought to occur and have a significant impact on toxic contaminants is the reach between Quebec and the Saguenay River which will be referred henceforth as the Upper Estuary of the St. Lawrence River.

The Upper Estuary is one of the most complex water bodies known due to its complicated bathymetry, vigorous tidal currents and turbulent mixing and pronounced gradients in density both horizontally and vertically due to input of fresh water into the St. Lawrence Estuary. In another setting the partitioning between the dissolved and particulate phases of zinc and lead are related to the freshwater and suspended sediment concentrations in a striking manner along the length of the Chesapeake Bay Estuary (Nichols, 1986). In the St. Lawrence, Bowers and Yeats (1978) have demonstrated the relation between suspended sediment concentration and total concentration of various trace metals. Additional complicating factor in the Upper Estuary.

with regard to water chemistry is presence of a sharp front of suspended sediments known as the turbidity maximum. Bowers and Yeats (1978, 1979) have drawn attention to the profound influence that the turbidity maximum has upon the distribution of trace metals in the Estuary. Although the sampling distribution undertaken by Bowers and Yeats was fairly detailed in space with one dozen stations along the axis and two transects across the Estuary at about four depths, the sampling resolution in time was not sufficiently detailed to discuss the large tidally induced fluctuations observed by others and therefore could not be expected to shed much light on the determining processes. Further aspects of the partitioning of cadmium in the St. Lawrence River upstream of the turbidity maximum are discussed by Lum et al. (1986).

During June and July 1986, observations of current, salinity and suspended sediment were taken concurrently with observations of trace metals and volatile hydrocarbons aboard the research vessel, C.S. Limnos, at four anchor stations and a controlled drift station in the Upper Estuary. In the following report an attempt is made to summarize the current state of knowledge on the flow, salinity and suspended sediment fields in this region as well as to present a preliminary analysis of the physical data taken during the field experiment.

### Physical Description of the Upper Estuary

An outline of the Upper Estuary of the St. Lawrence River and the sampling station locations are shown in Figure 1. The topography of this area is discussed in detail by (Muir, 1980). At the downstream end, the Upper Estuary is split into two distinct channels by Ile aux Lievres. The South Channel is a broad shallow region while the North channel is much deeper with depths up to 180m. These two channels converge at the upstream end of Ile aux Lievres but the Estuary is blocked near Pt. au Pic by a submerged bank. The maximum depth of water over this bank is about 36m and upstream of the bank the water deepens to about 85m near Goose Cape. The main channel takes a distinct bend in passing north of Ile aux Coudres. Upstream of Ile aux Coudres the Estuary again has two deep north and south channels with a suggestion of a central channel as well, as is shown by Figure 2 of Soucy et al. (1976).

### Residual Circulation

The net result of tidally related flood currents up the estuary along the northwestern shore and ebb currents concentrated along the southeastern shoreline is to produce a general counter clockwise circulation in the horizontal plane. The vertical



circulation according to measurements reported by Soucy et al. (1976) is that of the classical estuarine circulation with seaward flow near the surface and return flow in the saline bottom waters. This characteristic circulation is prevalent in the deep channel on the northwestern side but may be absent in the more shallow mid-channel region and on the southeastern channels where unidirectional seaward flow may be found.

### Tidal Regime

The tides of the Upper Estuary are strongly semi-diurnal and of the lunar type and are intermediate between a purely progressive wave in which the maximum current occurs at the tidal extremes and the standing wave type where the tidal extremes coincide with slack water.

Tides at Quebec during the survey period shown in Figure 2 are of a mixed type but strongly semi-diurnal as are the tides at Pointe au Pere downstream of Quebec. The tides at these two stations indicate that neap tidal conditions apply during the occupation of station 6-E-400, near neap at 6-E-200 and intermediate between neap and spring at stations 253, 6-E-100 and 6-E-300.

More precise information on the tidal currents of the Upper Estuary has been provided by Budgell and Muir (1975) and Muir (1978, 1979) who subjected long time series of current meter observations to harmonic analyses at 44 individual moorings in the estuary. They found that in addition to the usual astronomical tidal frequencies there were significant short term tides known as overtides of periods of several hours. These tides are thought to be generated locally in the process of dissipation of the tides. Because the presence of the strong overtides and the consequent rapidly changing conditions both these investigators recommended that current and salinity be sampled at 30 minute intervals. This sampling rate was followed when the logistics permitted during the 1986 field survey.

Tidal water level fluctuations are the only oceanographic phenomenon occurring in the Upper Estuary that have been successfully simulated to date. Two-dimensional numerical hydrodynamical models of the tidal elevations have been computed by Levesque (1977). A related phenomenon known as storm surges have discussed by Murty et al. (1979) and apparently are responsible for relatively minor deviations of the predicted tide heights.

### Suspended Sediments

Since the principal concern of the physical component of the field observations is the concentration and flux of suspended sediments it is appropriate to briefly review the prior work on suspended sediments of the Upper St. Lawrence Estuary.

The St. Lawrence Estuary is no exception to estuaries in general which exhibit zones of enhanced turbidity in the transition between river and sea water. This zone of maximum turbidity was the subject of study of the University of Laval in mid 1970's. A notable report by Soucy et al. (1976) was the first to describe the turbidity zone and relate it to such sedimentary processes as sediment flocculation and recycling due to the residual gravitational circulation. They found that augmented suspended sediment concentrations are more likely to be due to the estuarine circulation than flocculation and that much work needed to be done before a sediment transport model could be developed. In another study at this time d'Anglejan and Smith (1973) measured surface and bottom suspended sediments at several stations in the Upper Estuary and related them to vertical density differences over the tidal cycle. d'Anglejan and Ingram (1976) were the first to measure profiles of suspended sediment concurrently with current profiles and hence deduce the horizontal sediment transport. Unfortunately, their anchor stations were limited

to the zone downstream of Pt au Pic and hence not close to the turbidity maximum. They found that horizontal advection is more important than local resuspension over the tidal cycle in this deeper portion of the estuary and that concentrations of suspended sediments were maximum at mid-depth as opposed to near the bottom.

Silverberg and Sundby (1979) were the first to study the sediments the entire system from the fresh water region at Quebec to open sea conditions by the Saguenay Fjord as well as the examination of the seaward response of the suspended sediment distributions to fluctuations in river discharge. An important contribution was the determination of particle size spectra for upper (fresh water), middle (turbidity maximum) and lower (seawater) reaches of the estuary. Particles sizes are more uniform or better sorted within the turbidity maximum or middle portion than at either ends. Other findings were that local resuspension as opposed to horizontal transport was an important factor in suspended sediment distribution in the shallower upper reaches and that maximum turbidities occurred just after the start of the flood tide. No current measurements were taken in their study.

In a further elaboration of the particle size distribution in the Upper Estuary, Krank (1979) found that in the turbidity maximum the most frequent particle size remained in the range 10-20  $\mu\text{m}$  over the

tidal cycle both at the surface and bottom although the concentrations changed dramatically. She was the first to point out that the turbidity maximum is maintained by tidal current asymmetry which was inferred from one station where she noted that the peak bottom speed was greater during flood than during ebb conditions. d'Anglejan (1981) has reviewed the work on the suspended sediment dynamics of the Upper Estuary up to the late 1970's.

In an important recent study of high frequency suspended sediment concentration and sediment flux, d'Anglejan and Ingram (1984) measured bottom concentrations and currents over long periods with moored instrumentation. They were able to show seasonal trends in sediment concentration related to the fresh water discharge and the necessity for high frequency sampling of suspended material with their rapid response sensor. At two locations near the downstream end of the Estuary, horizontal advection was more important than local resuspension whereas in the middle portion local resuspension effects were identified.

#### River Discharge

The flow of the St. Lawrence River is subject to seasonal fluctuations of approximately 70% of the annual mean with the peak

discharge usually taking place in May. Unfortunately the river discharge during the study period was not available at the time writing at Quebec. Instead the discharge at La Salle near Montreal is shown in Figure 3. It is evident that the flow is about 10% greater than the previous 5-year average flow. From d'Anglejan (1981) the average flow at Quebec at the end of June is 11000 ( $\text{m}^3/\text{s}$ ). Thus the river flow in the study area may be estimated to be approximately 12000  $\text{m}^3/\text{s}$ .

#### Other Physical Studies

Besides a number of early investigations of the general hydrography, extensive profiles of current, temperature and salinity were measured from 1975 to 1979 by Budgell and Muir and Muir in the vicinity of 6-E-300 (Figure 1). Based upon these studies Muir (1980) and (1981) attempted to generalize these data in terms of internal tides. Muir concluded that internal waves are generated by the interaction of the upward propagating tidal waves with bottom irregularities and density stratification due to the presence of the salt wedge. Thus the internal wave regime is highly sensitive to the tidal conditions in the lower estuary such as the phase of the spring-neap cycle and the density conditions as controlled by river discharge and by the mixing induced by the dissipation of surface and internal

tides. The overwhelming complexity of the transient density and flow regime made it impossible to predict or even hindcast these internal tidal flows, density structure and circulation although these internal motions comprised a significant portion of the total flow. Thus currents and salinity data supporting chemical measurements must be measured simultaneously with the chemical observations as they cannot be reconstructed, at present. In a study now in progress the tidally averaged and cross sectional mean salinity distribution and vertical circulation are being modelled (K. Tee, personal communication) in the Upper Estuary.

### Methods

In the present survey where possible, currents were measured nominally at 10 depths evenly distributed over the water column at thirty minute intervals aboard the anchored ship. Calibration of the speed response was undertaken in the NWRI tow tank prior to field deployment. The calibration shown in Figure 4 is within the manufacturer's specifications of the Neil Brown direct reading current meter of 3% of full scale.

Currents, depths and temperatures were read directly from the deck display unit as the meter was dwelled at predetermined depths

while the ship was at anchor. Initial examination of the data revealed that flow directions were unreliable in the upper 3 m of the water column especially under flood conditions. As a result the current meter was henceforth lowered at the end of a boom projecting out about 3 m beyond the ship's hull. This arrangement appeared to eliminate the magnetic interference of the steel hull of the Limnos. The heaviest lead weight available was used to reduce the tilt and angle of the mooring line to an acceptable value. The raw data were entered directly on to computer coding forms.

A conductivity, temperature and depth profiler was obtained on loan from NHRI through E. Marles and others. The profiler is made by Applied Microsystems, model CTD-12. This self-recording instrument was initially lowered in line with the current meter until it was found that too much magnetic tape was used. Subsequently, the profiler was rapidly lowered and then turned off. The contents of the magnetic tapes were transferred to the mainframe computer by J. Bull whereupon the internal readings were converted to the physical variables of depth, temperature and conductivity using the manufacturer's and E. Marles' calibrations. The conductivity readings were converted to salinity using a standard oceanographic formula. Converted temperature data were edited by comparison to the readings from the current profiler and observations of conductivity at fixed depths taken by the ship's personnel during the anchor station. It is noted



that the salinity at the river station 253 was considered to be too low to be detectable by the profiler. Finally salinity data were averaged at 10 depth intervals uniformly spaced over the station depth.

Profiles of percentage optical transmission were recorded in analogue fashion usually at 1 hr intervals with a 50 cm path length transmissometer. Unfortunately, this sensor did not have the dynamic range required for the widely varying turbidities of the Upper Estuary and consequently no usable data were obtained at station 6-E-100 and some data were lost at station 6-E-300. Percentage optical transmissions of the profiler system is related in Figure 5 to suspended sediment through comparison of individual readings to two-hour averaged suspended sediment concentrations at two fixed depths as determined by the centrifuging of 600 L of water. Despite the large scatter, these data suggest a break point in the relation and as a result, the data were fitted visually by the two linear segments shown in Figure 5 for the purpose of estimating suspended sediment concentration from the digitized profiles of percentage transmission. It would have been most useful to have had access to seston samples as a means of evaluating this approach to suspended sediment measurement. At the time of writing no other means of estimating suspended sediment concentration was available.

Standard surface meteorological observations taken hourly while at anchor completed the physical data set.

In estuarine studies often tidally averaged quantities are of interest. A number of early studies including Soucy et al. (1976) the maximum and minimum flow over the tidal cycle was simply averaged. Another approach is to observe at uniform time intervals over the tidal cycle or at integer lunar hours. However, it is easier and much more accurate to sample at hourly or half-hourly intervals and take all readings into account employing the straightforward methods for dealing with harmonic time series outlined by Bloomfield (1976). It is considered that this method of calculation of tidal residuals is more accurate in view of the strong overtones mentioned earlier. This is outlined in Appendix G.

The field data described above with the exception of the meteorological data were displayed in machine produced plots in profile form. Final edited data which are the basis of the analysis to follow are presented in Appendices A through F. In Appendix G the magnetic tape on which the edited physical data are stored is listed. Values at the surface and bottom of each profile along with the time of the bottom reading in GMT are presented on the plots. Limited data are available from station 6-E-200 where strong tidal currents required that the ship drift rather than anchor.

Comparison of profiles of current and salinities listed in Appendix D may be made with the past measurements of Muir (1978) in Appendix F. The stations in 1975 were located within several 100 m of station 6-E-300 so provide an opportunity to access the effect of the phase of the tide and river discharge on the repeatability of the physical data. The two sets of data have been similarly displayed for ease of comparison. The salinity profiles in 1975 are less stratified and exhibit lower salinities than in the case of 6-E-300. Tidal current amplitudes are somewhat stronger in 1975 than in 1986 although display similar structure. Close inspection of the two episodes in 1975 also reveal considerable differences. For example, the stratification is weaker on May 29 than on May 19.

#### Tidal Averaged Data

Mean salinity profiles averaged over at least one full tidal cycle according to the method described above are shown in Figure 6 range from near fresh water conditions at 6-E-100 to sea water at 6-E-400. Similarly averaged along channel components of flow demonstrate seaward flow at stations 6-E-100 and 6-E-300 and a complex three layer residual circulation at 6-E-400. The small downstream flow at the bottom may be due to local bathymetric influences of the shallow anchorage. The corresponding cross channel residual

(Figure 8) is surprisingly large in comparison with the along channel component at station 6-E-300 and 6-E-400 and indicates the three-dimensional nature of the flow fields. There appears to be a steady northwestern drift of the surface layers and a weak counterflow at the bottom.

The downstream flow at stations 6-E-100 in the high turbidity zone and at 6-E-300 somewhat downstream is curious in the light of the understanding of the maintenance of the turbidity maximum by effect of the gravitational circulation on recirculating the suspended sediment particles. Figure 9 shows this concept as applied to the St. Lawrence by Soucy et al. (1976). Riverborne particle sinking to the lower level return flow are returned upstream whereupon they are entrained into the upper layer again. Since this picture did not appear to hold in the present data, unpublished residual along channel currents from the anchor station data of Muir taken in 1975 show in Figure 10, that while the classical estuarine circulation holds along the northwestern side it does not always obtain at mid channel or along the southern shore. Residual currents in these regions are sensitive to the phase of the fortnightly tidal cycle.

The question arises as to whether the upstream flow along the northern shoreline is sufficient to maintain the turbidity maximum

or if some other mechanism such as the ebb-flood current asymmetry suggested by Krank (1979) is responsible.

Besides the tidal averaging of primary physical variables it is instructive to form averages of the product of fluctuating quantities over a tidal cycle. Figure 11, gives the averaged salt flux as determined by the product of the tidal fluctuations of along channel flow and salinity. It is not surprising that the tidal residual salt flux is nearly always upstream since the balancing advective flux as provided from Figures 6 and 7 is overwhelmingly downstream. This example of the transport of salt in a tidally dominated flow illustrates that it is necessary to take into account not only the mean concentration and flow field but also the fluctuating components in the estimation of net transport.

Returning to the question of the maintenance of the turbidity maximum this principle is applied to suspended sediment at station 6-E-300 where the hourly profiles of suspended sediment over a tidal cycle provide an opportunity of estimating the residual suspended sediment flux. Mean concentrations of sediment increase monotonically to the bottom at this location which when coupled with the downstream flow of Figure 7 lead to a net downstream advection of suspended sediment as seen in Figure 11. The tidally averaged sediment flux,  $\overline{u'ss'}$ , is evidently upstream at the bottom which at this mid channel location provides a means of maintaining the

turbidity maximum in a similar way to the balance of salt. A more in-depth study of the mechanisms controlling the upstream turbidity flux at Station 6-E-300 follows. Fluctuation of suspended sediments, salinities and two components of horizontal sediment flux at each of the 4 stations occupied during the cruise are discussed by Hamblin et al. (1987). These data suggest that local resuspension in contrast to horizontal advection (d'Anglejan and Ingram, 1976) is the controlling factor in suspended sediment distributions particularly at station 6-E-300.

#### Model of Vertical Transport of Suspended Sediment

The finding that local resuspension of sediments over a tidal cycle is an important process in the Upper Estuary and need for further understanding of the residual upstream diffusive flux of sediment has lead to the development of a one-dimensional mathematical model of the vertical transport of sediment.

In Figure 12, bottom stress along the channel has been estimated from measured bottom currents, the standard aerodynamic stress law and the bottom stress coefficient of  $1 \times 10^{-3}$  recommended in the recent study of tidal flow of Dewey and Crawford (1987) employing the dissipation method. The asymmetry of the peak bottom

stress between ebb and flood as suggested by Krank (1979) is not evident but rather there is asymmetry about the time of occurrence of slack water. This type of ebb-flood asymmetry has been examined in detail by Dronkers (1986) who points out that since the flow reverses more quickly as it goes from ebb to flood than from flood to ebb there will be more material remaining in suspension during the flood cycle than in the ebb cycle. Thus there is a net landward transport of suspended sediment at the bottom.

From the viewpoint of the tidal analyst the slack water asymmetry observed in this study and the peak ebb-flood asymmetry reported by Krank (1979) may be explained by overtides. Fortunately the current meter moorings of Muir and Budgell of the lower portion of the Upper Estuary have been submitted to harmonic analysis. In most cases the dominant overtide is the M<sub>4</sub> tidal constituent having a period of 6.2 hr. In moorings where several current meters were established in a line the data of Muir and Budgell show that the M<sub>4</sub> increases relative to the predominant M<sub>2</sub> constituent in the lower current meters and that in the case of meter 77-07C-10A080 (Muir, 1979) at a depth of 80 m and 1.5 m above the bottom the amplitude of the M<sub>4</sub> is 22% of the M<sub>2</sub> constituent compared to 5.4% at a depth of 10 m. The phasing of these two constituents is not available in order to calculate whether the M<sub>4</sub> constituent would produce the correct asymmetry for landward transport.

As well as the slack water asymmetry clearly evident in Figure 12, further landward transport may be caused by fluctuations in the vertical transport linked to mixing coefficients. A one-dimensional model ought to be able to provide insight into this process. Additionally, it may be noted in Figure 12 that allowing for some lag the suspended sediment concentration rises in general when the magnitude of the bottom stress exceed 0.12 pa and falls when it is less than this value. This observation will be incorporated into the simulation model to be outlined below.

### Mathematic Model

The vertical transport model for fine grained newly-deposited sediments is described by Teeter (1986) as follows. The one-dimensional transport equation is

$$\frac{\partial C}{\partial t} - W_s \frac{\partial C}{\partial Z} = \frac{\partial}{\partial Z} \left( K_z \frac{\partial C}{\partial Z} \right) \quad (1)$$

where C is the concentration of the suspended sediment which varies over depth, Z, and time t. Ws is the unknown settling velocity and the vertical eddy diffusivity, Kz is given by Fischer et al. (1979) by the standard formula



$$K_z = k u^* Z (h - Z)/h (1 + 3.33 Ri)^{-1.5}$$

where  $k$  is the von Karman constant, .4,  $u^*$  is the friction velocity of the bottom boundary layer;  $u^* = \sqrt{1 \times 10^{-3}} U_b$  ( $U_b$  is the bottom current speed),  $h$  is the depth of the water and  $Ri$  is the Richardson number

$$Ri = g \frac{\partial \rho}{\partial Z} / \left[ \left( \frac{\partial U}{\partial Z} \right)^2 + \left( \frac{\partial V}{\partial Z} \right)^2 \right]$$

where  $g$  is the acceleration of gravity and the density,  $\rho$  of the water is a function of the measured temperature, salinity and suspended sediment concentration. Measured values of the flow field and density structure are required to evaluate  $K_z$ . The observed distribution of  $K_z$  and a highly smoothed version are shown in Figure 13. The extreme variability of this quantity is related to the variation of the bottom current, Figure 12, and to the stabilizing effect on mixing of the salt wedge on the flood. These two effects reinforce on the slack following the flood tide to produce mixing coefficients of the order of  $10^{-6} \text{ m}^2/\text{s}$  whereas during the ebb diffusivities are in the order  $10^{-2} \text{ m}^2/\text{s}$ .

Boundary conditions at the surface,  $Z = h$ , are no flux of sediment through the surface or

$$W_s C + K_z \frac{\partial C}{\partial Z} = 0$$

and at the bottom  $z = 0$  there are three possible conditions;

$$(1) \text{ Free settling, } K_z \frac{\partial C}{\partial Z} = 0,$$

$$(2) \text{ Equilibrium (no flux), } W_s C + K_z \frac{\partial C}{\partial Z} = 0,$$

$$(3) \text{ Erosion, } W_s C + K_z \frac{\partial C}{\partial Z} = -e.$$

From Figure 12 condition (1) obtains when the bottom stress is less than 0.12 pa, condition (2) when it has a value of 0.12 pa and (3) when the stress is greater than 0.12 pa. The erosion rate is assumed to be given by  $9 \times 10^{-5} (U_b - 35)^2 \text{ g/(m}^2\text{s)}$  based upon the discussion of Teeter (1986) and some initial sensitivity tests. The bottom speed 35 cm/s in the above expression corresponds to a bottom stress of 0.12 pa. The above model was solved by discretization of depth into 40 vertical grid points and an explicit integration of the advection diffusion equation (1). Flux boundary conditions were tested with a known analytical solution and finally the sediment settling experiments of Dhamotharan et al. (1981) were duplicated by

the numerical model. In the application of the model to tidal flows the initial conditions were assumed to be zero and the model was run until the concentrations were periodic over a tidal cycle (10 to 12 tidal cycles). The unknown vertical settling velocity was assumed to be constant and was determined to be  $3.0 \times 10^{-4}$  m/s on the basis of the best visual match between the observations and the model output.

In Figure 14 the observed time history of the vertical distribution of the suspended sediment concentration at Station G-E-300 is compared to the computed distribution for the smoothed diffusivity and in Figure 15 for the unsmoothed distribution. The smoothed results illustrate somewhat more clearly the physics of the influence of vertical mixing on the horizontal landward transport of sediment in the lower layers. Since the bottom current is symmetrical there are two equal pulses of high turbidity at the bottom each tidal cycle but due to the reduced upwards transport by the small diffusivities of the flood more suspended water is retained in the lower layers and less in the upper layers than on the ebb. This explains why there is only one maximum and minimum per tidal cycle at the surface but two at the bottom. The net effect is to transport sediment landward in the lower layer and seaward in the upper layers.

Once a model of this type is reasonably well calibrated it is possible to infer additional information related to the chemistry

of contaminants. For example, the vertical flux of suspended sediment over the tidal cycle may be estimated at any level. Two levels of particular interest are mid-depth where the exchange with the seaward moving volume takes place and the bottom where the recycling with the landward displacing phase occurs. Figure 16 shows what the mid-depth flux is in phase with the bottom flux and is about one-half of the bottom flux. The instantaneous vertical sediment flux at the bottom is at least 1000 times less than the horizontal flux of suspended matter as measured by Hamblin et al. (1987).

From the magnitude of the vertical flux an approximate residence time for particles in suspension may be estimated. The residence time based on a vertically averaged concentration of 35 mg/L and a water depth of 25 m is 10 hours. This may be compared to the vertical advection time scale or settling time of a particle starting from the surface of 23 hours. Finally the vertical settling velocity of  $3 \cdot 10^{-4}$  m/s may be related to a mean particle size through the Stokes law relation which gives a size of 15  $\mu\text{m}$ . The size corresponds closely to the average particle size in the turbidity maximum of 10 to 20  $\mu\text{m}$  (Krank, 1979).

It is of some interest to construct a simple two-box model of suspended sediment based on exchanges between the boxes established by the continuous vertical transport model. This generalization of

the data at G-E-300 as shown in Figure 17 may be useful in accounting for the contaminant chemistry.

## CONCLUSIONS

While there has been considerable work on the hydrodynamics and physical oceanography of the Upper St. Lawrence Estuary the only successful prediction model in this water body is that of the standard surface tidal model. Internal flows and density distributions are much too complex to be predicted at this point. Long term circulation and response of the density fields to changing river discharge are active research areas but without proven modelling capability at this stage. Flow fields and salinity distribution as may be required to interpret processes responsible for contaminant transport and reaction must at this stage be directly measured along with the chemical concentrations. While there is considerable past data from anchor station and moored current meters it has little value in supplying the needed fields as they would be taken under different conditions of tide, river discharge and surface meteorology.

The situation on suspended sediments is even less satisfactory as there have been only a handful of past studies. Apparently

there has only been one attempt to connect sediments with hydrodynamics on a quantitative basis and no studies of such key processes as the resuspension of fine grained sediments. Again direct observations of current and salinity are required to understand the dynamics of sediment resuspension.

#### ACKNOWLEDGEMENTS

The loan of the conductivity-depth profiler by E. Marles is gratefully acknowledged as well as the assistance of J. Bull in translating the data tapes. Field support of P. Heally, K. Brown, and C. Fergusson as well as the officers and crew of the CS Limnos contributed substantially to the success of the data collection. M. Comba is thanked for providing suspended sediment concentrations during the transmission profiles. L.R. Muir kindly permitted access to his unpublished data files of current meter observations. K.R. Lum is thanked for making possible the author's participation in the cruise on the St. Lawrence.

**REFERENCES**

Allan, R.J. and K.R. Lum. 1985. National Water Research Institute, St. Lawrence River, Toxics issue, overview and plans. Unpublished report, NWRI.

d'Anglejan, B. and E.C. Smith. 1973. Distribution, transport and composition of suspended matter in the St. Lawrence Estuary, Can. J. Earth Sci., Vol. 10, pp. 1380-1396.

d'Anglejan, B. and R.G. Ingram. 1976. Time-depth variation in tidal flux of suspended matter in the St. Lawrence estuary. Estuarine and Coastal Marine Sciences, 4:401-416.

d'Anglejan, B. 1981. On the advection of turbidity in the Saint Lawrence Middle Estuary. Estuaries, Vol. 4, pp. 2-15.

d'Anglejan, B. and R.G. Ingram. 1984. Near bottom variations of turbidity in the St. Lawrence Estuary. Estuarine, Coastal and Shelf Science, Vol. 19, pp. 655-672.

Bewers, J.M. and P.A. Yeats. 1979. The behaviour of trace metals in estuaries of the St. Lawrence Basin. Naturaliste Can., Vol. 108, 149-161.

\_\_\_\_\_. 1978 trace metals in the waters of a partially mixed estuary. Estuar. Coastal Mar. Sci., 7:147-162.

Bloomfield, P. 1976. Fourier analyses of time series: An introduction, John Wiley and Sons, pp. 258.

Budgell, W.P. and L.R. Muir. 1975. St. Lawrence River Current Survey 1974 Data Report. Ocean and Aquatic Sciences Dept. of Environment, Burlington. Unpublished report.

Dewey, R.K. and W.R. Crawford. 1987. Bottom stress estimates from vertical dissipation profiles on the continental shelf. Manuscript submitted or publication.

Dhamotharan, S., Gulliver, J.S. and Stefan, H.G. 1981. Unsteady one-dimensional settling of suspended sediment. Water Res., Vol. 17, pp. 1125-1132.

Dronkers, J. 1986. Tide-induced residual transport of fine sediment. In: Physics of Shallow Estuaries and Bays. Ed. J. Van der Kreeke. Springer-Verlag, pp. 228-244.

Fischer, H., E.J. List, R.C.Y. Koh, J. Imberger, N.H. Brooks. 1979. Mixing in inland and coastal waters. Academic Press.



Hamblin, P.F., K.R. Lum, M.E. Comba and K.L.E. Kaiser. 1987. Observations of suspended sediment flux over a tidal cycle in the region of the turbidity maximum of the Upper St. Lawrence River Estuary. Proceedings of Symposium of Hydrodynamics and Sediment Dynamics of Tidal Inlets.

Krank, K. 1979. Dynamics and distribution of suspended particulate matter in the St. Lawrence Estuary, *Le Naturaliste Can.*, Vol. 106, pp. 163-173.

Lum, K.R., M. Callaghan and P.R. Youakim. 1986. Dissolved and particulate cadmium in the St. Lawrence River. Proceedings of Symposium.

Levesque, L. 1977. Étude du modèle mathématique de la propagation des marées dans l'estuaire du Saint Laurent. *Cahier d'information No. 2, Section D, Oceanographie, Université du Quebec, Rimouski*, pp. 161.

Murty, T.S., M.I. El-Sabh and J. M. Briand. 1979. Storm surge amplitudes in the St. Lawrence Estuary. *J. Can. Hydrogr. Assoc.*, 20:8-16.

Muir, L.R. 1978. St. Lawrence River Current Survey. 1975. Data Report Unpublished Report Data Report 78-2, Fisheries and Environment Canada.

Muir, L.R. 1979. St. Lawrence river oceanographic survey. 1977. Data Report Vol. 1 Tidal, Meteorological and Current Meter Data. Data Report Series 79-1, Fisheries and Oceans.

Muir, L.R. 1980. Internal tides in a partially mixed estuary. 2nd Stratified Flow Symposium, Trondheim, pp. 538-547.

Muir, L.R. 1980. Internal tides in a partially mixed estuary. Ocean Science and Surveys Central Region Fish. Ocn. Can., MSR No. 9.

Muir, L.R. 1981. Internal tides in a partially mixed estuary. MS Rep. Ser. 9, Fisheries and Oceans, Burlington.

Nichols, M.N. 1986. Effects of fine sediment resuspension in estuaries. In Estuarine Cohesive Sediment Dynamics. Ed. A.J. Mehta, Springer-Verlag. pp. 5-42.

Silverberg, N. and B. Sundby. 1979. Observation in the turbidity maximum of the St. Lawrence Estuary. Can. J. Earth Sci., Vol. 16: 939-950.

Soucy, A.Y., Y Berubé, J.P. Fronder and P. Marie. 1976. Évolution des suspensions et sédiments dans l'estuaire moyen du Saint Laurent, Le Cahier de Centreau, 1(5):67.

Teeter, A. 1986. Vertical transport in fine-grained suspension and newly deposited sediment. In Estuarine Cohesive Sediment Dynamics, Ed. A.J. Mehta, Springer Verlag, pp. 170-191.

**FIGURE CAPTIONS**

1. Station locations of the 1986 survey in the Upper St. Lawrence River Estuary.
2. Tides at Quebec during the field survey based on Canadian Hydrographic Service Tide tables.
3. Daily discharge at La Salle, during study period, Inland Waters Branch, October 1986. Five-year average 1981 - 1985 discharge.
4. Tow tank speed versus direct reading current meter speed.
5. Percentage optical transmission versus suspended sediment concentration, mg/L at three stations Upper St. Lawrence Estuary.
6. Averaged salinity profiles over a tidal cycle.
7. Tidally averaged along channel flow, positive flow in seaward direction.
8. Tidally averaged cross-channel flow, positive to northwest.

9. Estuarine circulation St. Lawrence Estuary according to Soucy et al. (1976).
10. Along-channel tidal residual current Pt au Pic, 1975, profiles measured at different times at a station are plotted along the axis of the channel. Sp = spring tides, NP = neap tides.
11. Tidal residual salt flux, u's'.
12. Suspended sediment concentration at bottom, — — — — —.  
Along-channel component of bottom stress, Pa, \_\_\_\_\_.  
Station 6E300.
13. Time history over the water column of the vertical eddy diffusivity at station 6E300 ( $m^2/s$ ) over a tidal cycle. (a) Unsmoothed, (b) smoothed. E is ebb; S is slack and F is flood.
14. Time history of suspended sediment concentration at Station 6E300 (mg/L), (a) observations based on transmissometer profiles, (b) simulated with smoothed diffusivity.

15. Same as Figure 14 but simulated with unsmoothed diffusivities.
16. Upward vertical flux of suspended sediment  $\text{mg}/(\text{m}^2 \text{s})$  at (a) mid-depth, (b) bottom over the tidal cycle predicted from vertical transport model.
17. Two-box model of suspended sediment, C, and salinity S and associated horizontal and vertical exchanges at Station 6E300.

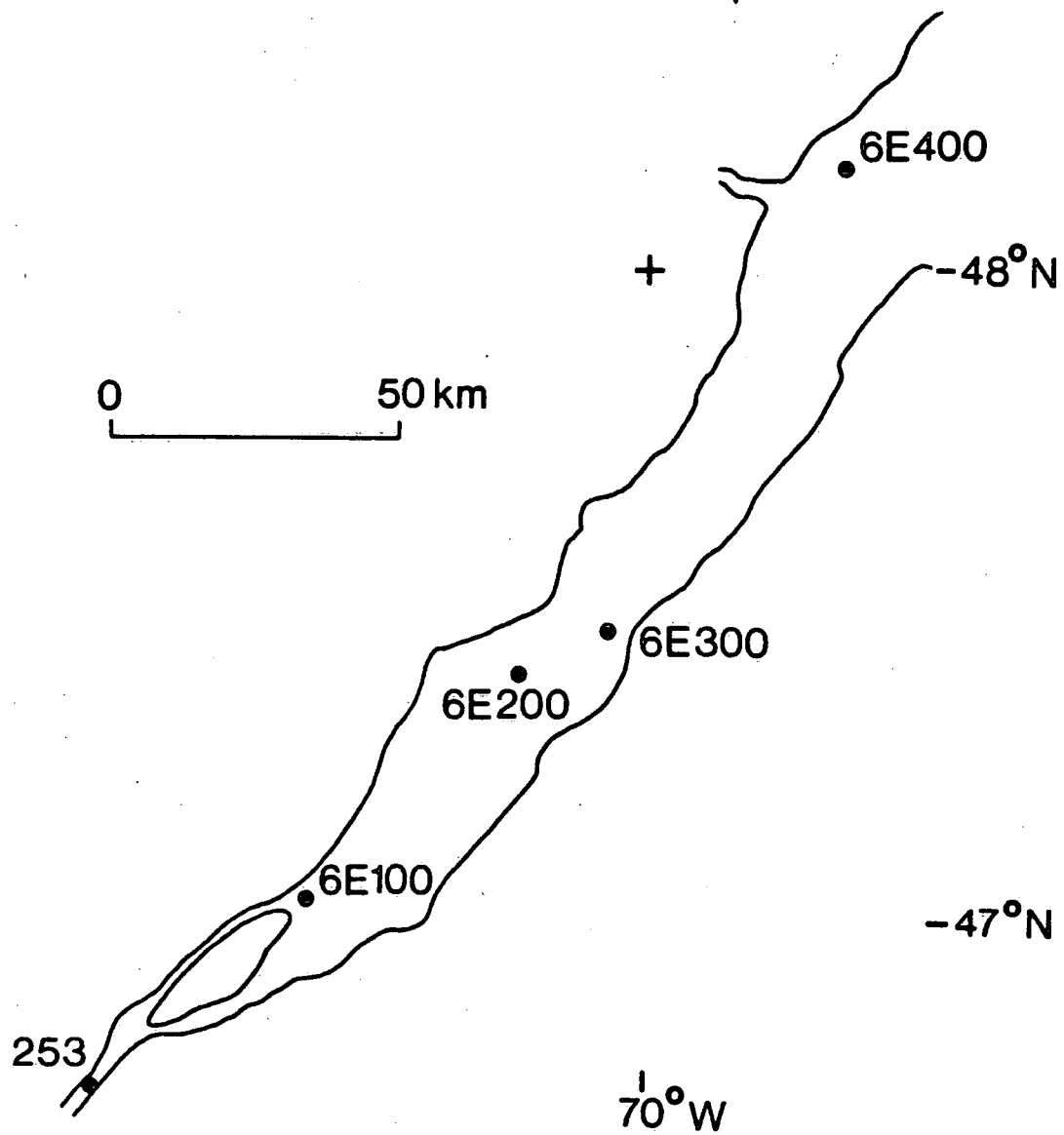


Figure 1.

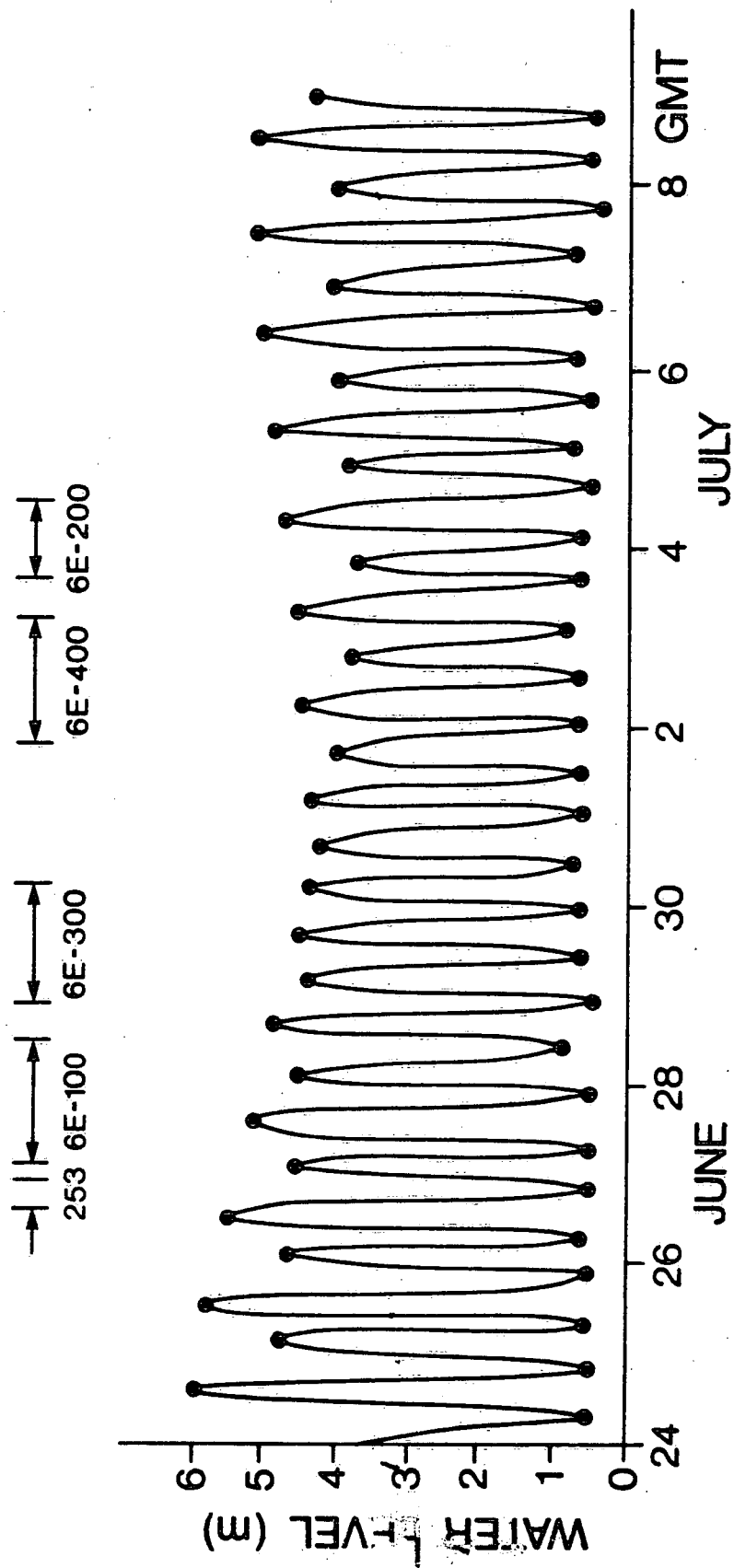


Figure 2.



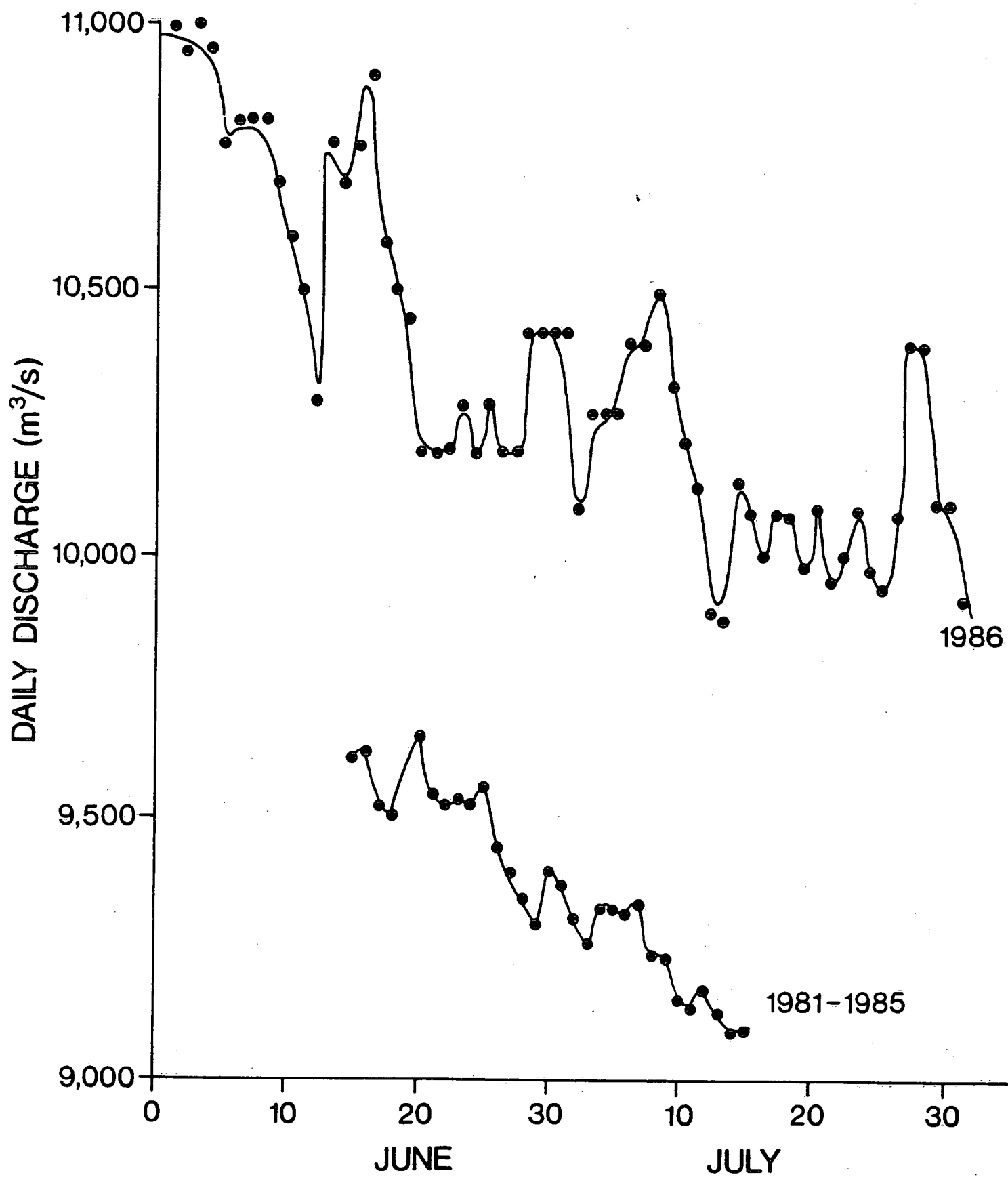


Figure 3.

NEIL BROWN DRCM

JUNE 13, 1986

(low speed)

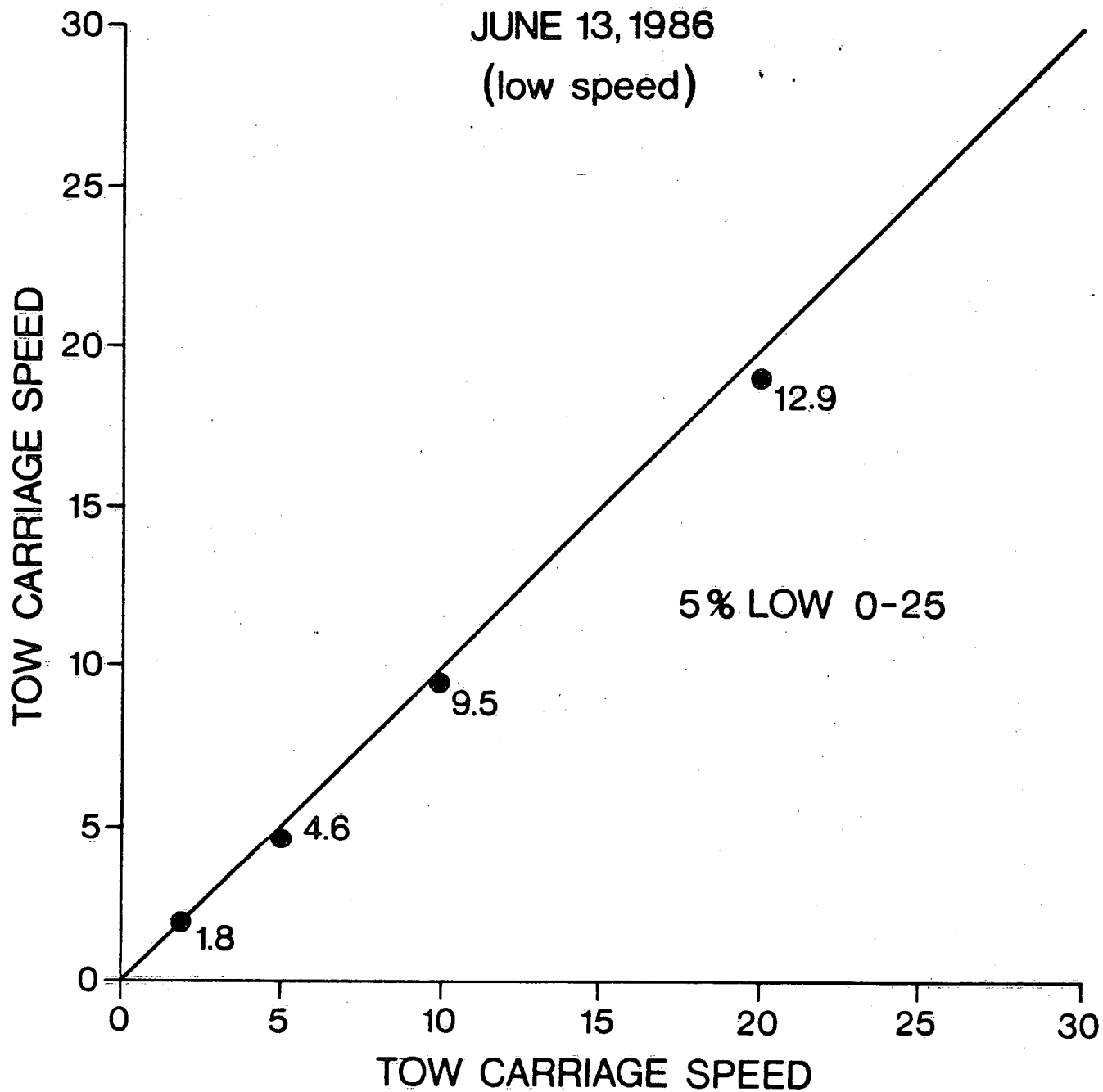


Figure 4.

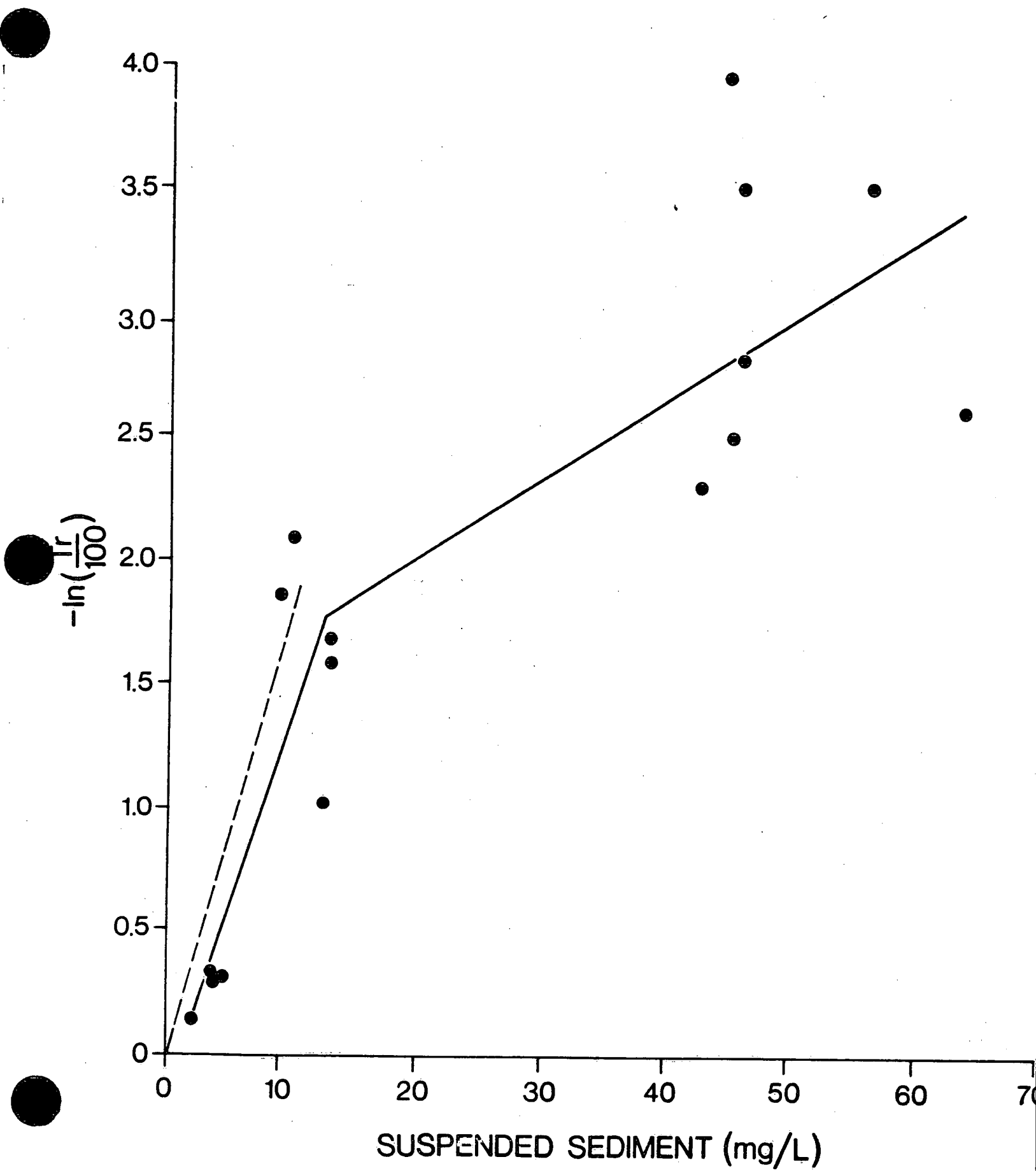
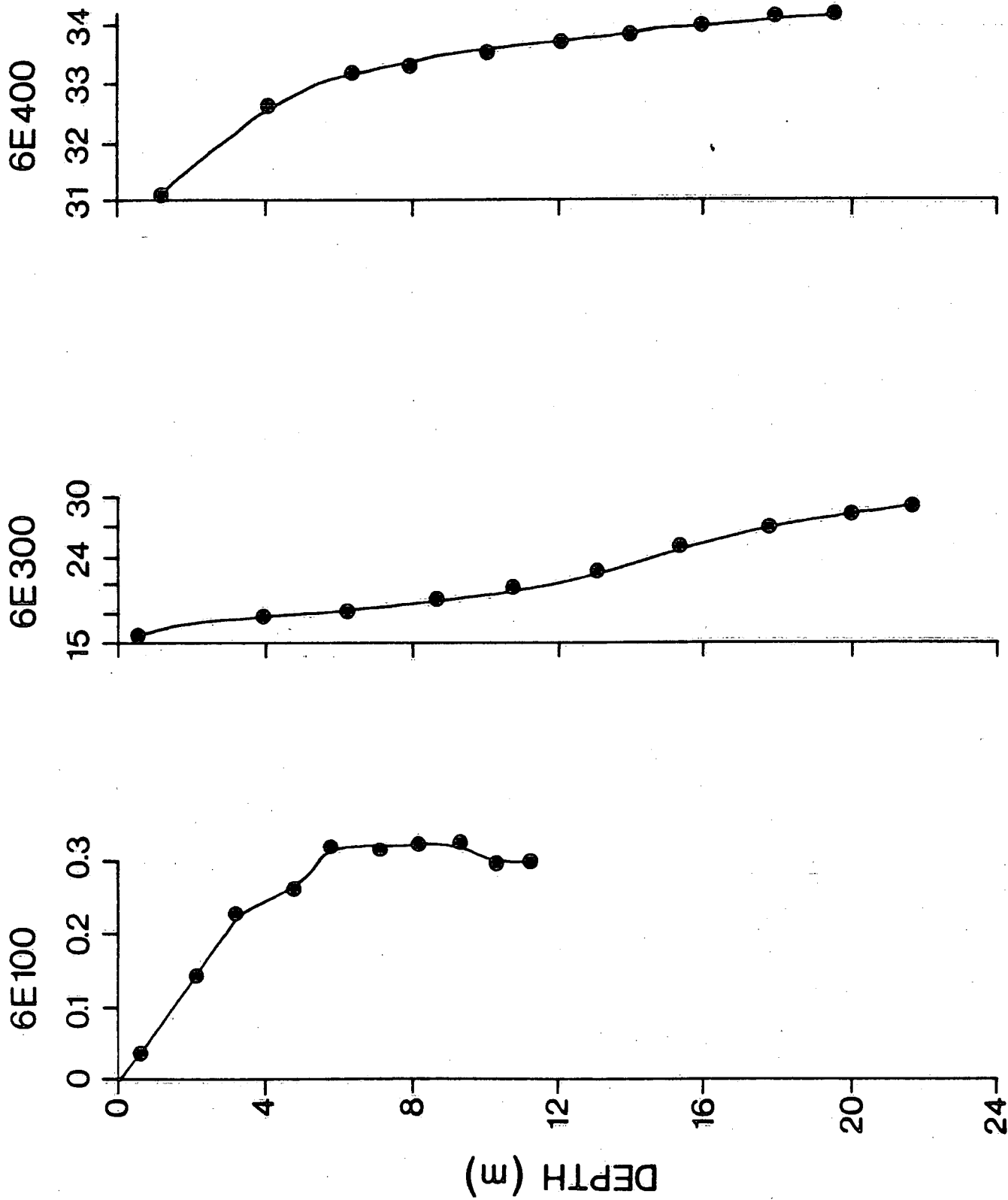


Figure 5.



SALINITY, ‰

Figure 6.

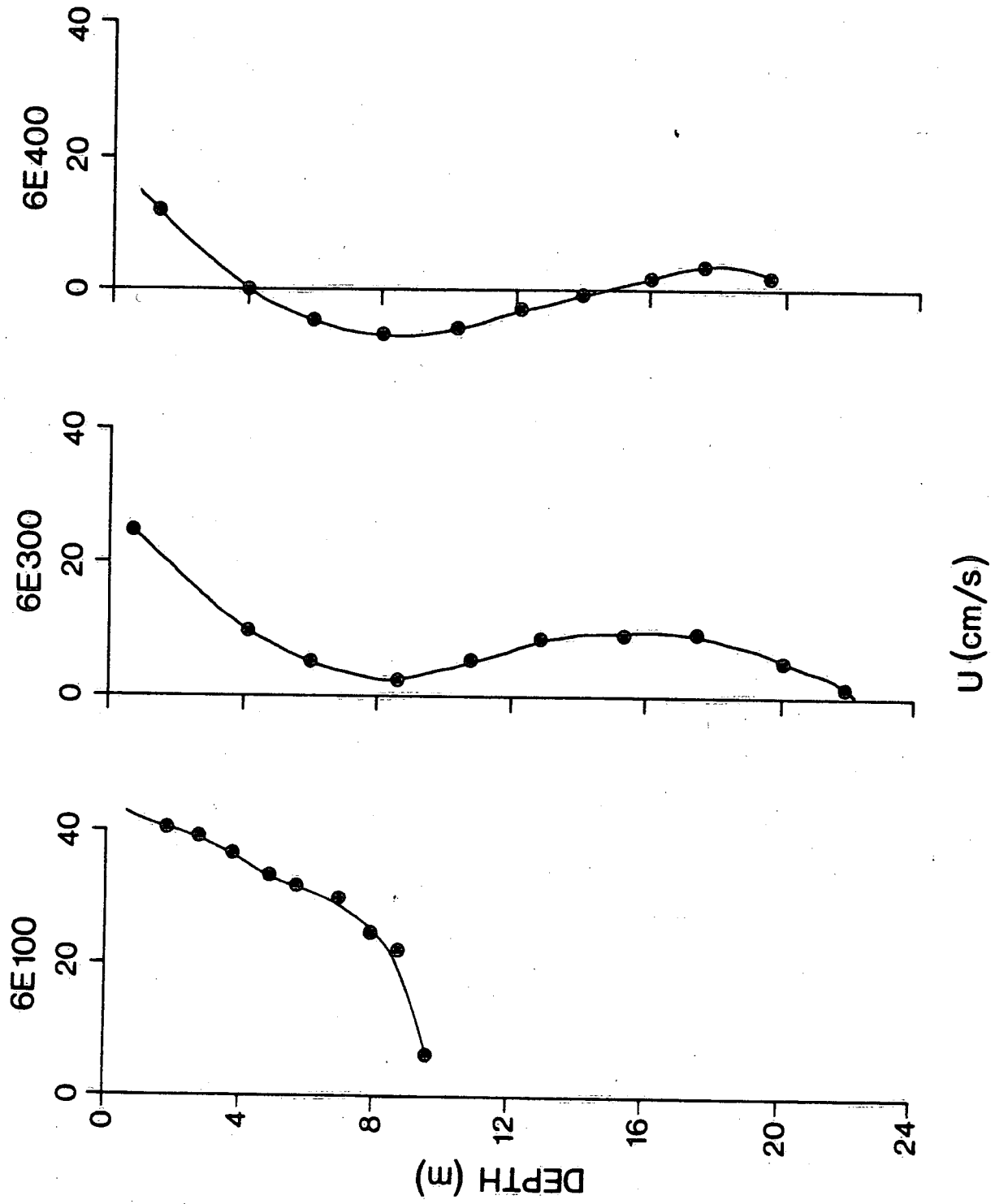


Figure 7.

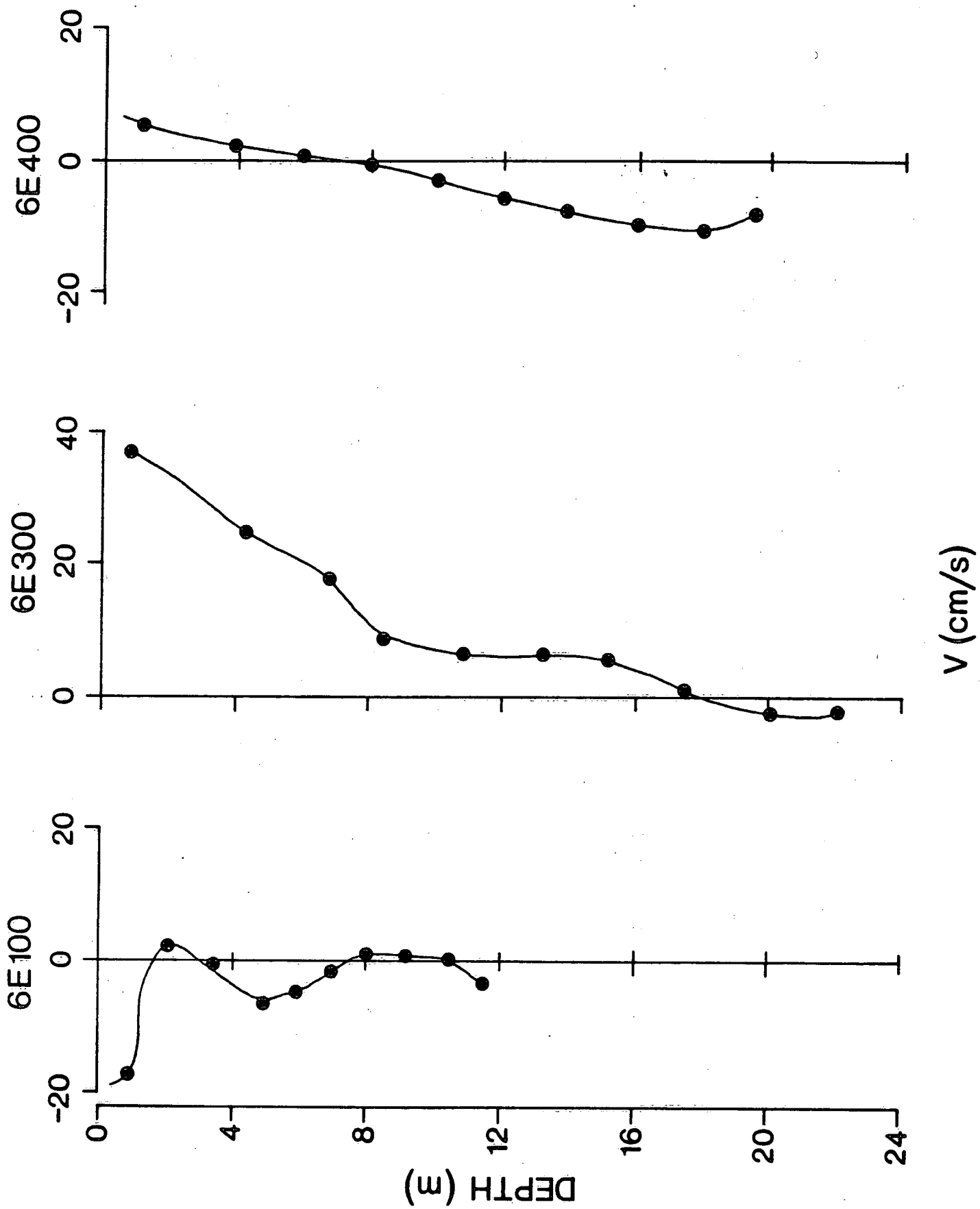


Figure 8.

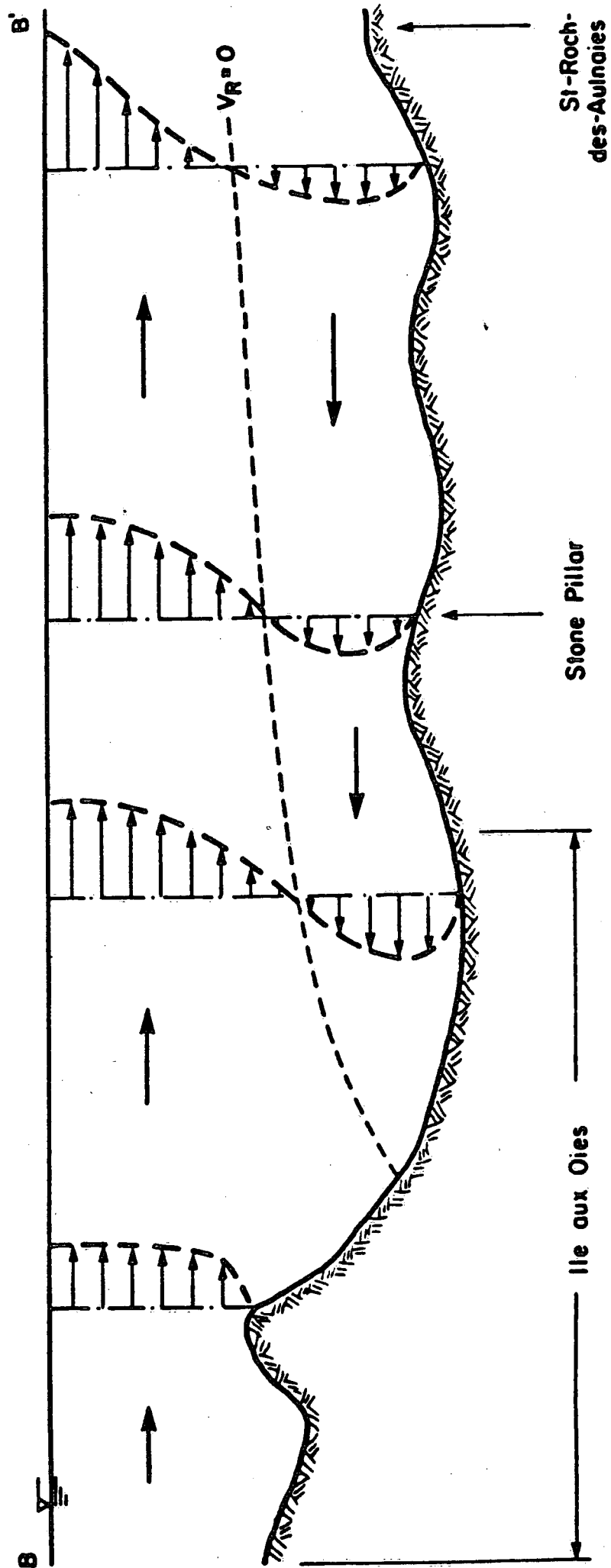


Figure 9.

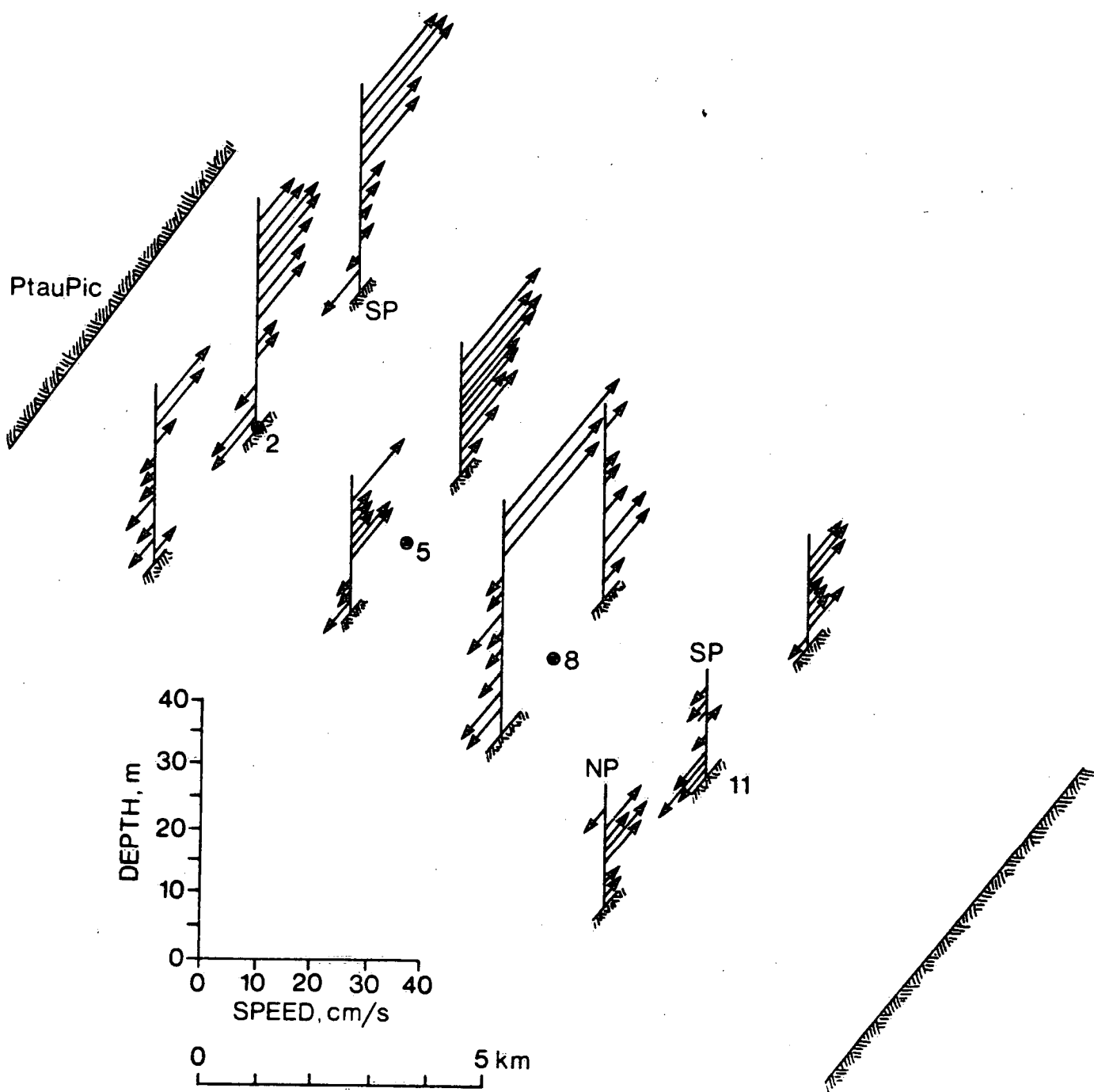


Figure 10.



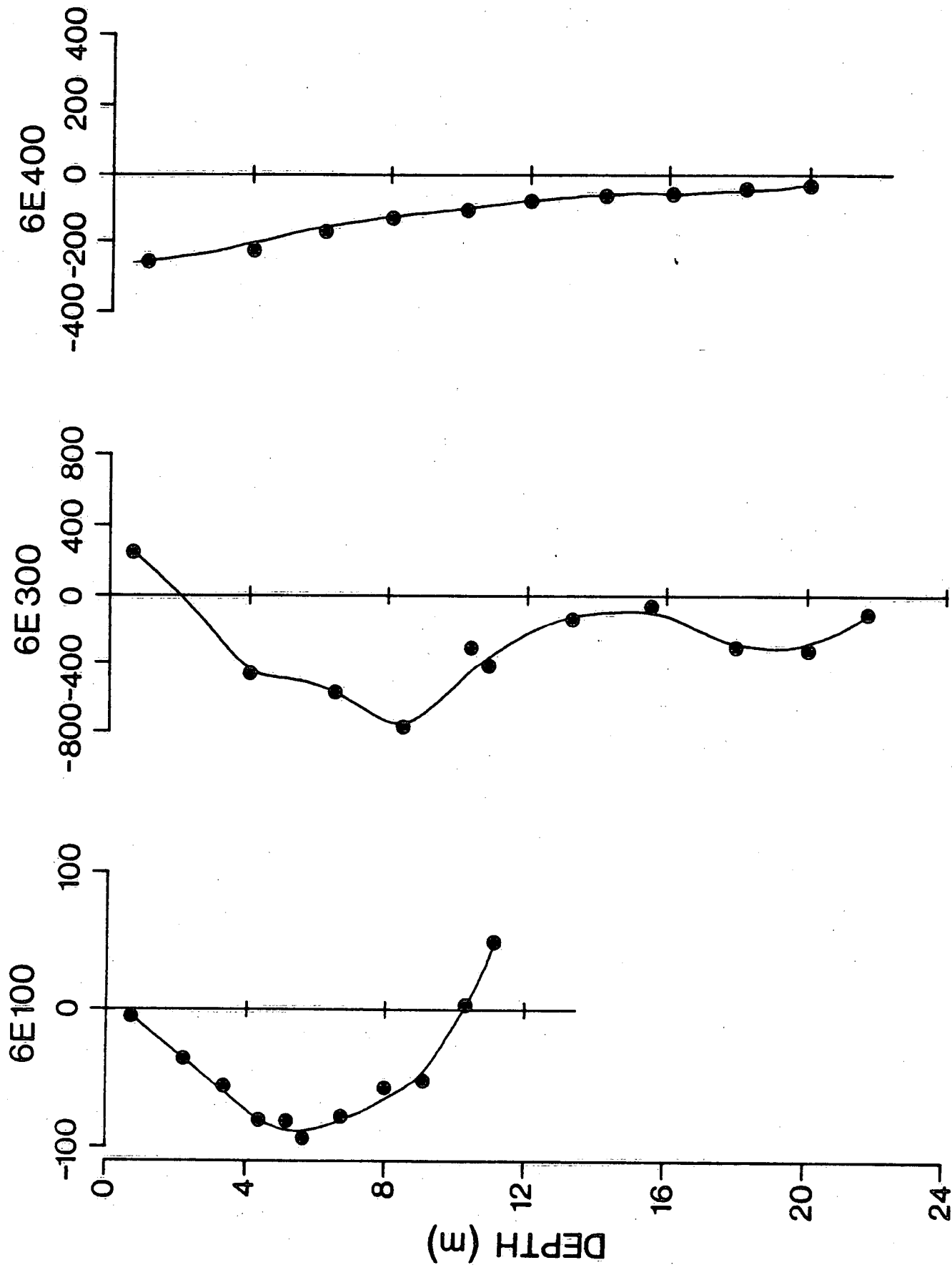


Figure 11.

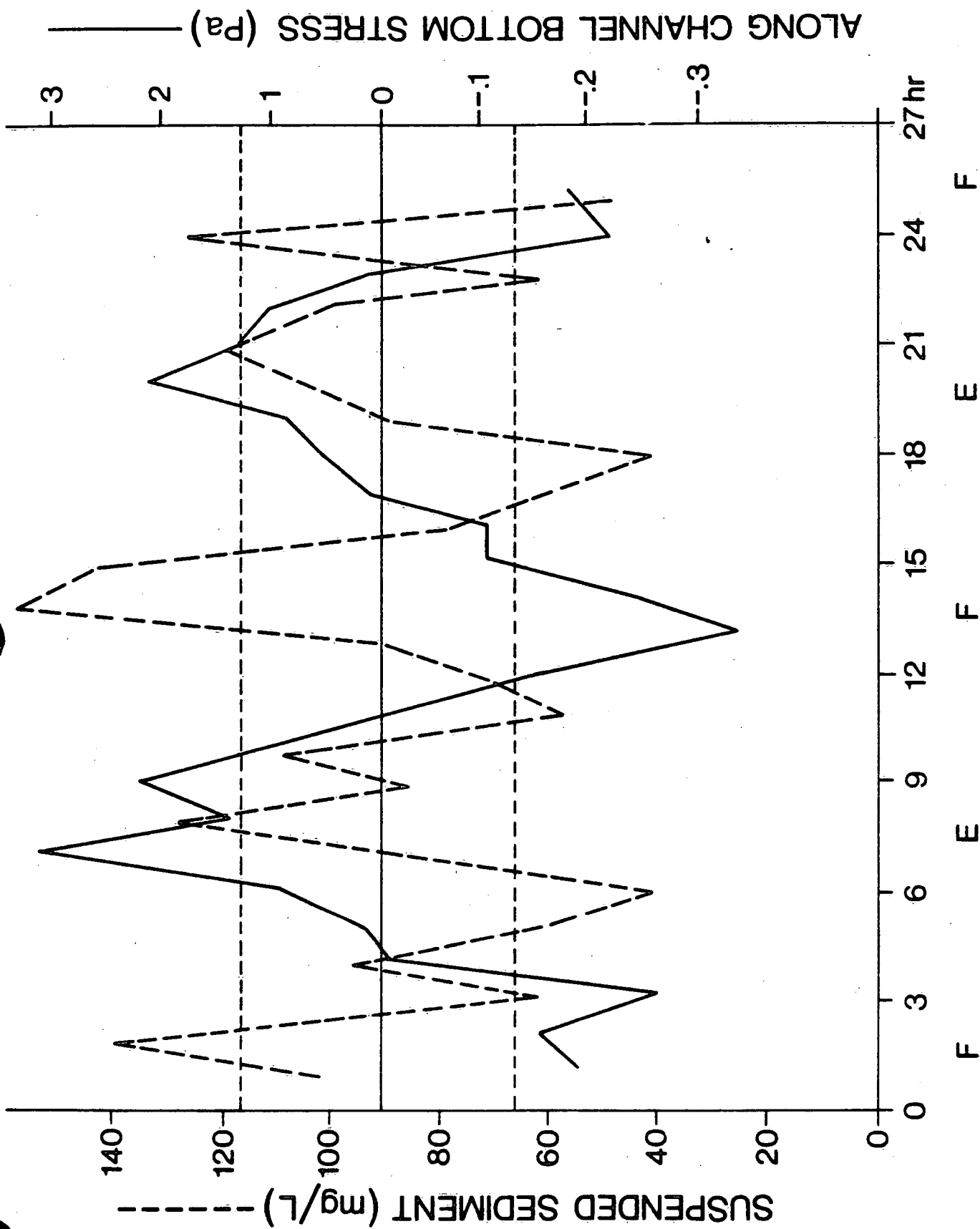


Figure 12.

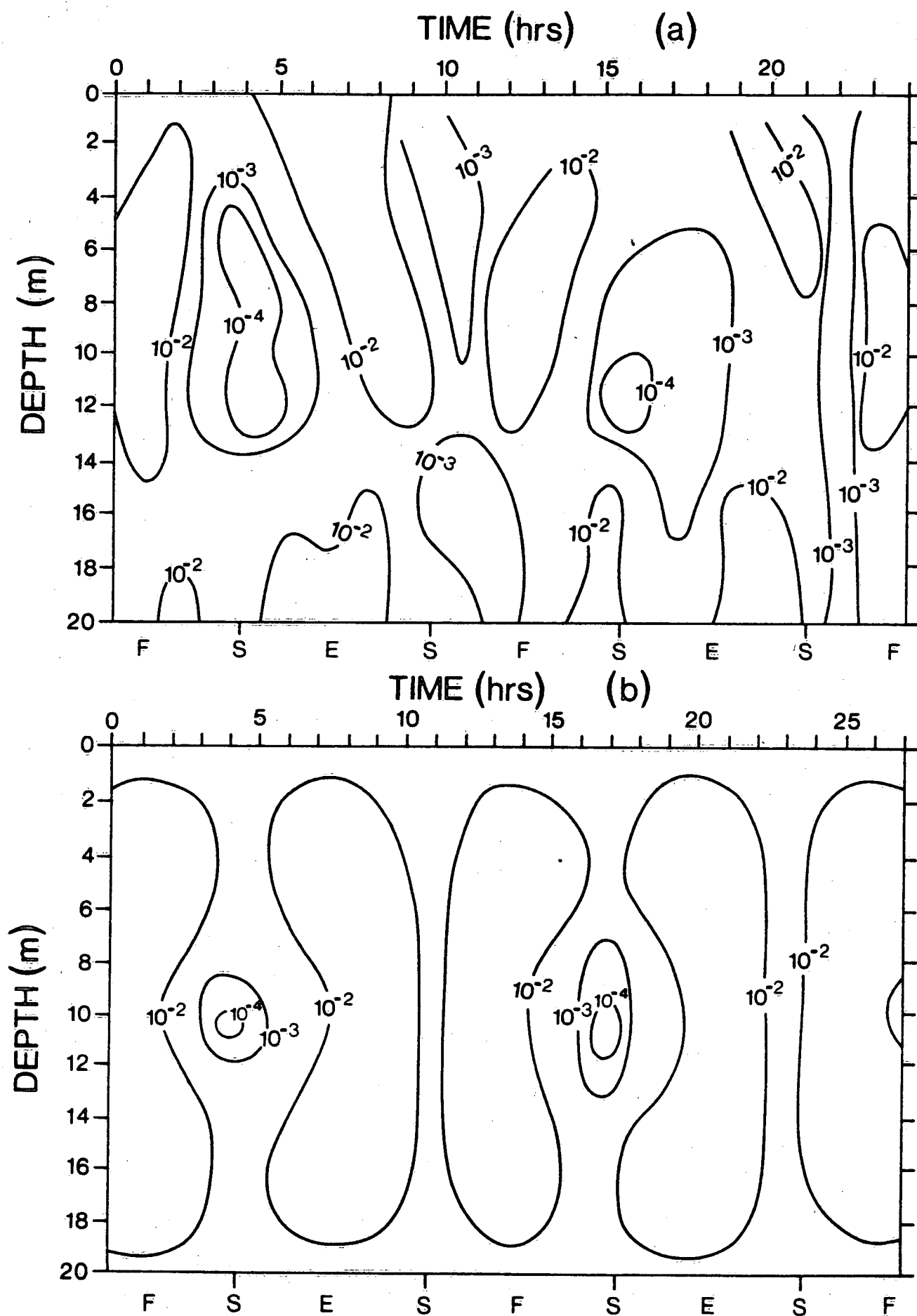


Figure 13.

STATION 6E 300

JUNE 28-30, 1986

GMT

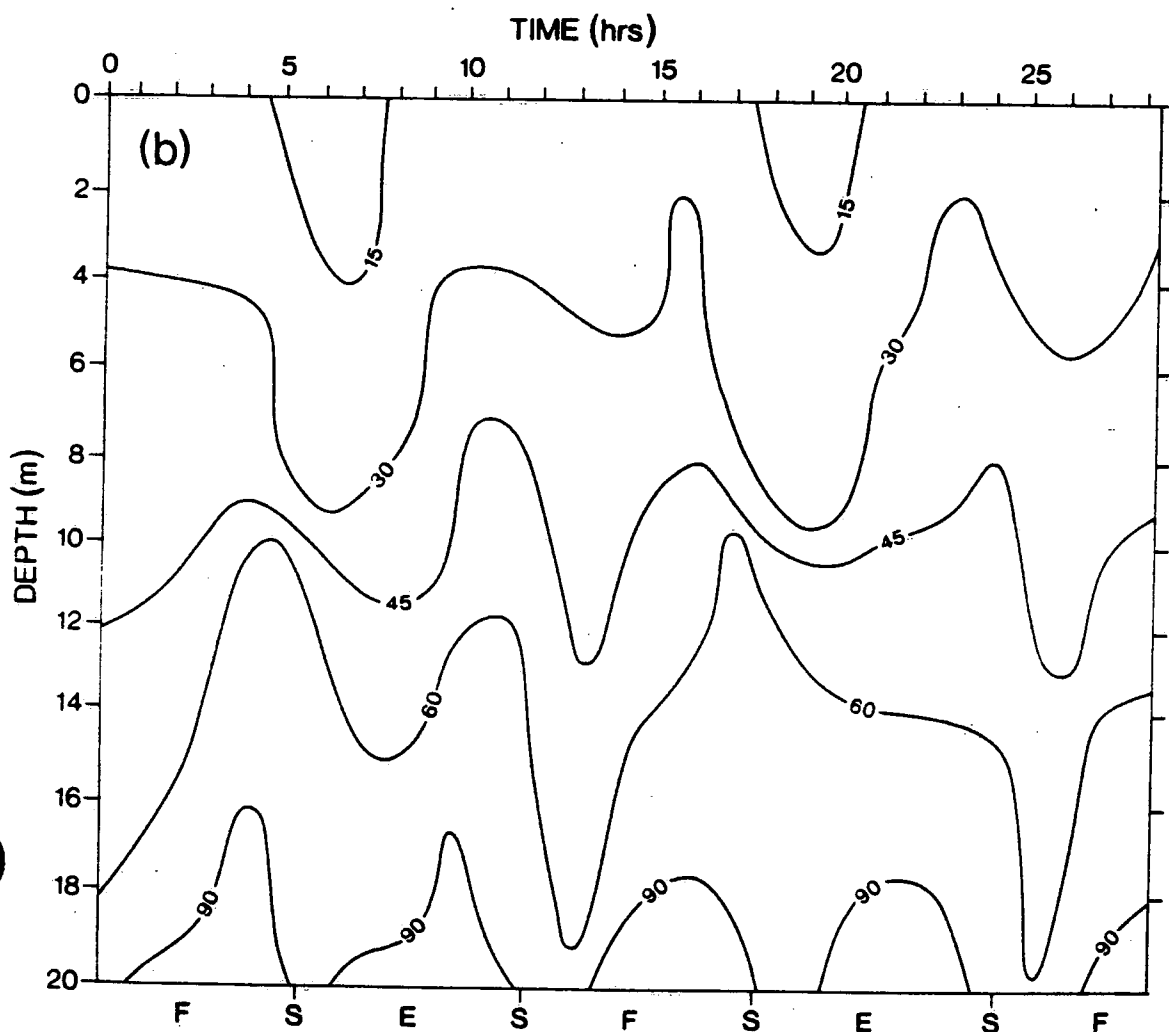
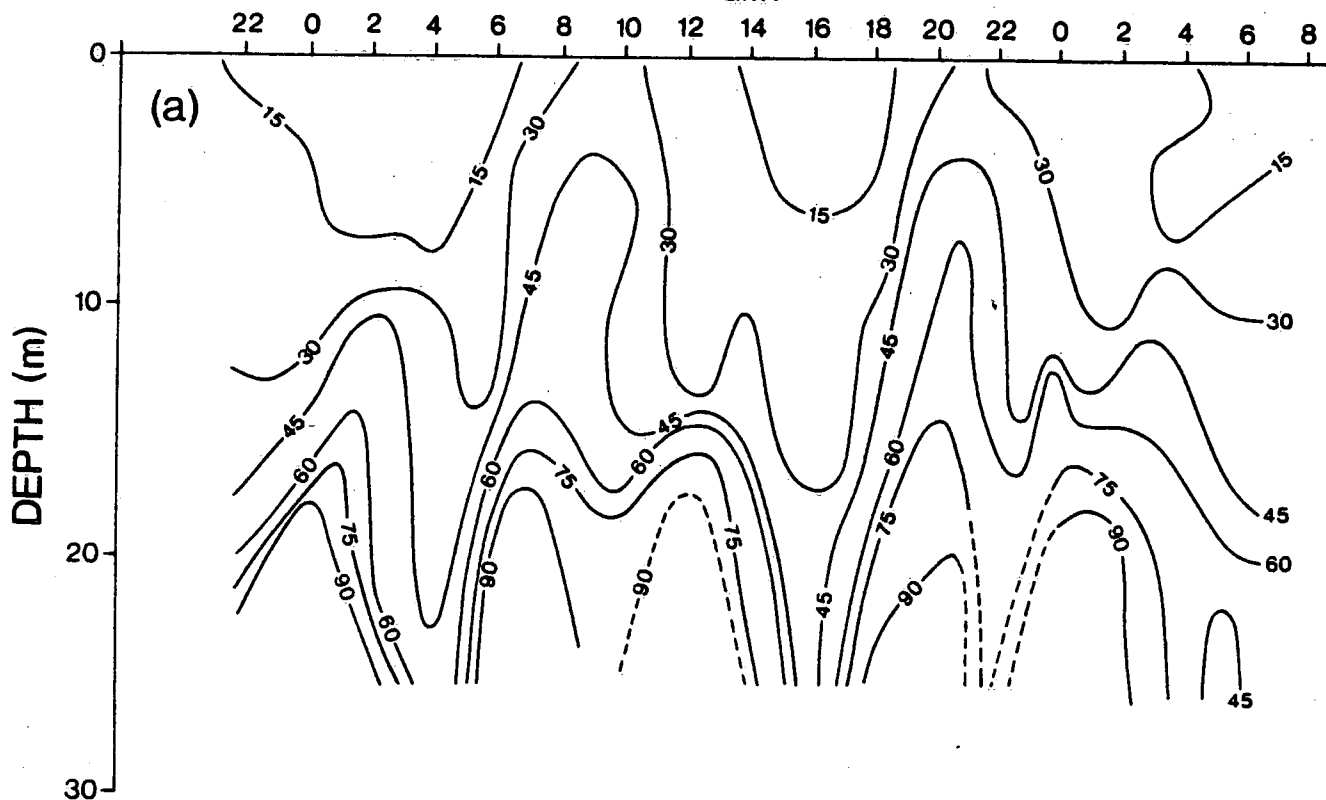


Figure 14.

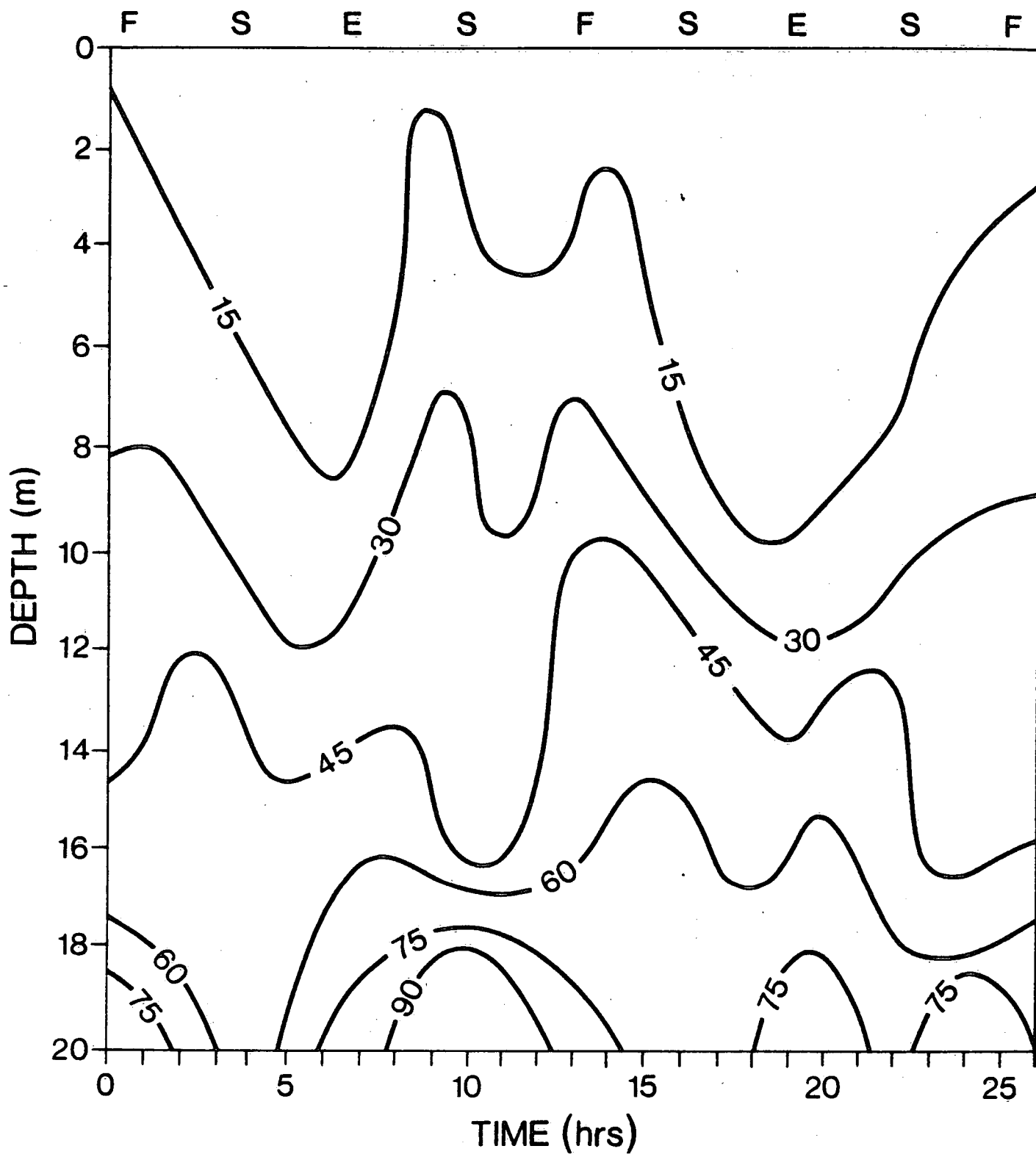


Figure 15.

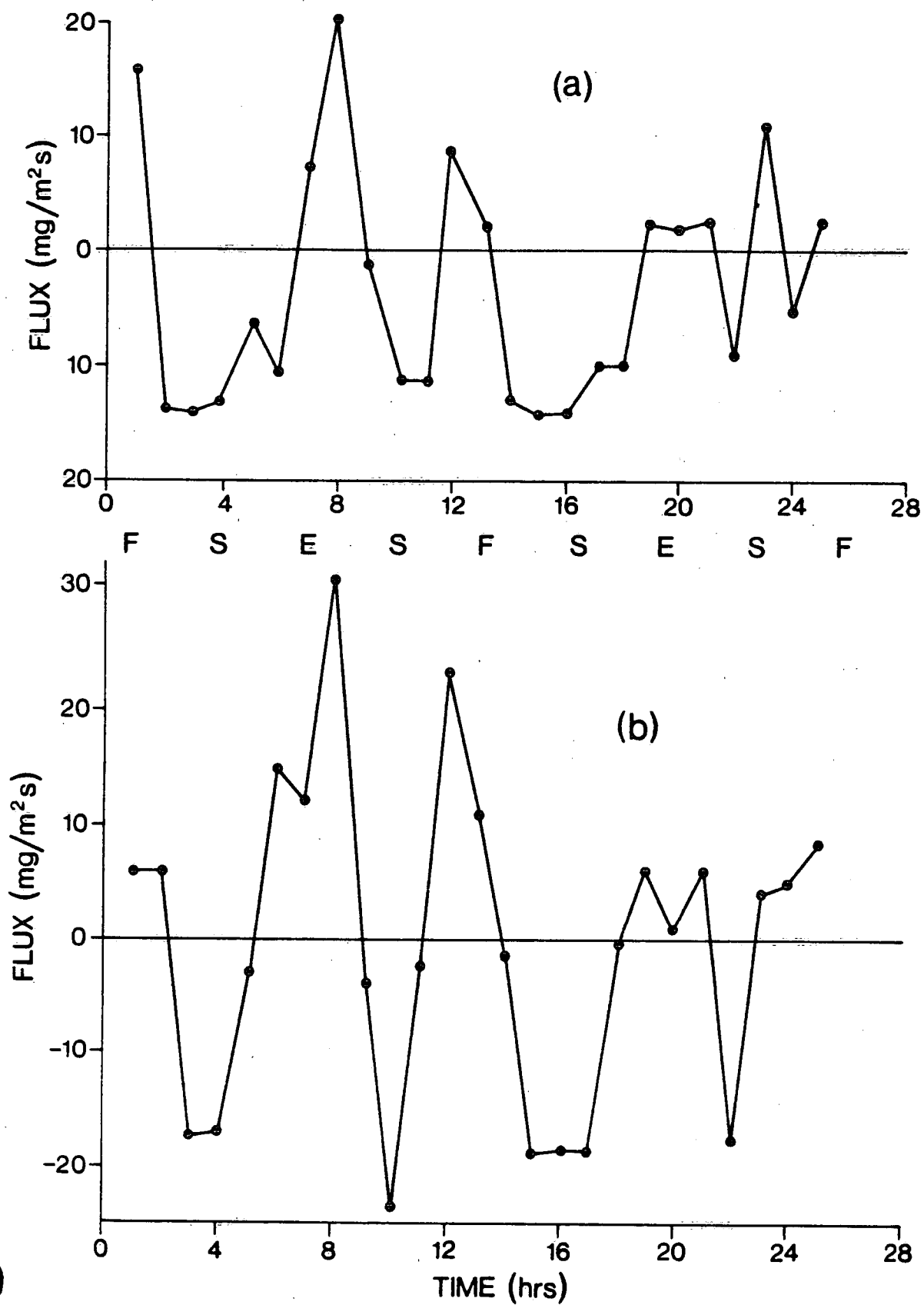


Figure 16.

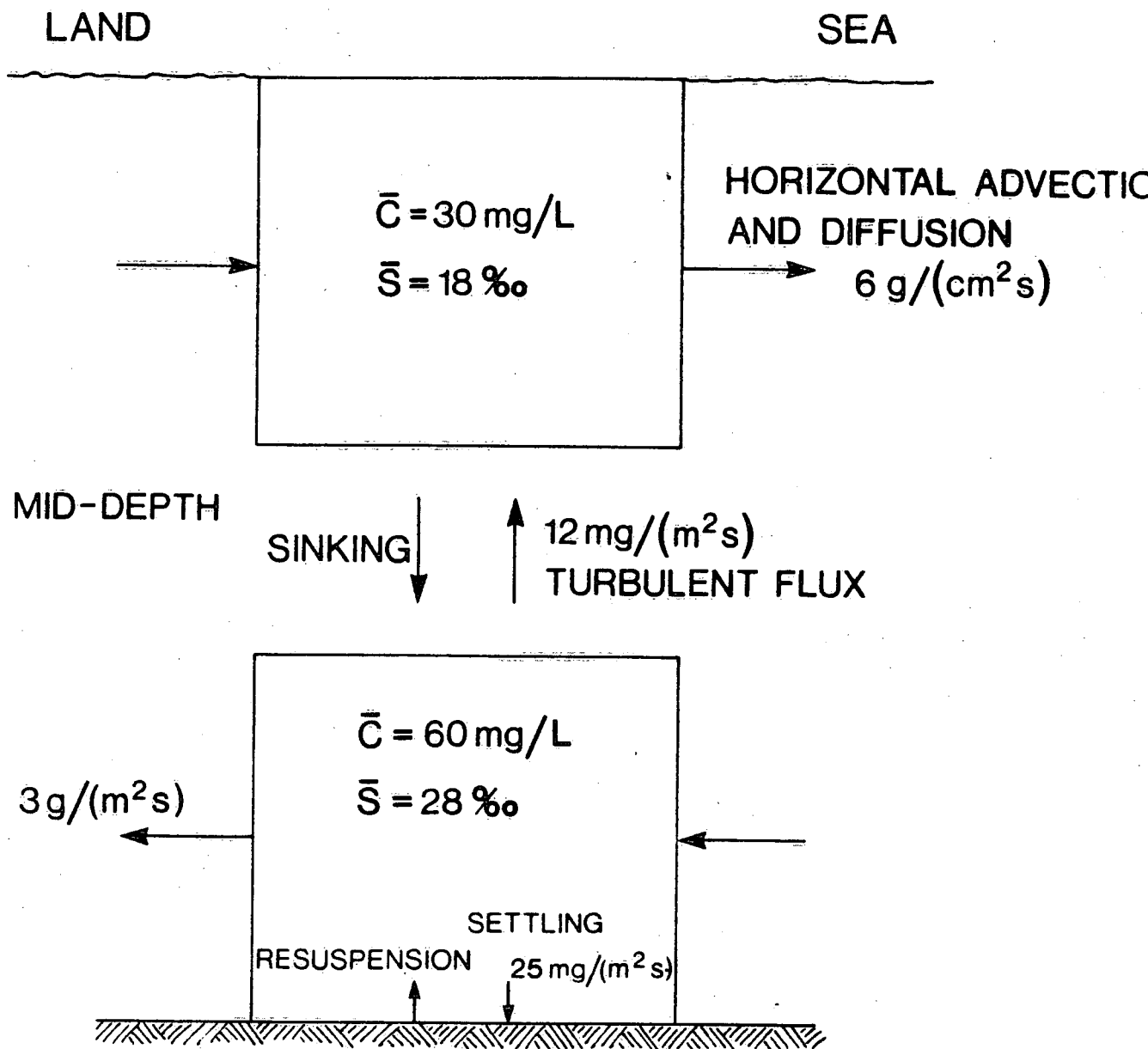


Figure 17.

## APPENDIX A

Station 253      Latitude N      46°42'58"  
Longitude M      71°22'42"

## List of Figure Captions

Figure A.1 Profiles of (a) temperature (b) along-channel flow cm/s (c) cross-channel flow (positive to SE) m/s (d) suspended sediment. Time of bottom reading (GMT) at bottom of profile.



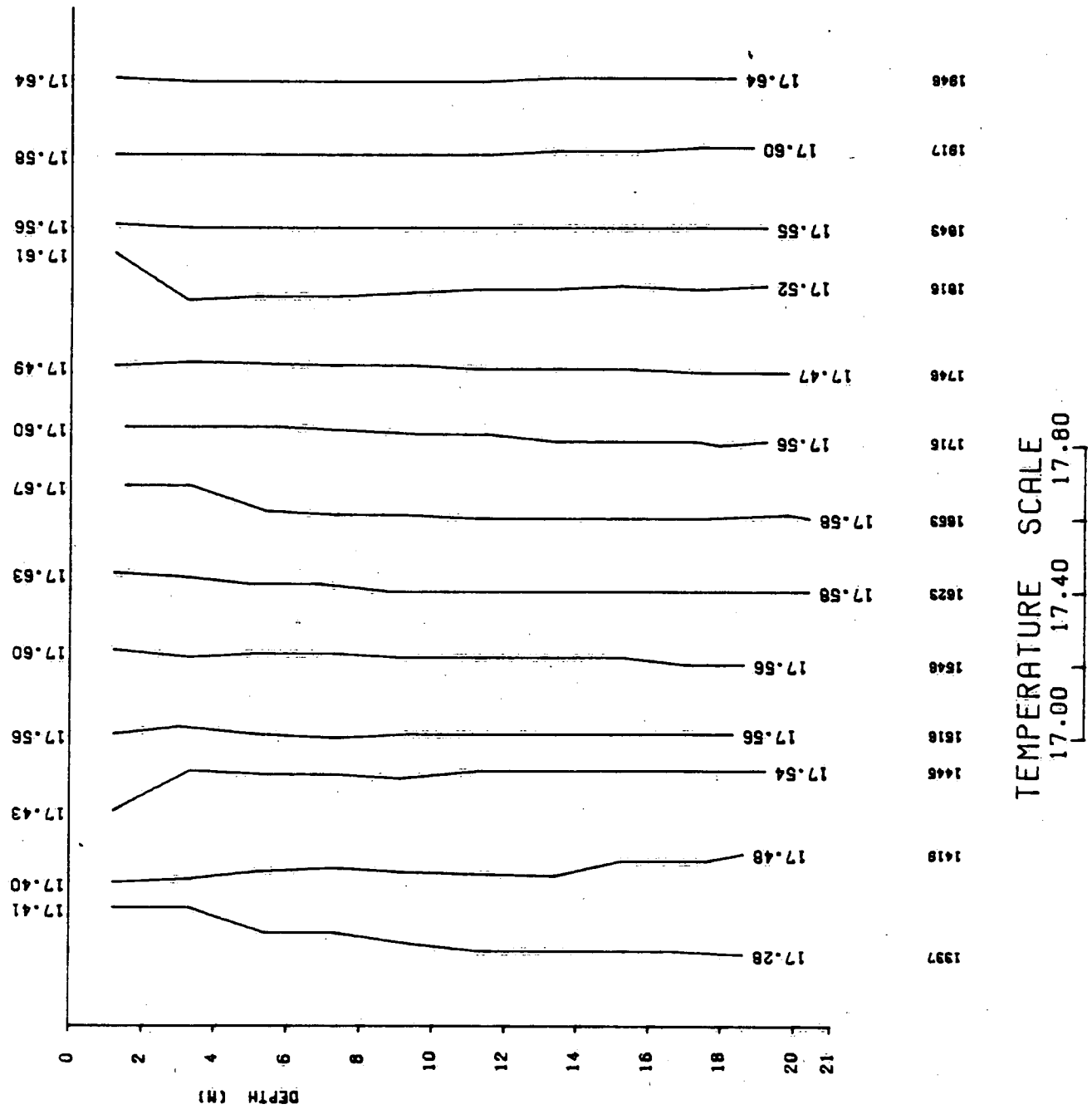


Figure A.1(a)

ST LAWRENCE STN 253 JUNE 26 1986

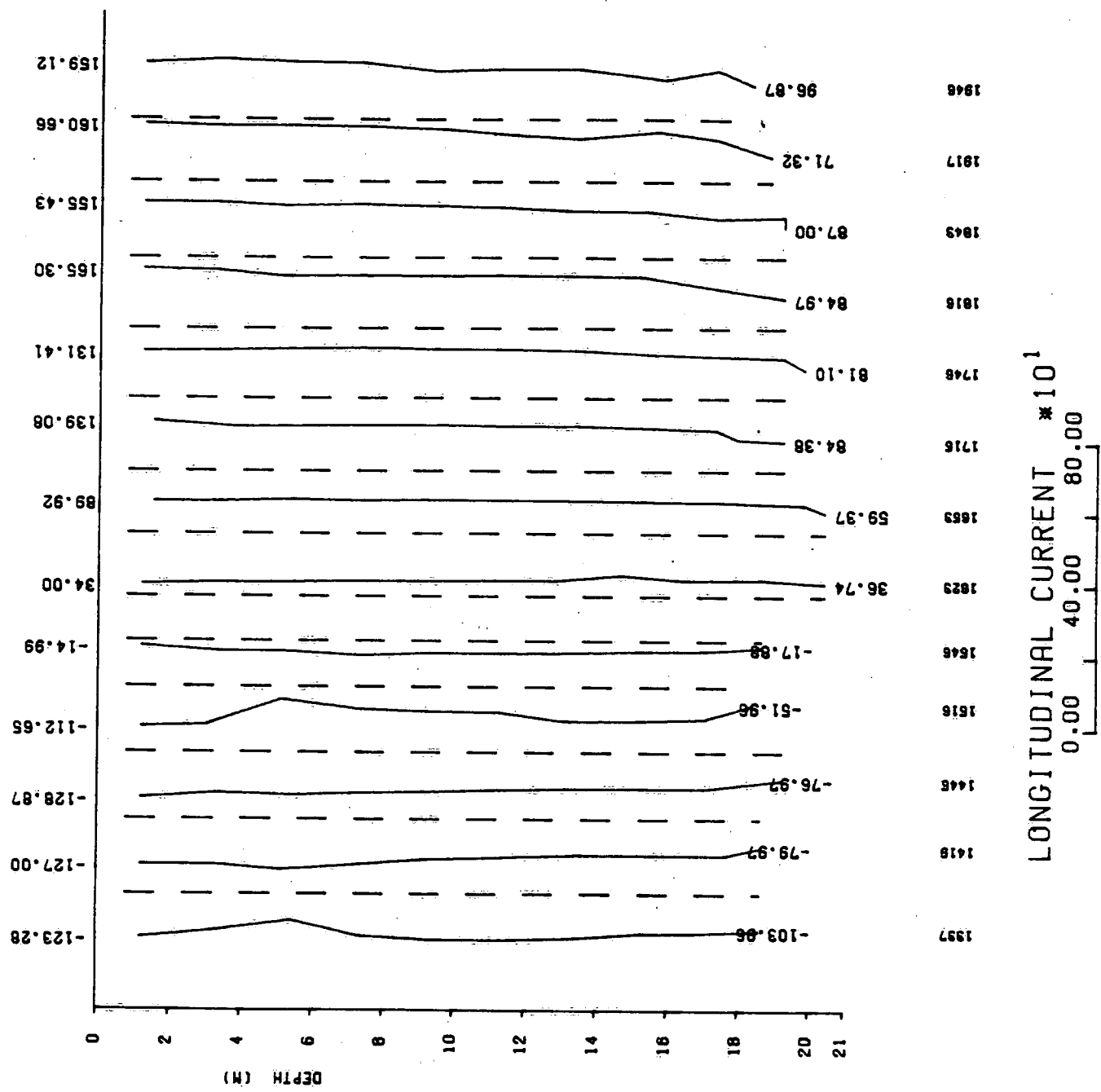


Figure A.1(b)

ST LAWRENCE IN 253 JUNE 26 1986

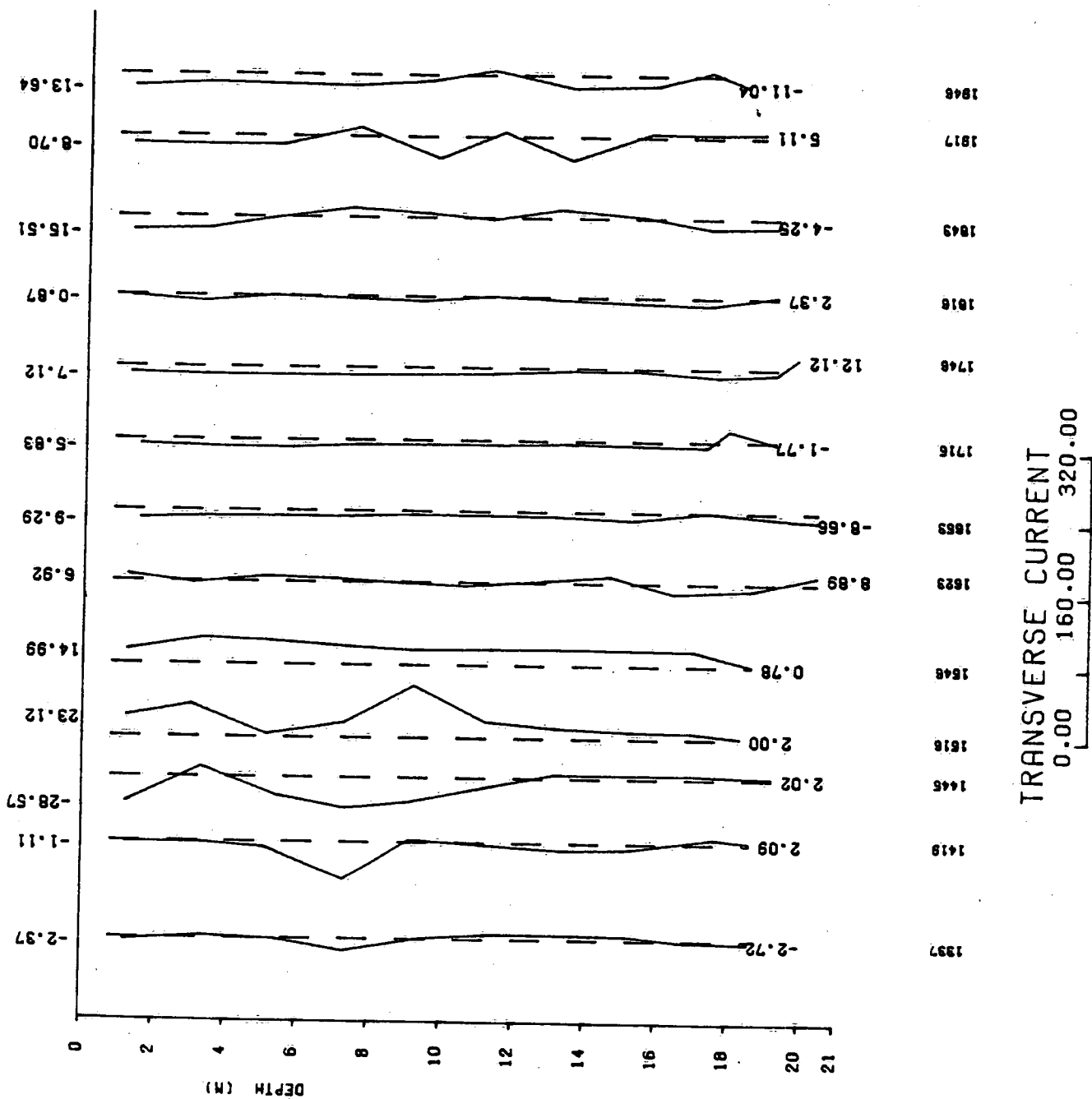
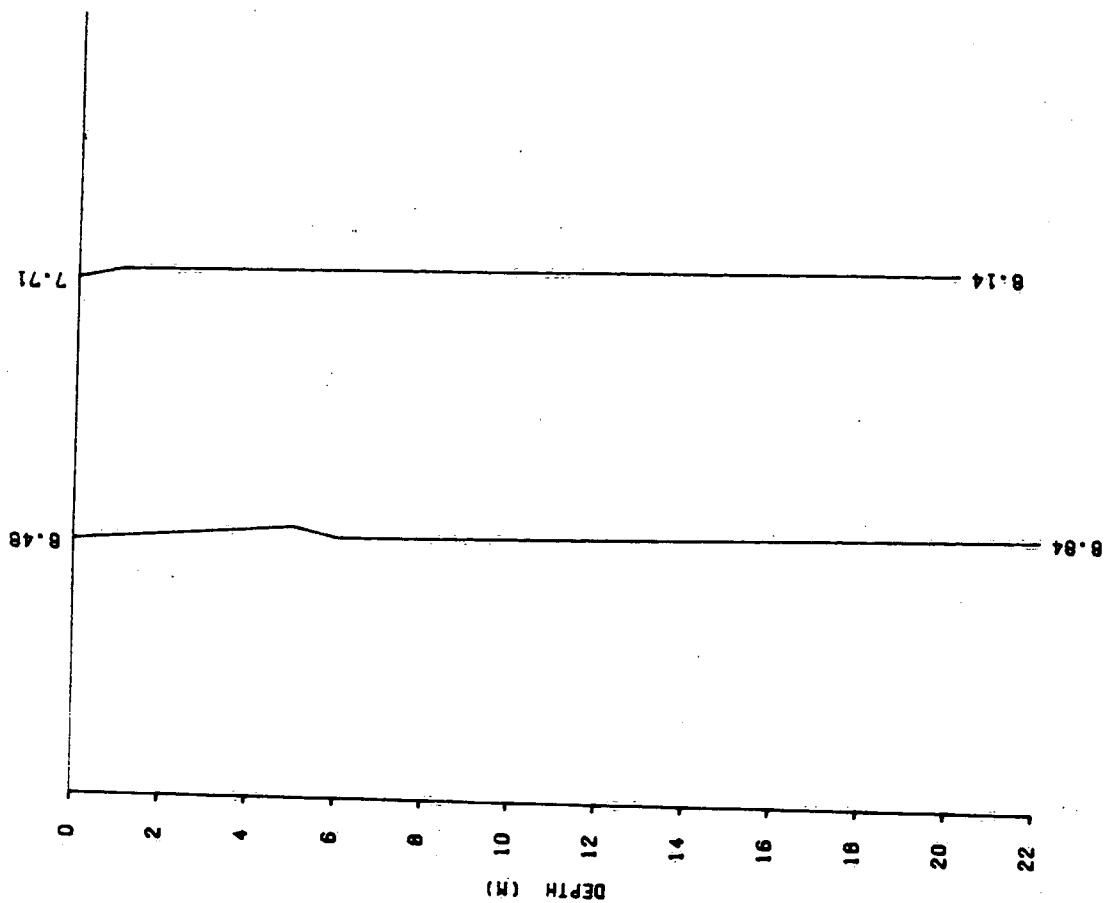


Figure A.1(c)

ST LAWRENCE STN 255 JUNE 1986



25/1306 26/1942

Figure A.1(d)

SUSPENDED SEDIMENT (MG/L)  
0.00 4.00 8.00

**APPENDIX B**

Station 6E100   Latitude N   47°02'28"  
Longitude W   70°48'24"

**List of Figure Captions**

- Figure B.1.   Profiles from 03:13 to 09:41 June 27, 1986 (GMT) of (a) temperature, (b) salinity, (c) along-channel current and (d) cross-channel current (positive to SE).
- Figure B.2.   Profiles from 10:07 to 16:17 June 27, 1986 (GMT) of (a) temperature, (b) salinity), (c) along-channel flow and across-channel flow (positive to SE).
- Figure B.3.   Profiles from 16:42 to 23:47, June 27, 1986 (GMT) of (a) temperature, (b) salinity, (c) along-channel flow and (d) across-channel flow (positive to SE).
- Figure B.4.   Profiles from 00:13 to 06:11, June 28, 1986 of (a) temperature, (b) along-channel flow (c) cross-channel flow (positive to SE).

Figure B.5. Profiles from 06:36 to 12:44, June 28, 1986 (GMT) of (a) temperature, (b) along-channel flow and (c) cross-channel flow (Positive to SE).

ST LAWRENCE 6E100 JUNE 27 1986

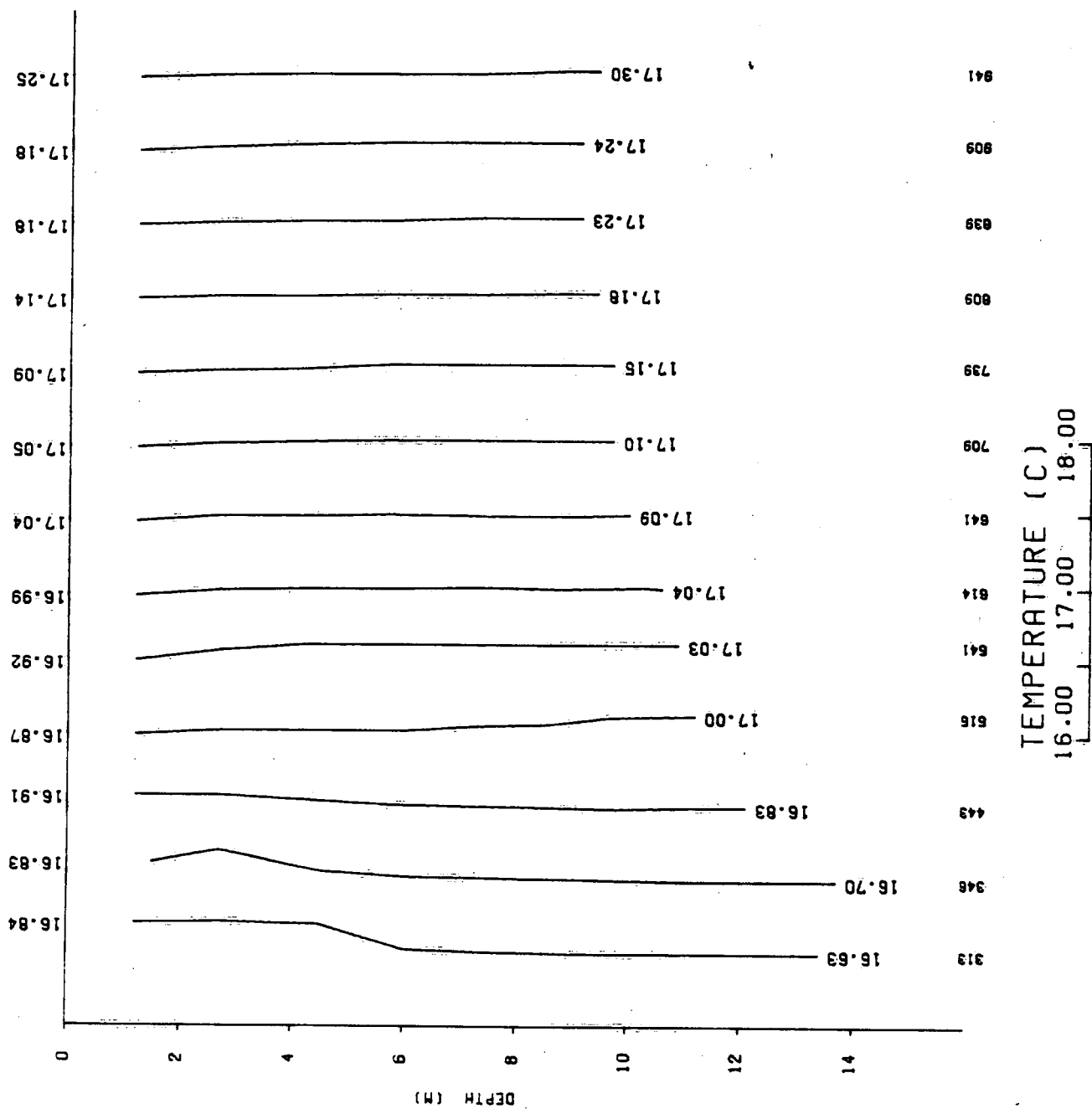


Figure B.1(a)

[illegible]

**Figure B.1(b)**



ST. LAWRENCE IN 6E100 JUNE 27 1986

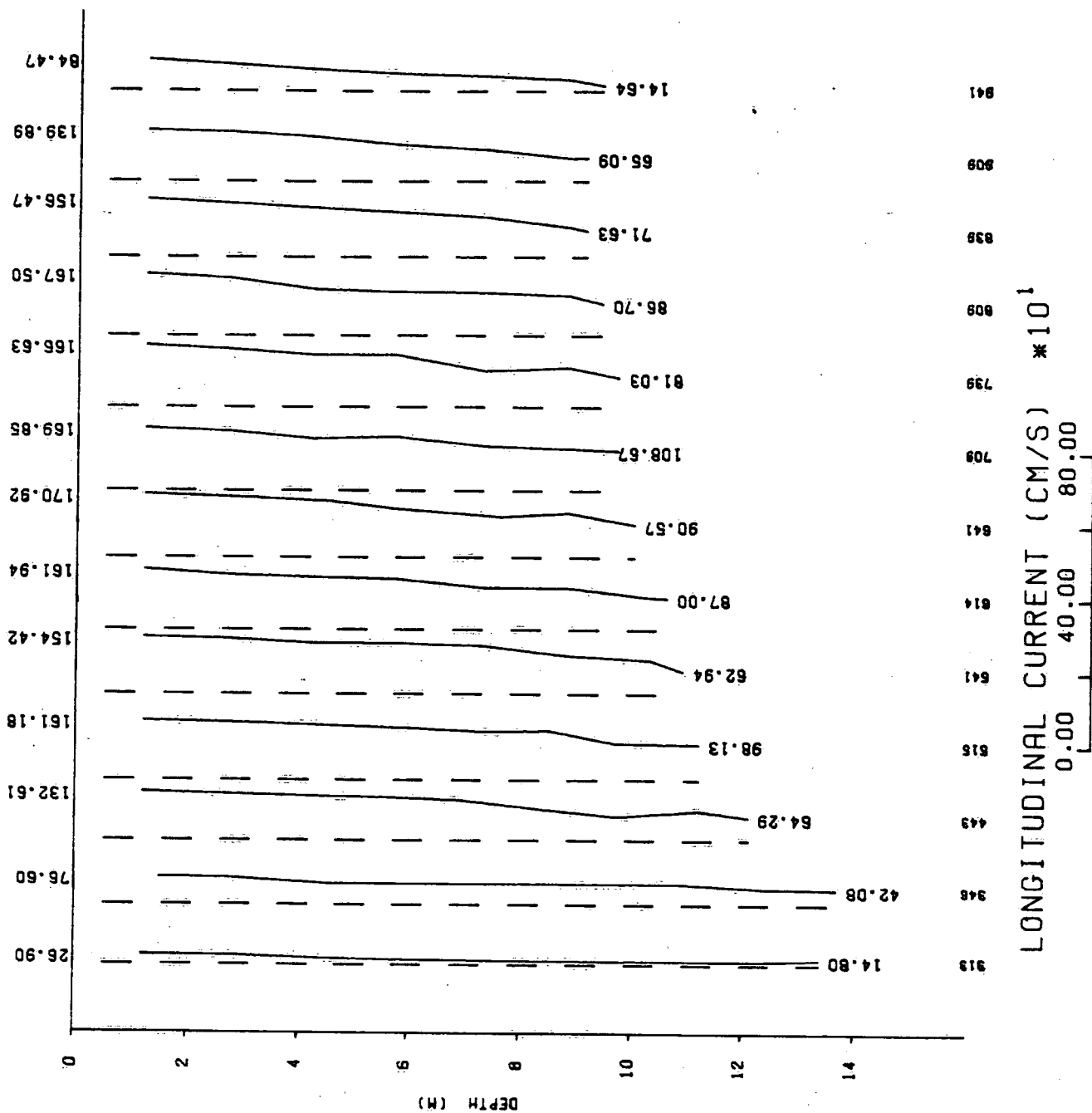


Figure B.1(c)

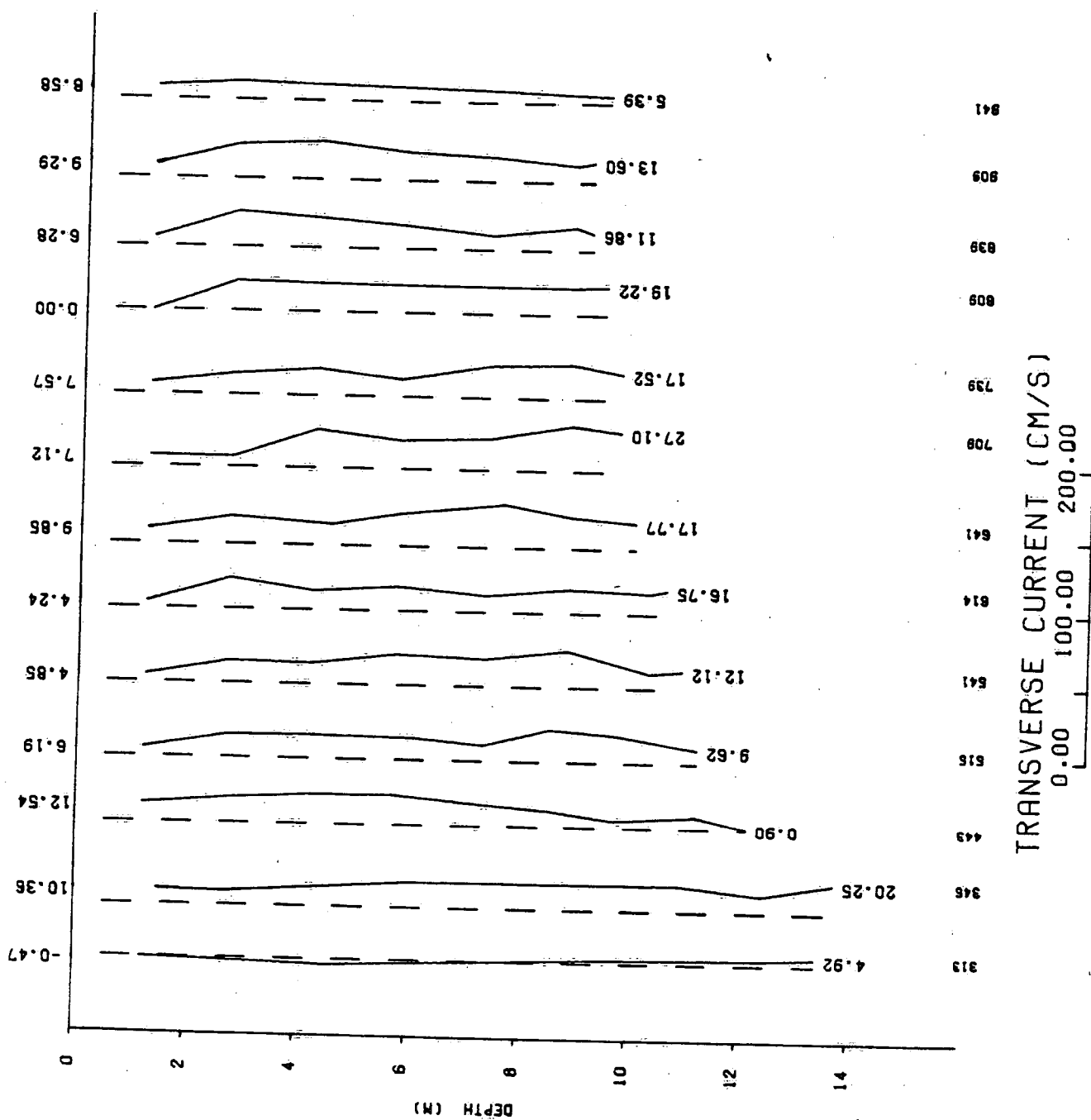


Figure B.1(d)

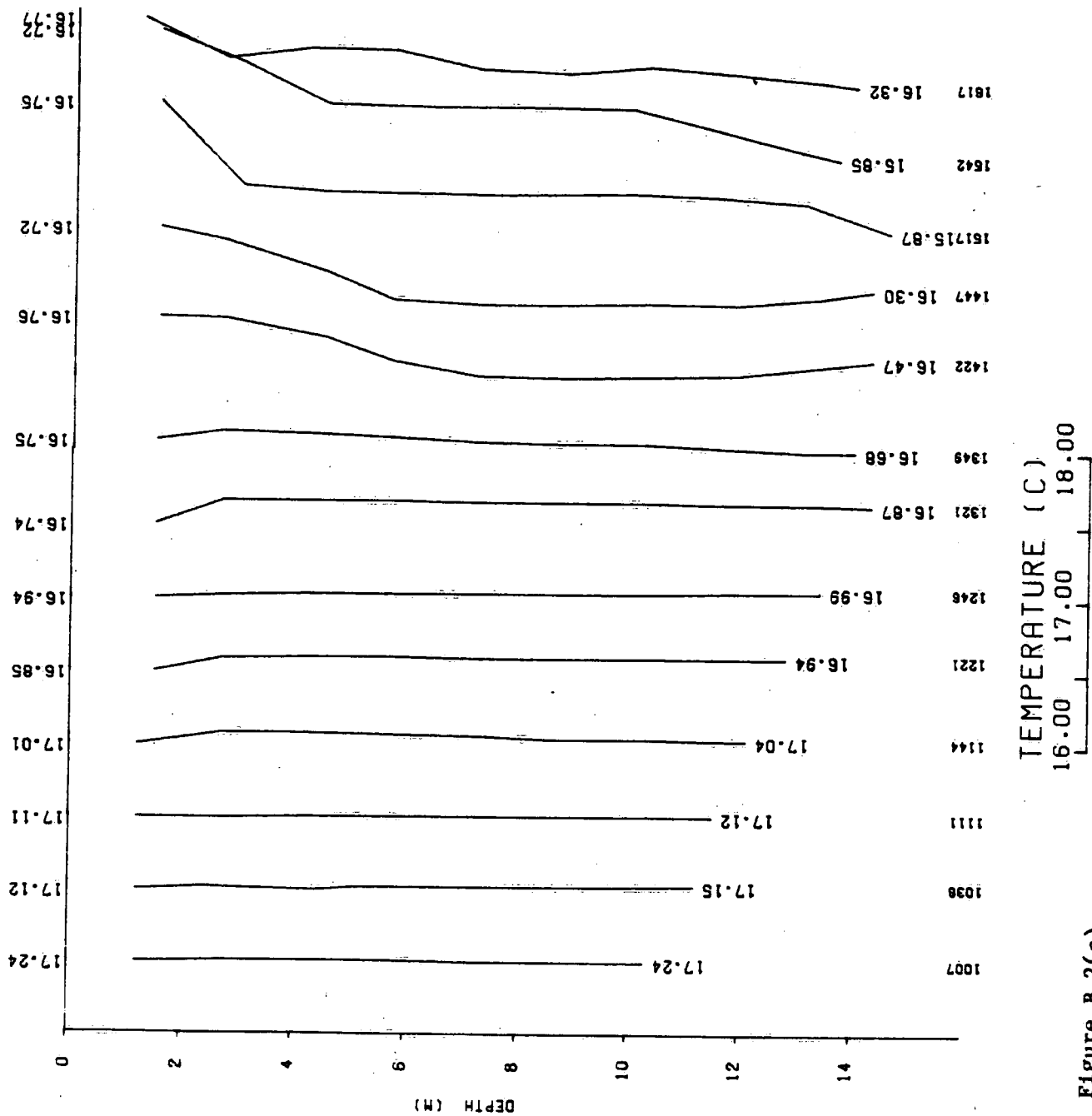


Figure B.2(a)

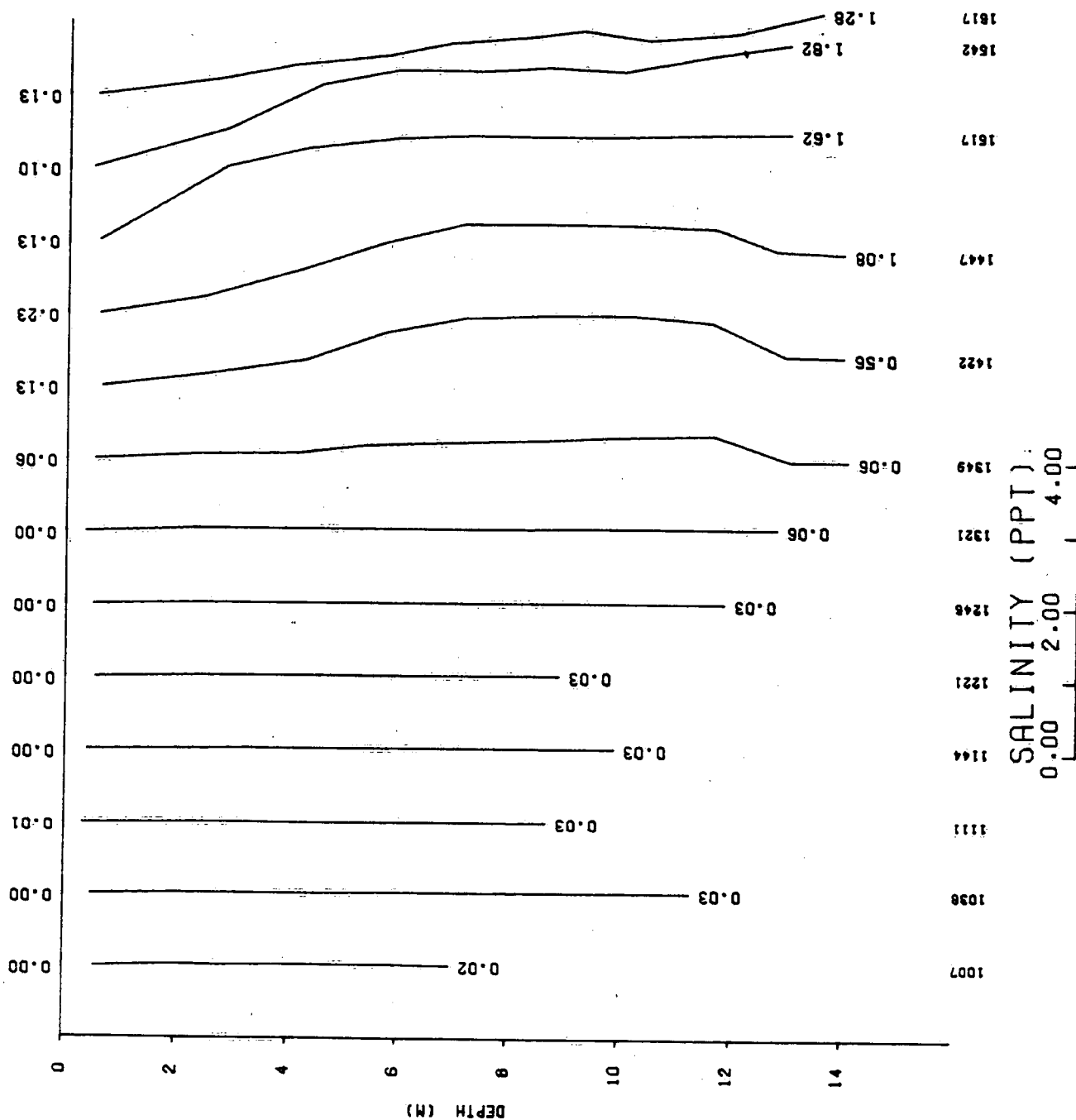


Figure B.2(b)

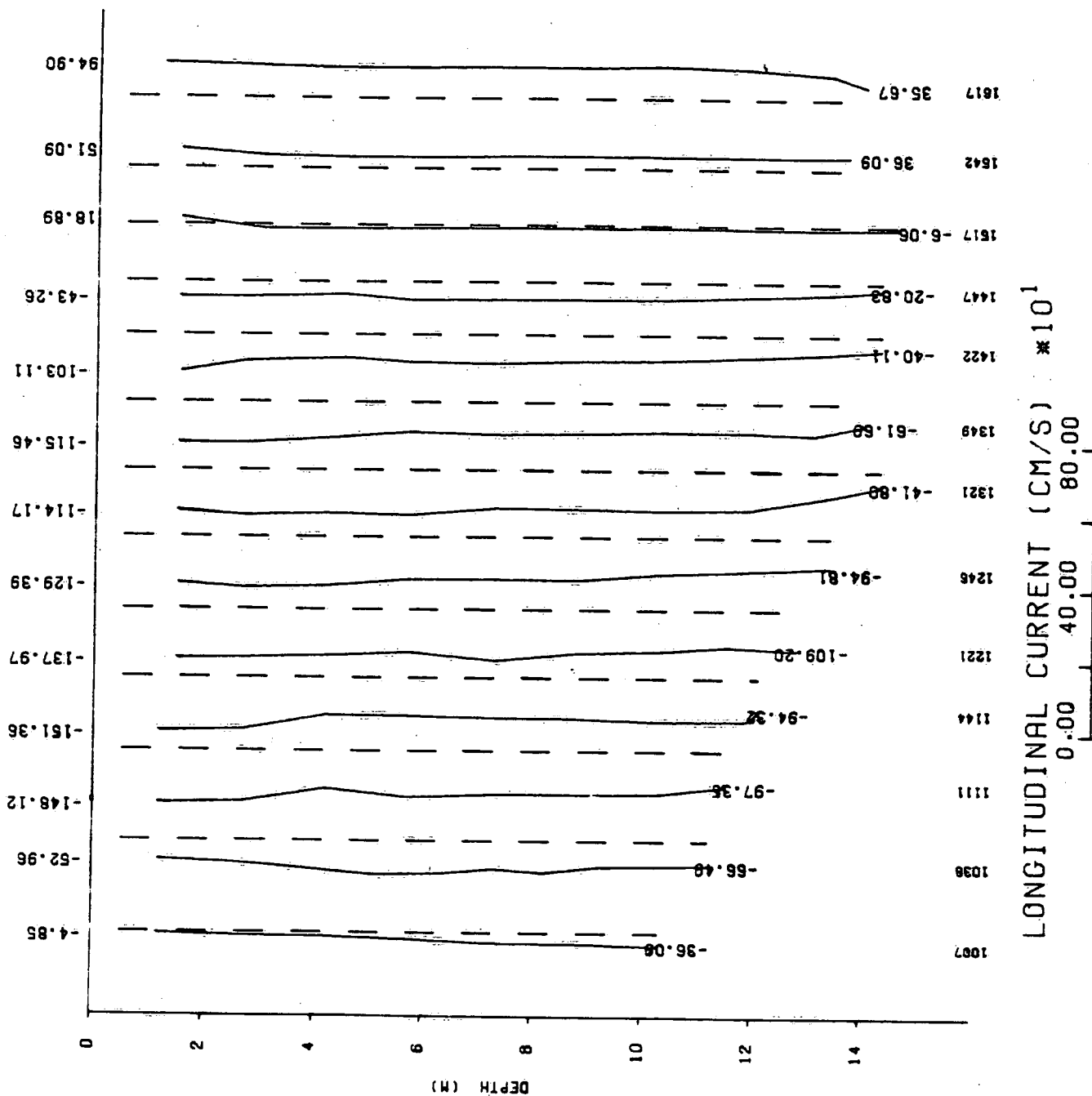


Figure B.2(c)

ST LAWRENCE S 100 JUNE 27 1986

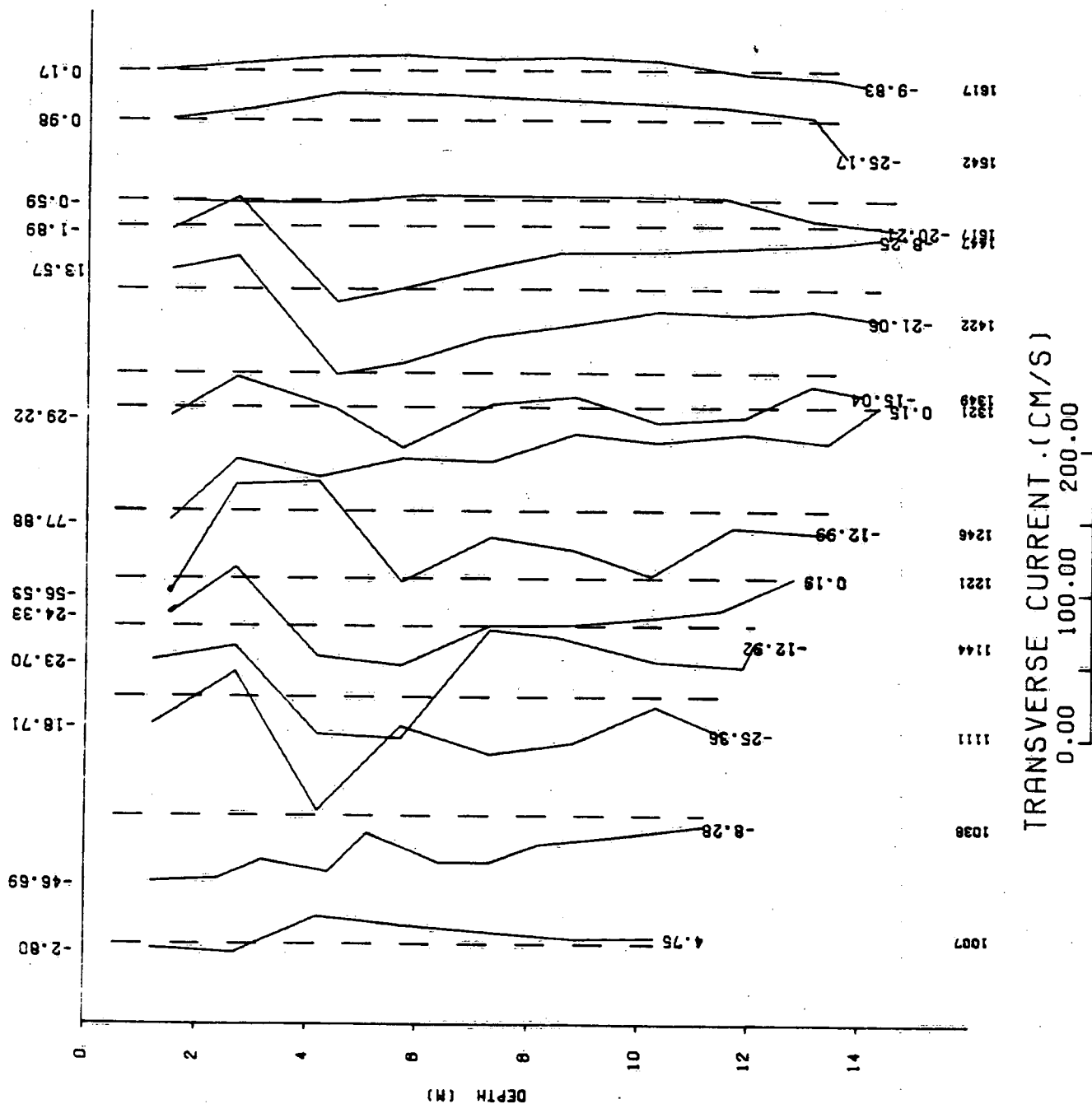


Figure B.2(d)

ST LAWRENCE TN 6E100 JUNE 27 1986

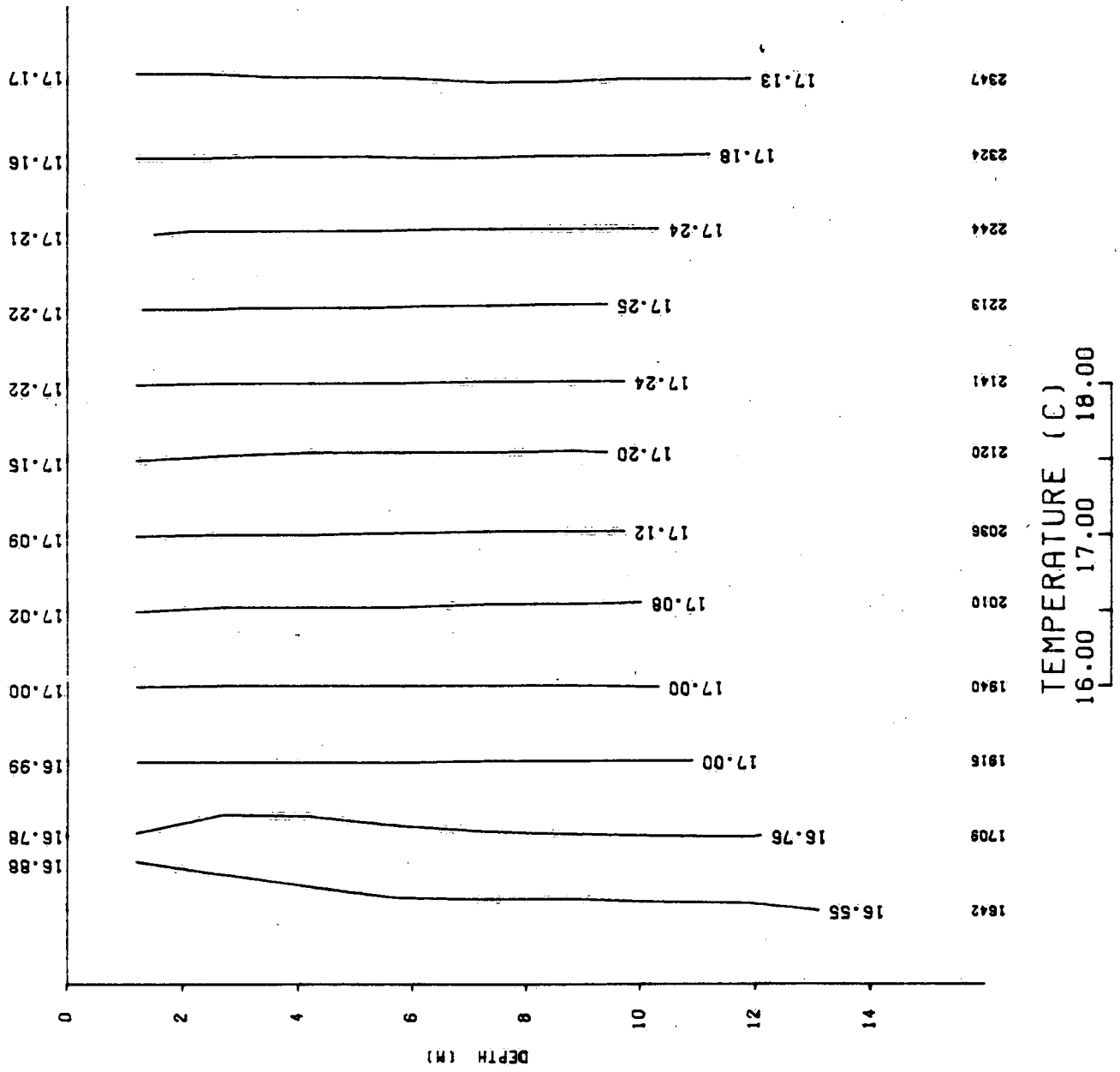


Figure B.3(a)

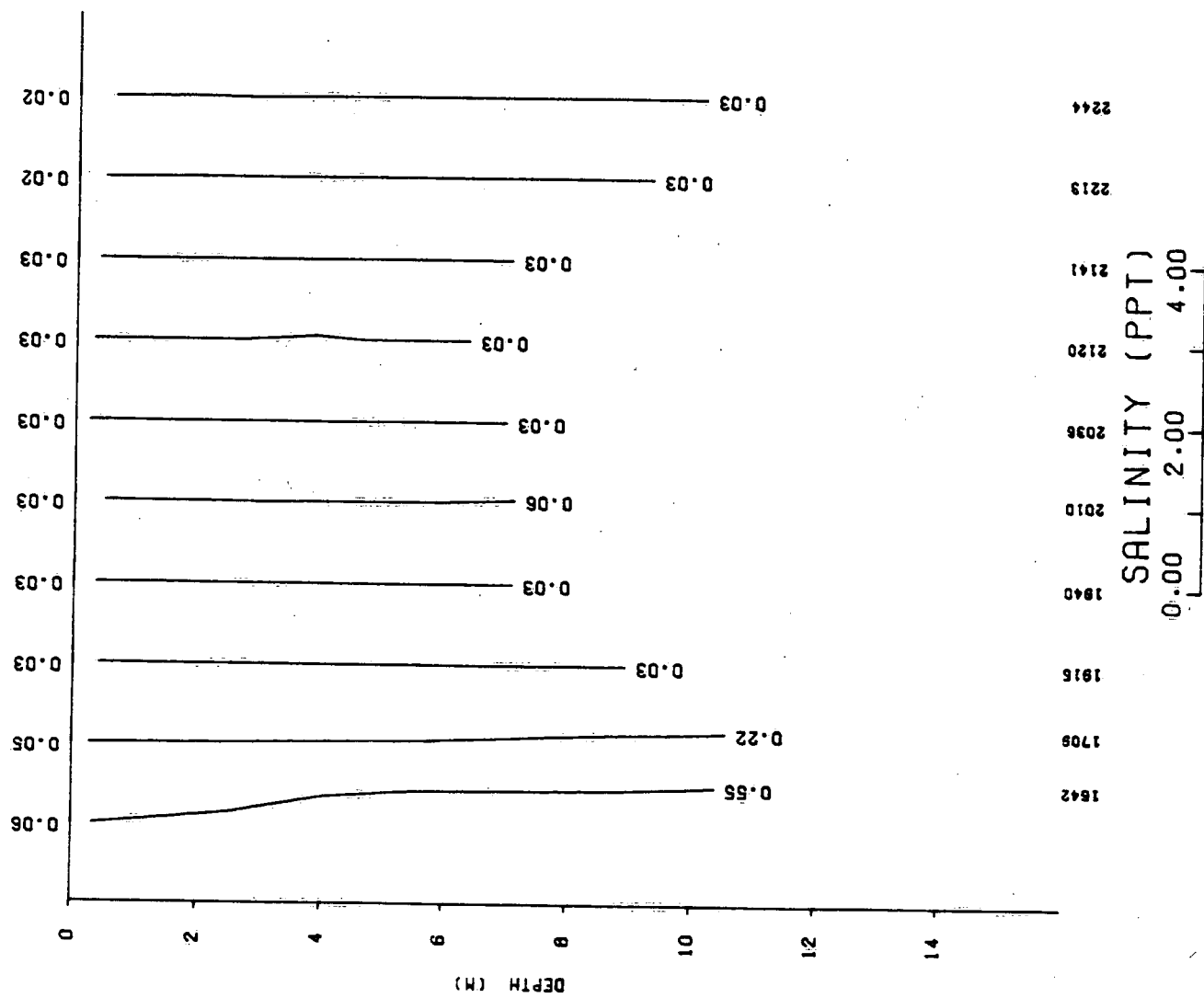


Figure B.3(b)



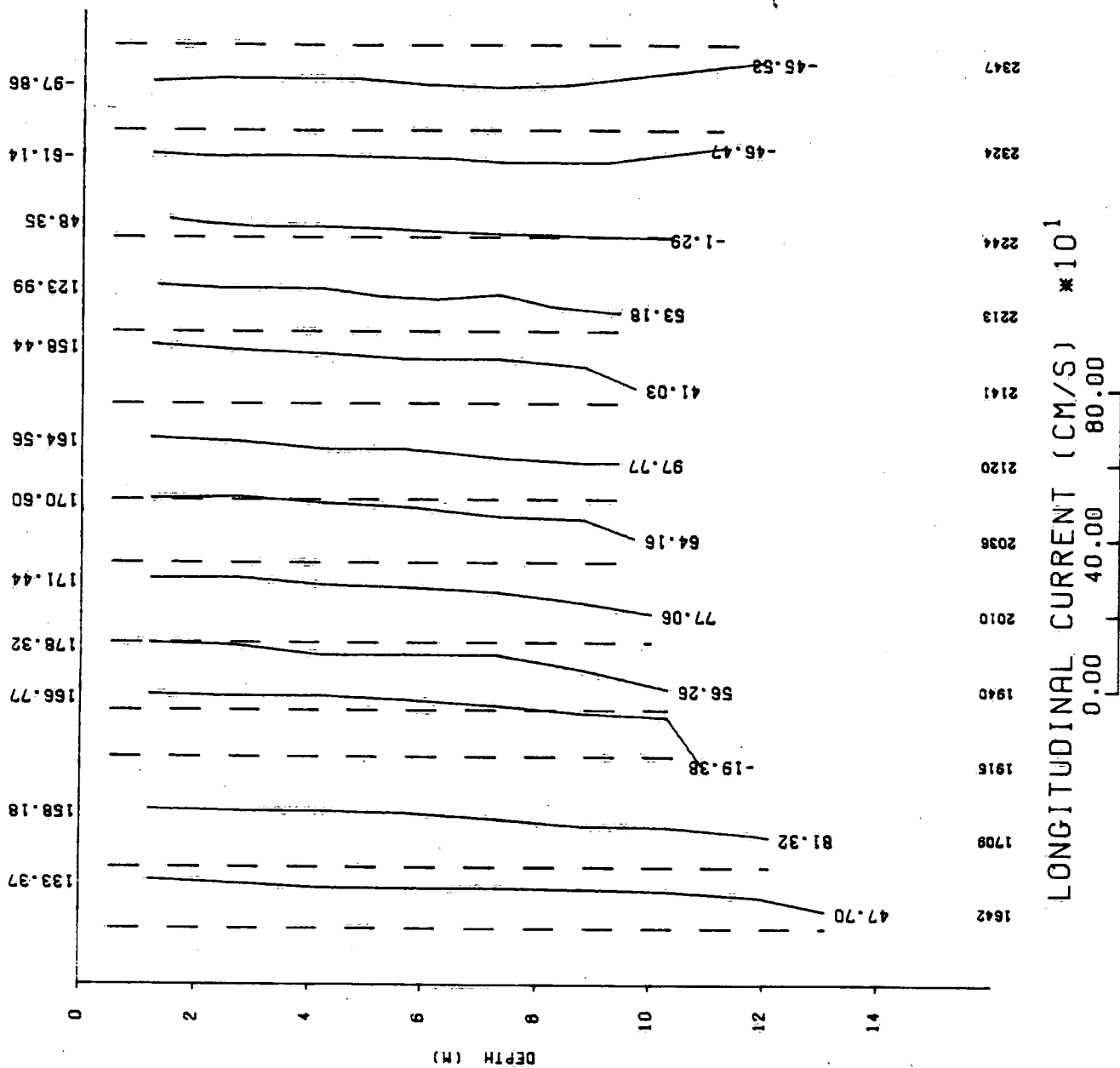


Figure B.3(c)

ST LAWRENCE ST 100 JUNE 27 1986

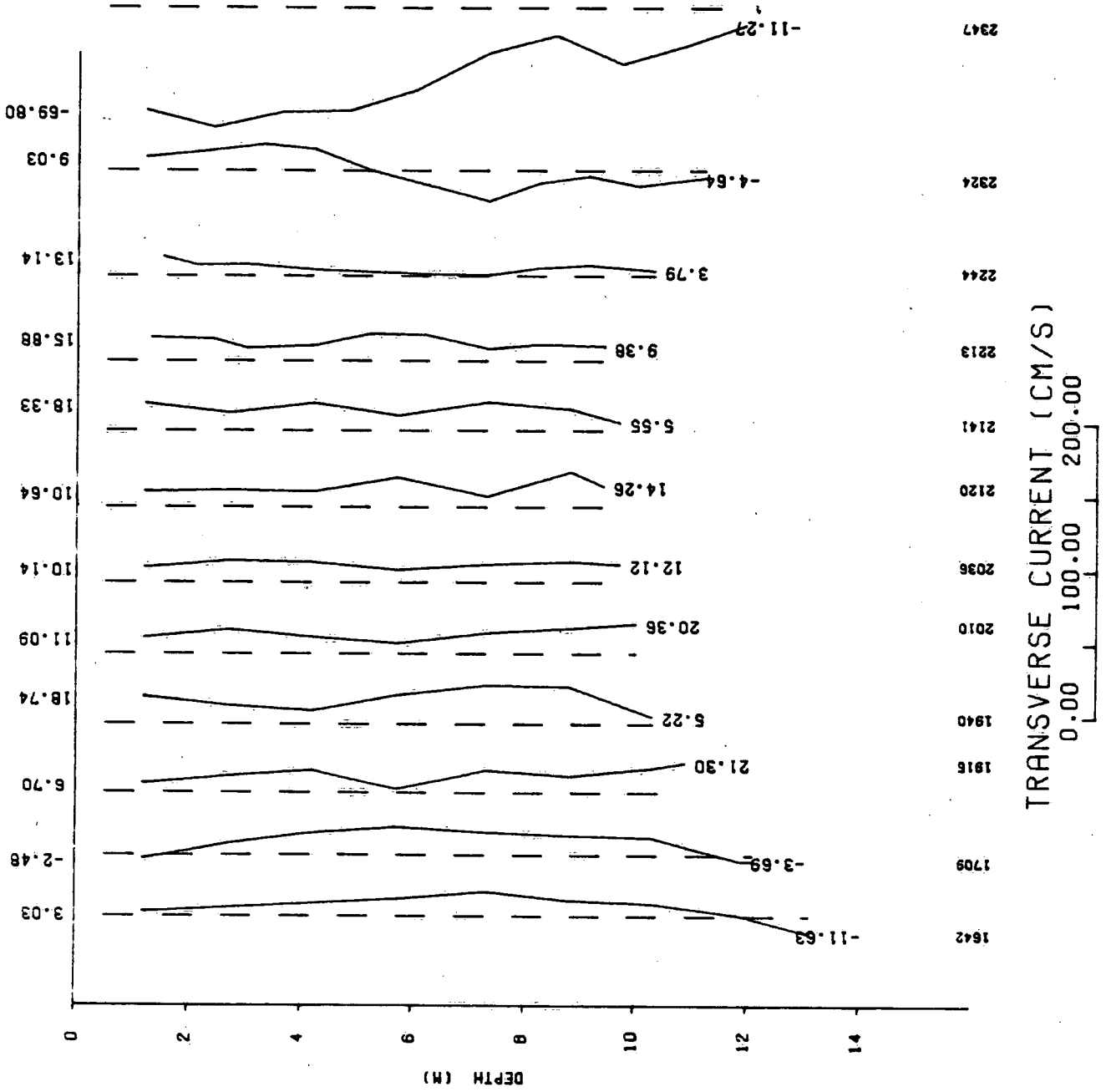


Figure B.3(d)

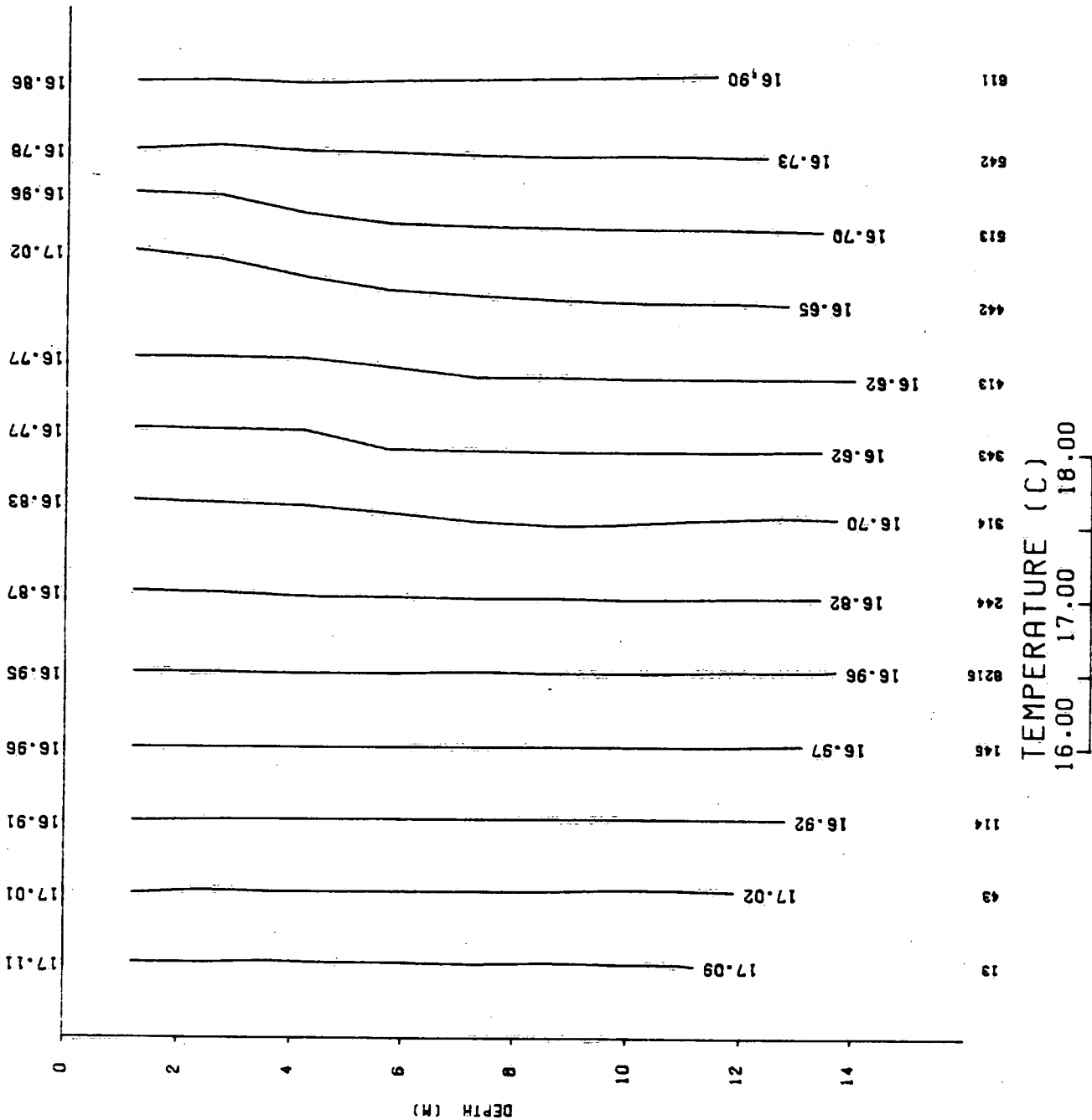


Figure B.4(a)

ST LAWRENCE 6E100 JUNE 28 1986

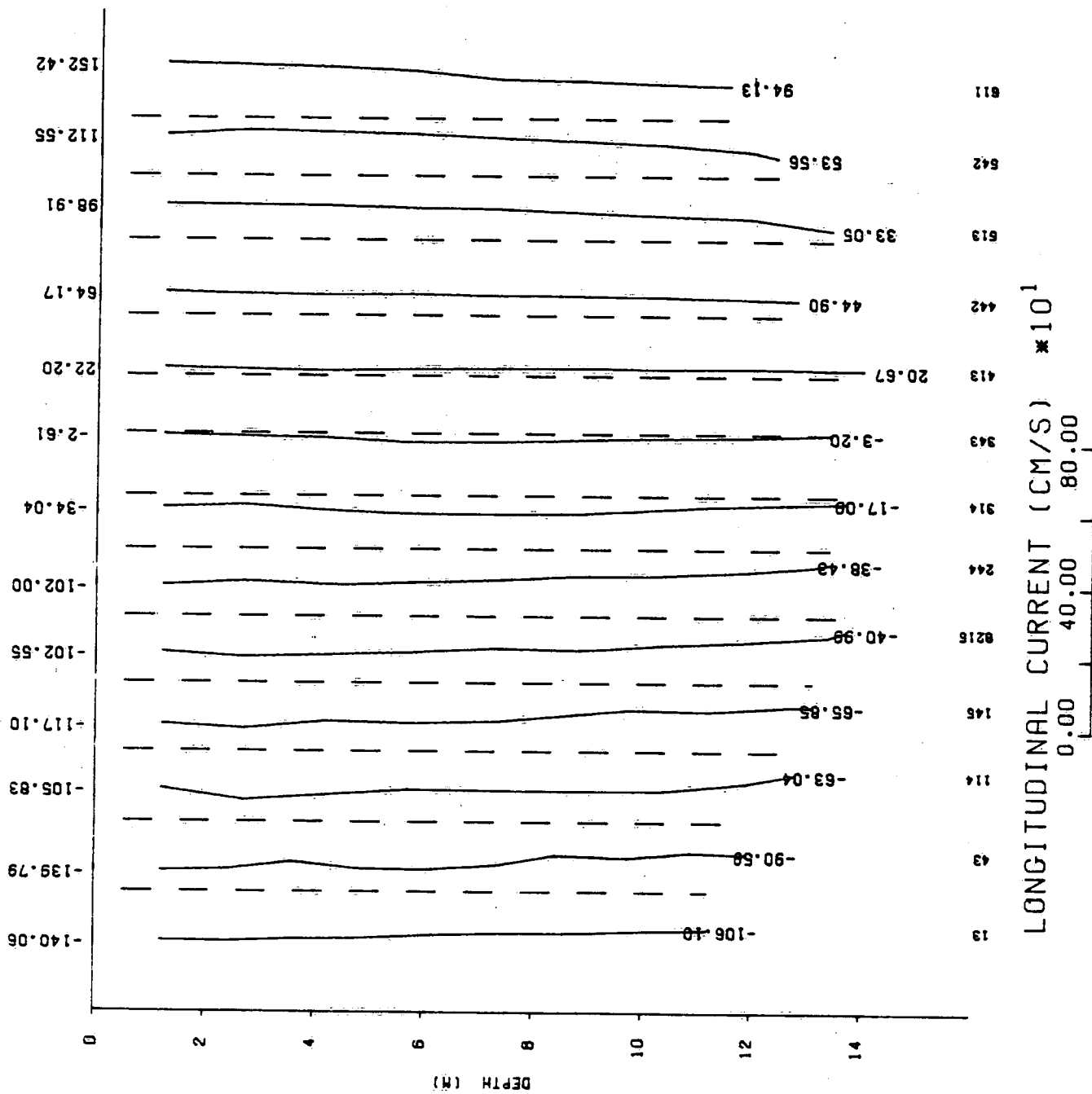


Figure B.4(b)

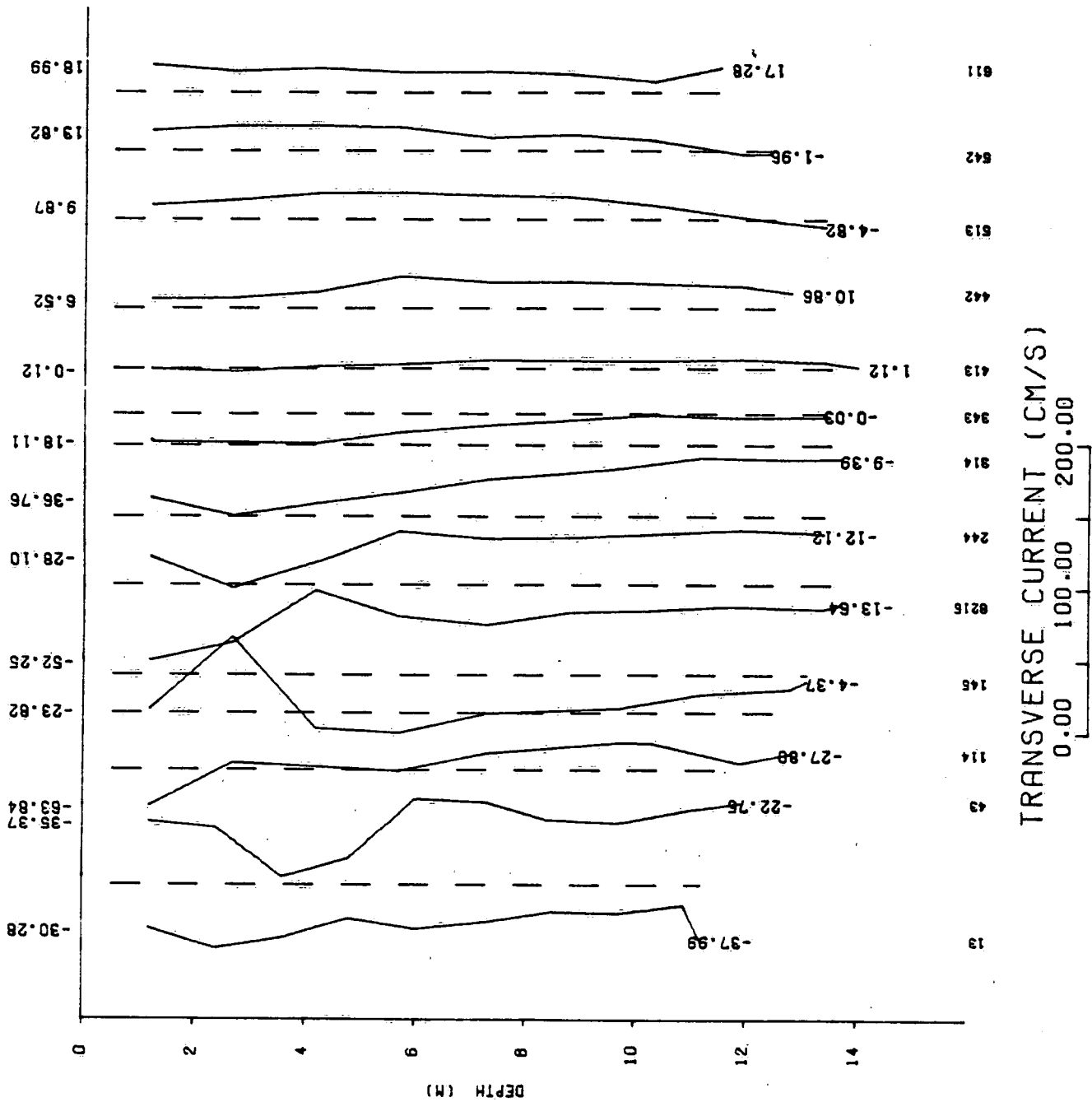


Figure B.4(c)

ST LAWRENCE STN 00 JUNE 28 1986

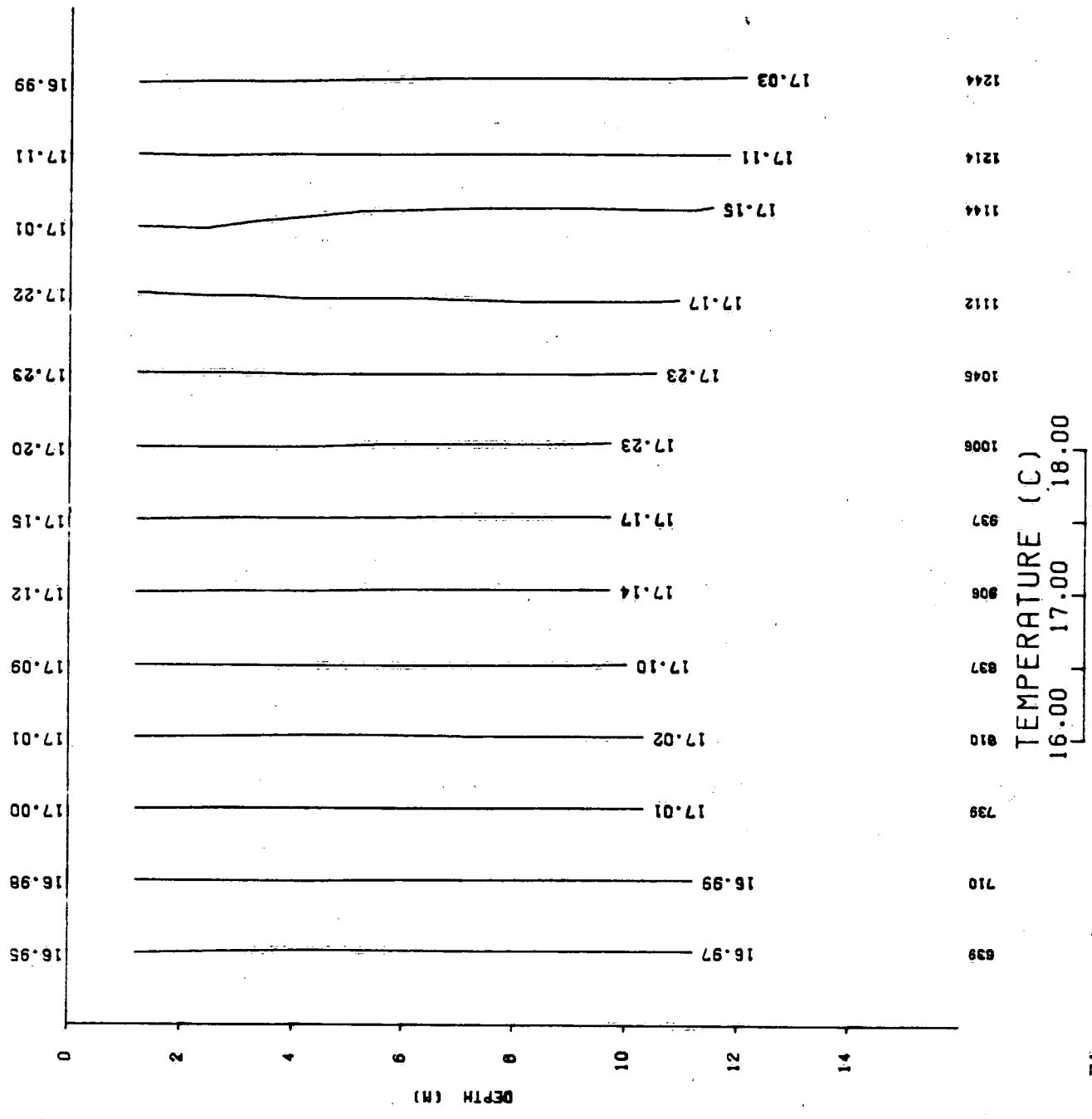


Figure B.5(a)

ST LAWRENCE STN 6E10 NE 28 1986

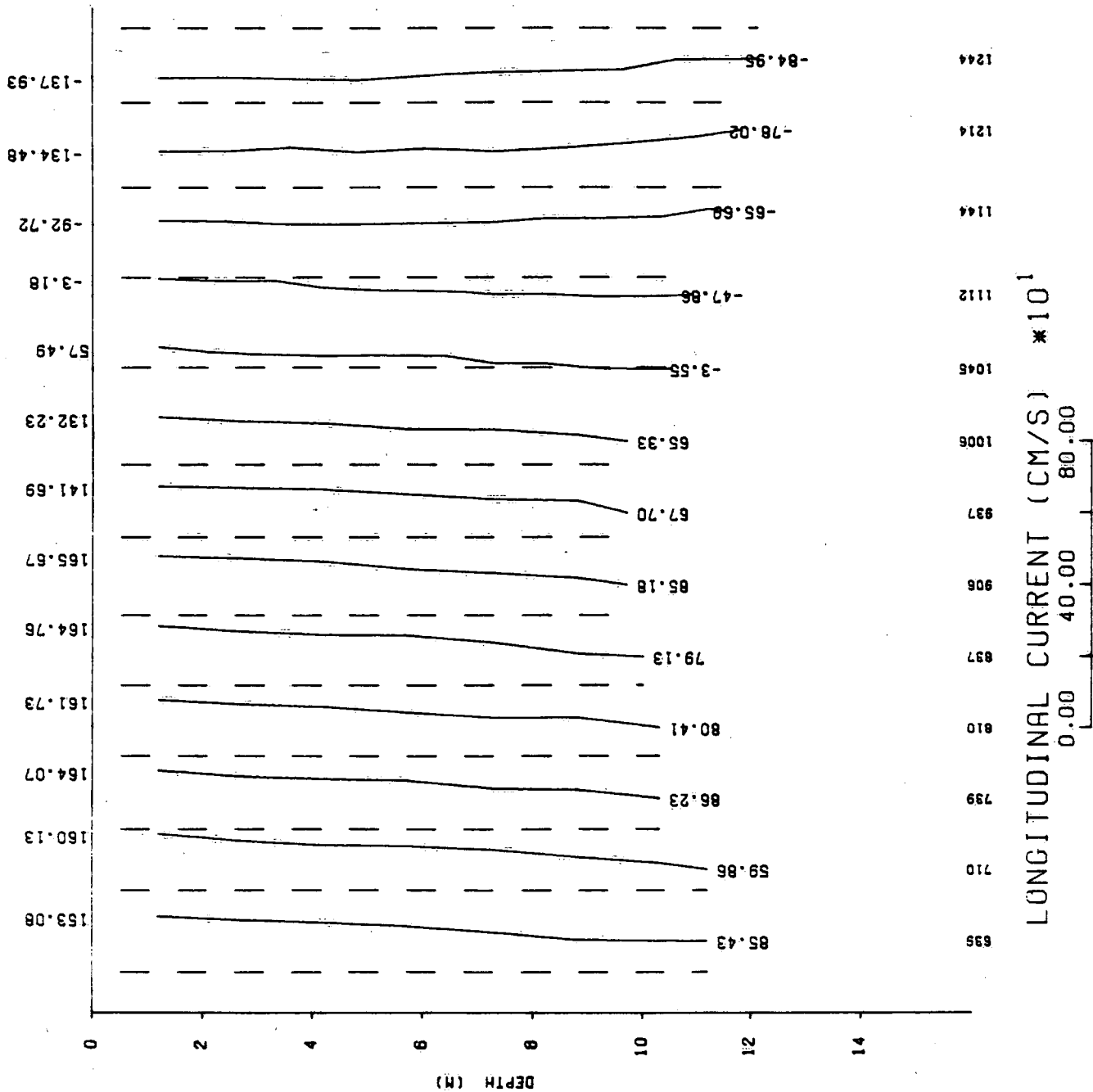


Figure B.5(b)

ST LAWRENCE STN 6E100 JUNE 28 1986

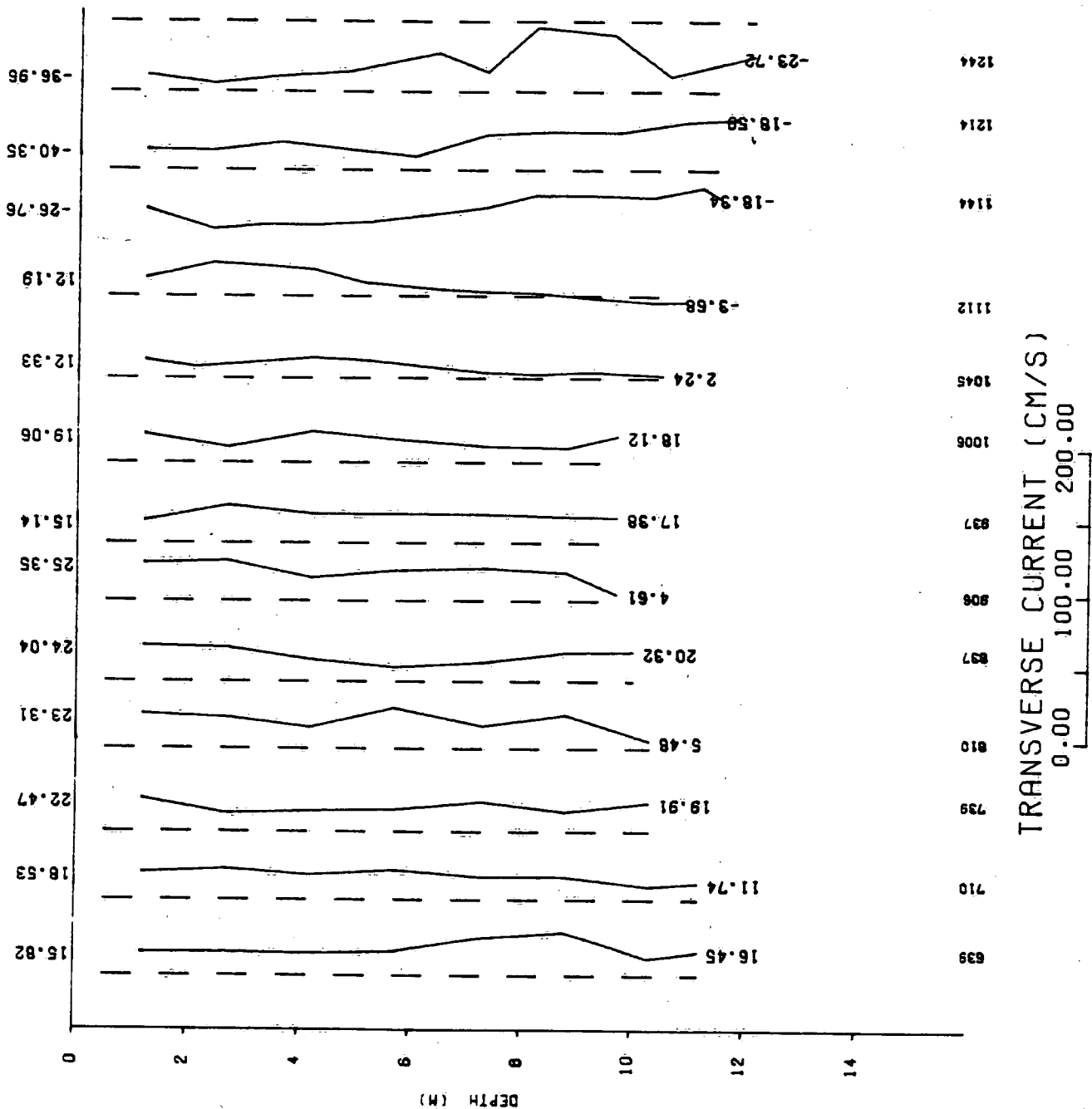


Figure B.5(c)



**APPENDIX C**

Station 6E200 Latitude N 46°42'58"  
Longitude W 71°22'42"

**List of Figure Captions**

Figure C.1. Profiles from July 3 to 4, 1986, (a) salinity, (b) suspended sediment (July 3) and (c) suspended sediment July 4.

SI LHWKLN SIN 06200 JULY 3 1986

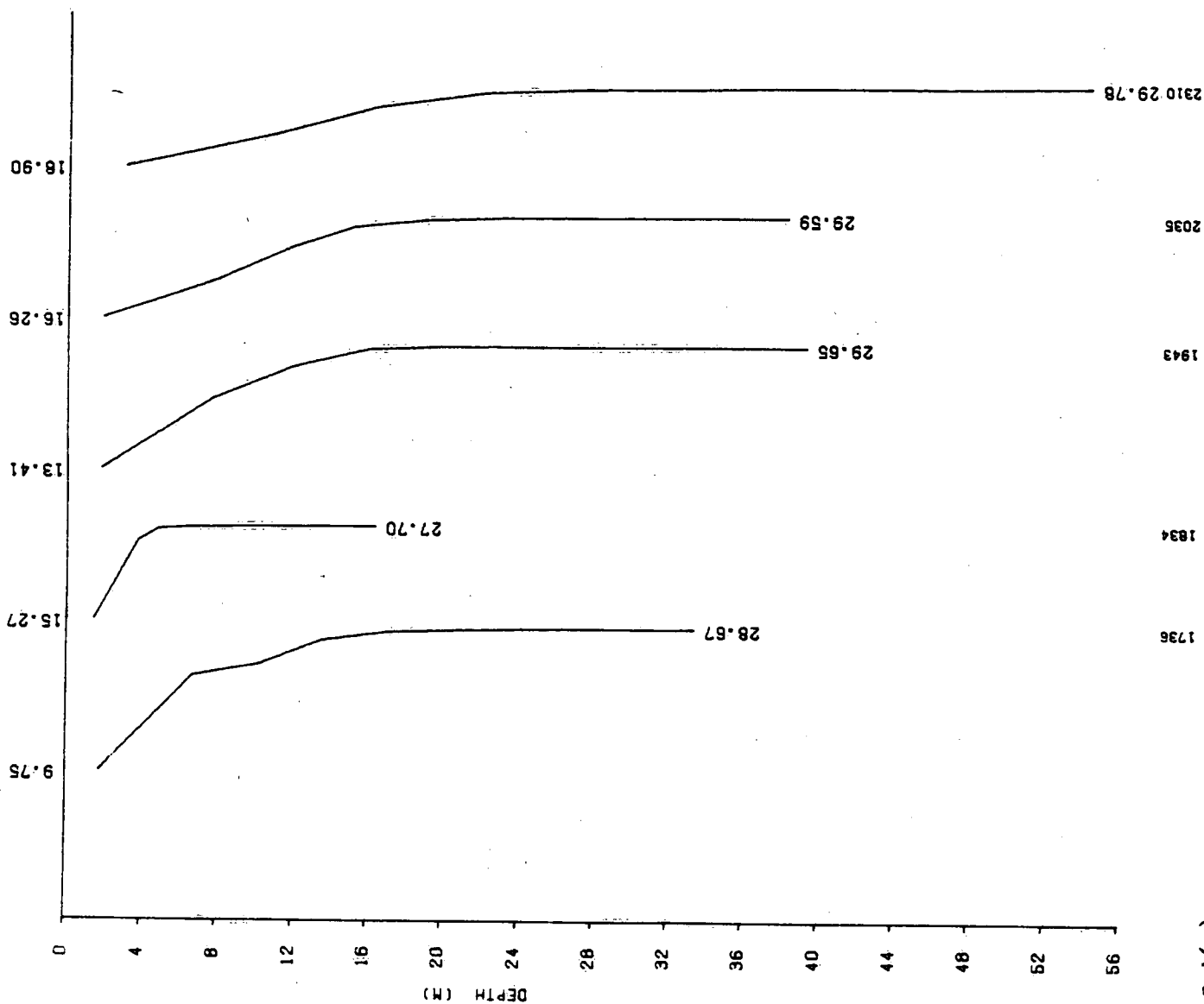


Figure C.1(a)

ST LAWRENCE STN 0200 JULY 1986

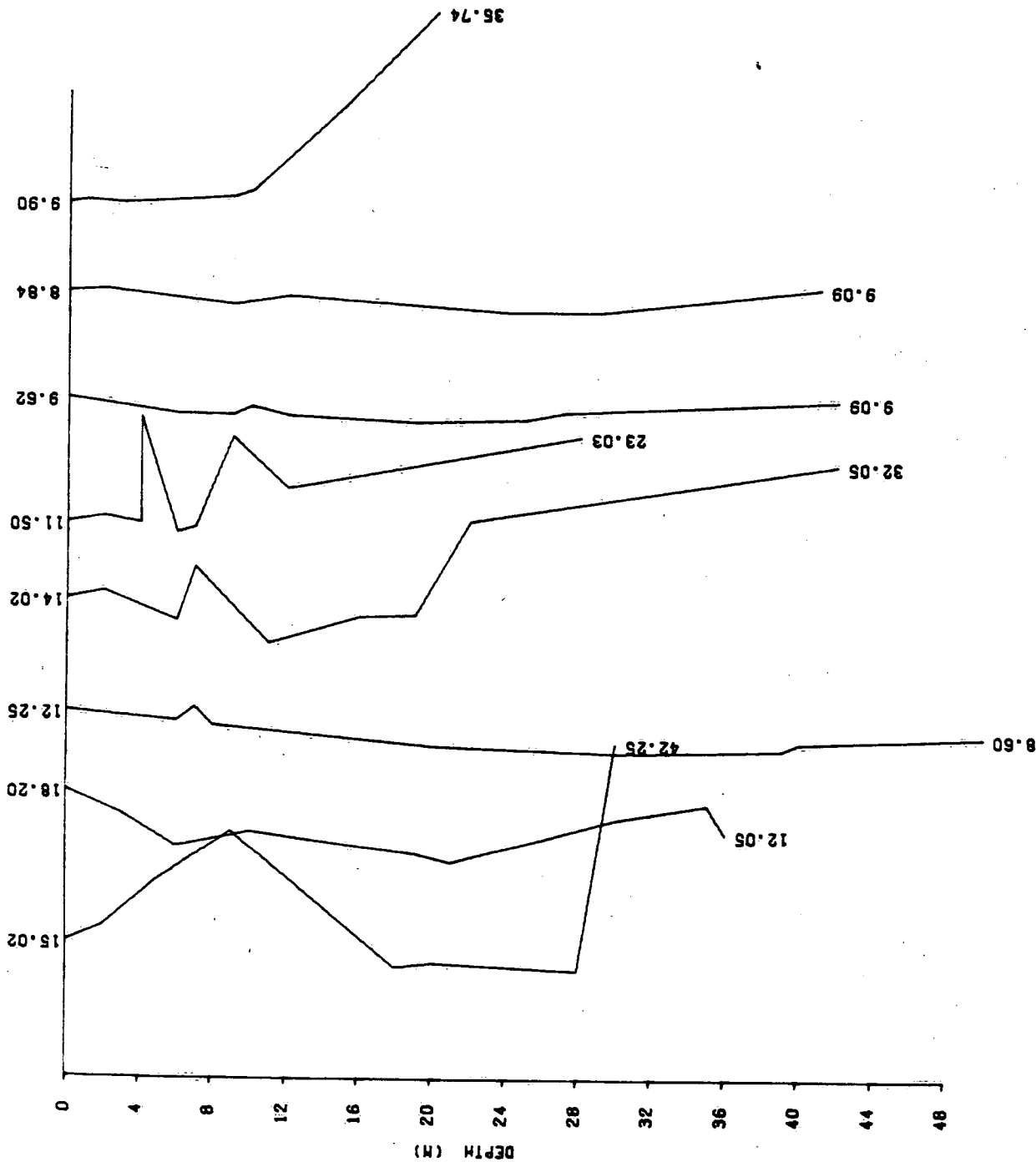


Figure C.1(b)

ST LAWRENCE STN 6E200 JULY 1986

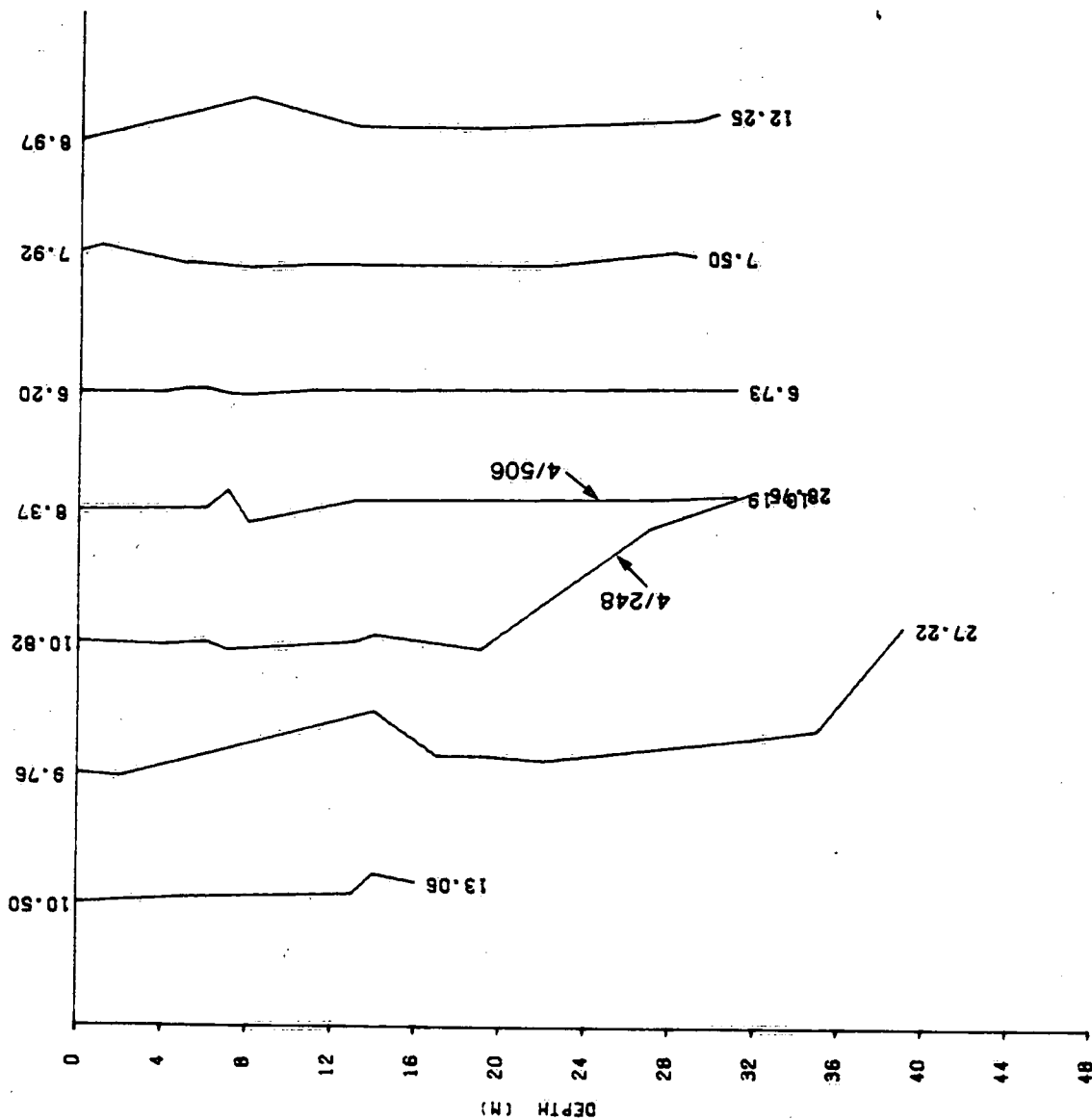


Figure C.1(c)

**APPENDIX D**

Station 6E300 Latitude N 47° 29'19"

Longitude W 70° 04'47"

List of Figure Captions

Figure D.1. Profiles from 23:06, June 28, to 06:10 June 29, 1986 (GMT) of (a) temperature, (b) salinity, (c) along-channel flow and (d) cross-channel flow (positive to SE).

Figure D.2. Profiles from 5:41 to 11:41 June 29, 1986 (GMT) of (a) temperature, (b) salinity, (c) along-channel flow and (d) across-channel flow (positive to SE).

Figure D.3. Profiles from 12:12 to 18:10, June 29, 1986 (GMT) of (a) temperature, (b) salinity, (c) along-channel flow and (d) across channel flow (positive to SE).

Figure D.4. Profiles from 18:40 to 23:42, June 29, 1986 (GMT) of (a) temperature, (b) salinity, (c) along-channel flow and (d) across-channel flow (positive to SE).

Figure D.5. Profiles from 00:09 to 05:40, June 30, 1986 (GMT) of (a) temperature, (b) along-channel flow, and (c) and transverse flow.

Figure D.6. Profiles of suspended sediments (a) from 19:42, June 28 to 07:00, June 29, 1986, (b) from 09:00 to 20:00 June 29, 1986 and (c) from 21:00 June 29 to 06:00 June 30, 1986.

ST LAWRENCE STN 6E3 JUNE 29 1986

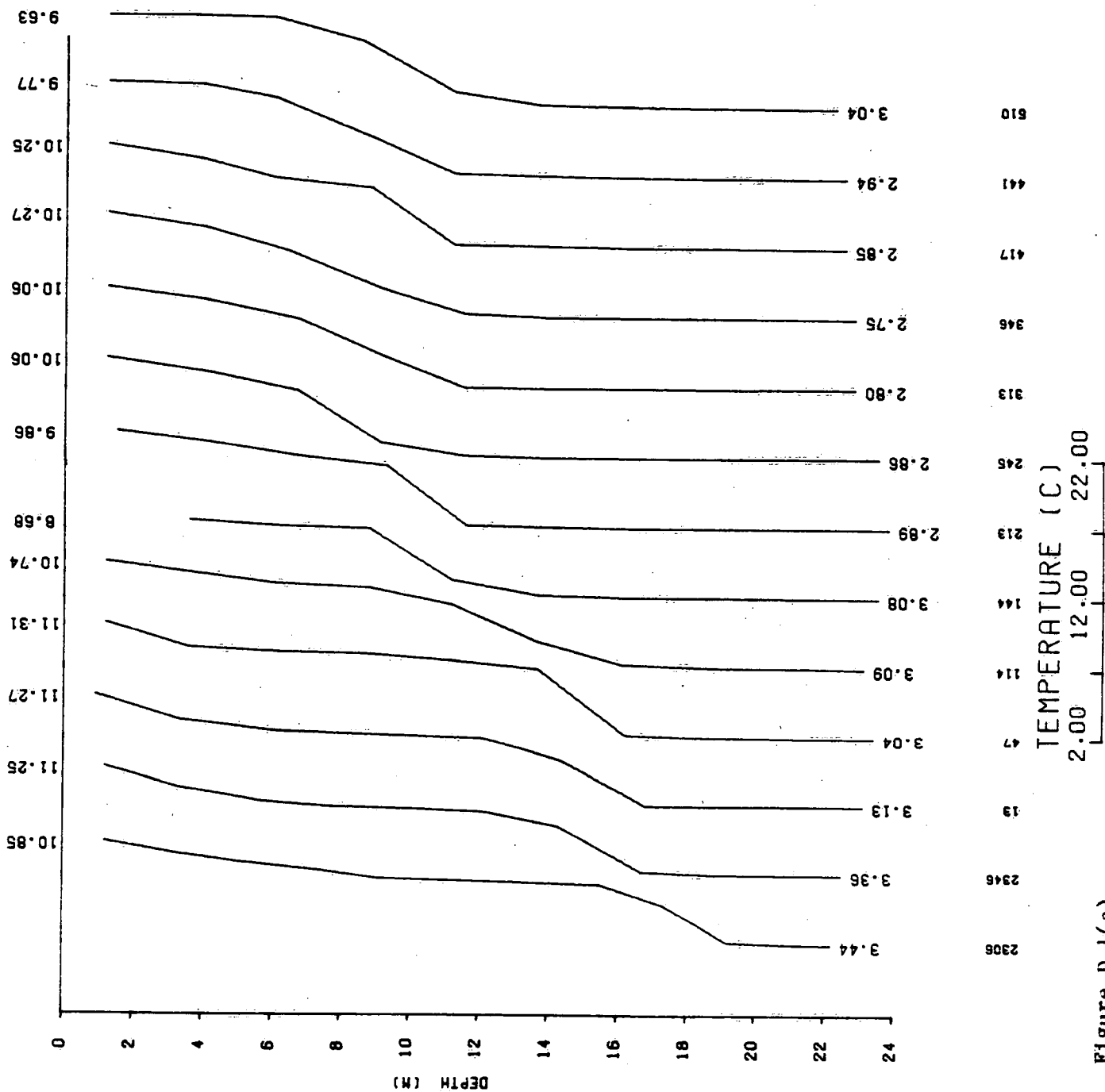


Figure D.1(a)

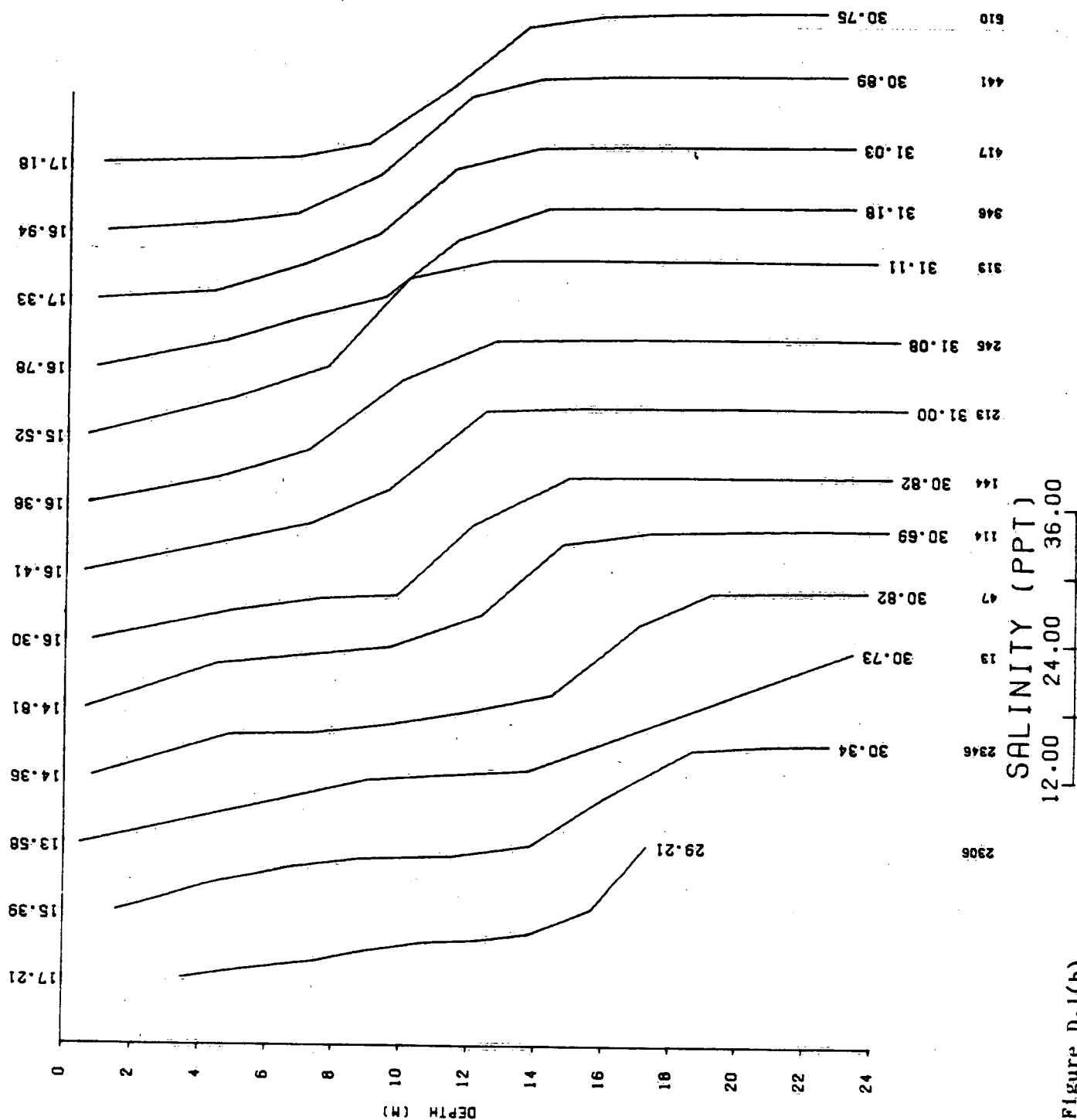


Figure D.1(b)



ST LAWRENCE ST 800 JUNE 29 1986

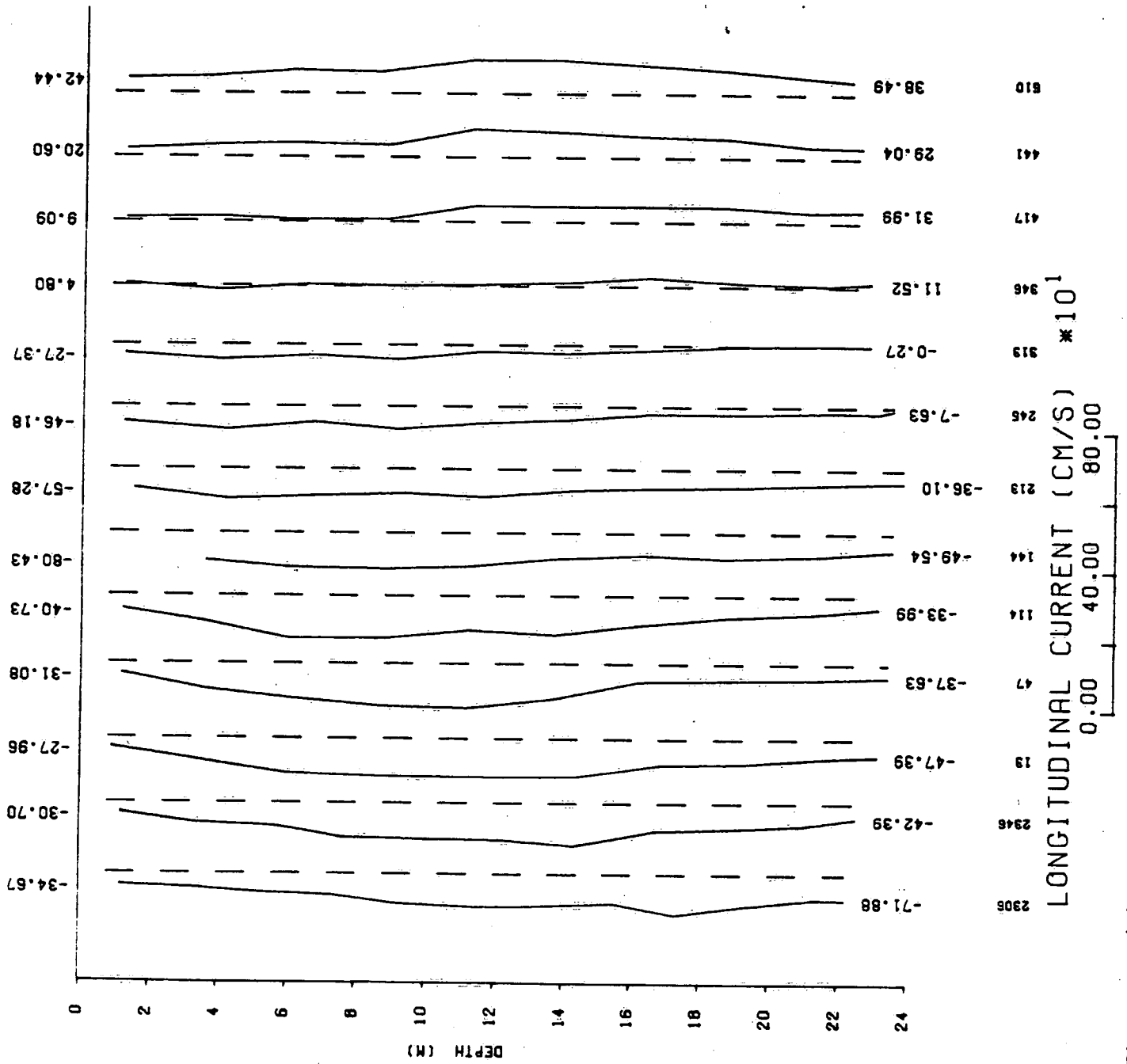


Figure D.1(c)

ST LAWRENCE STN 6E30 NE 29 1986

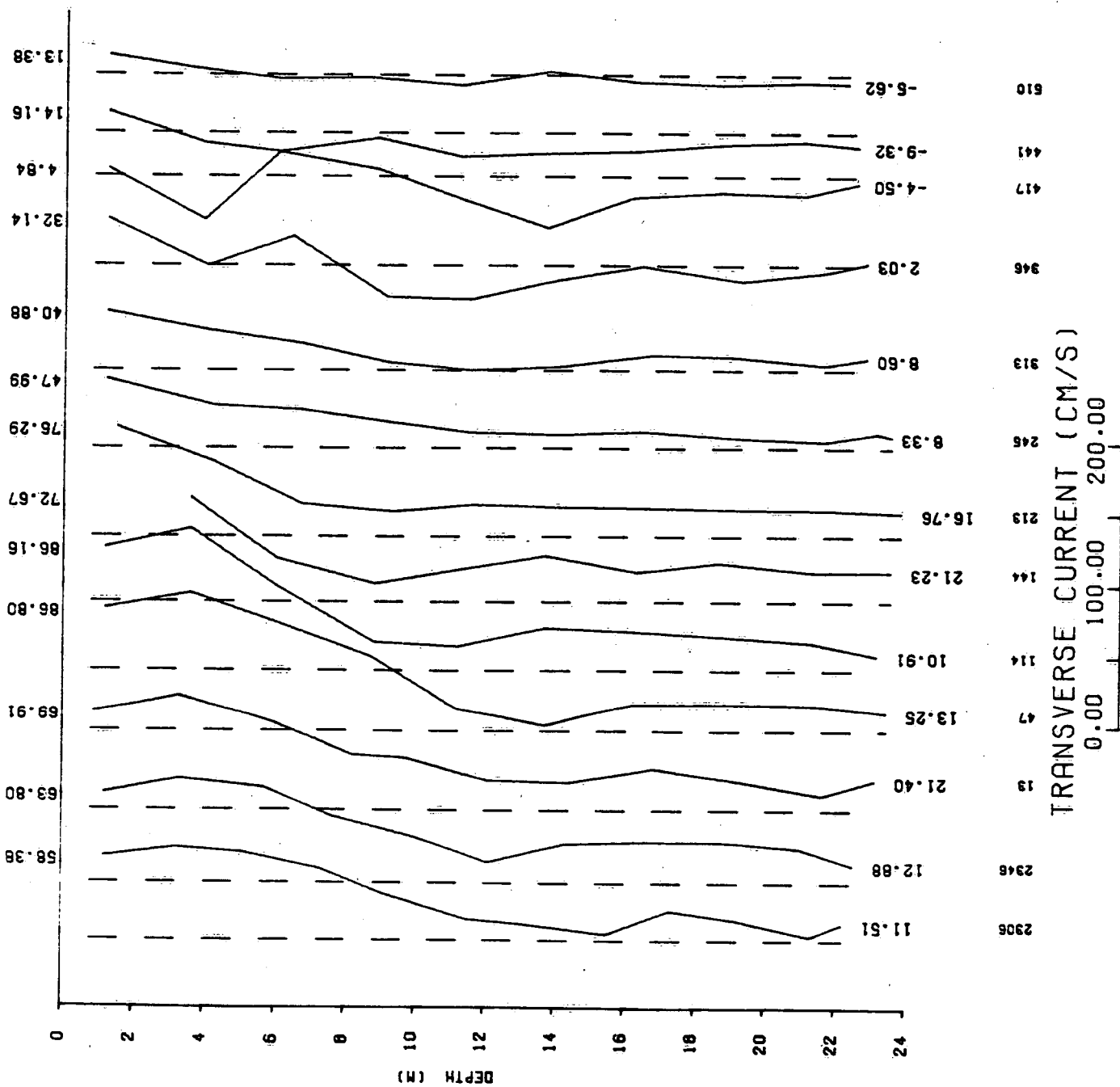


Figure D.1(d)

ST LAWRENCE STN 6E300 JUL 9 1986

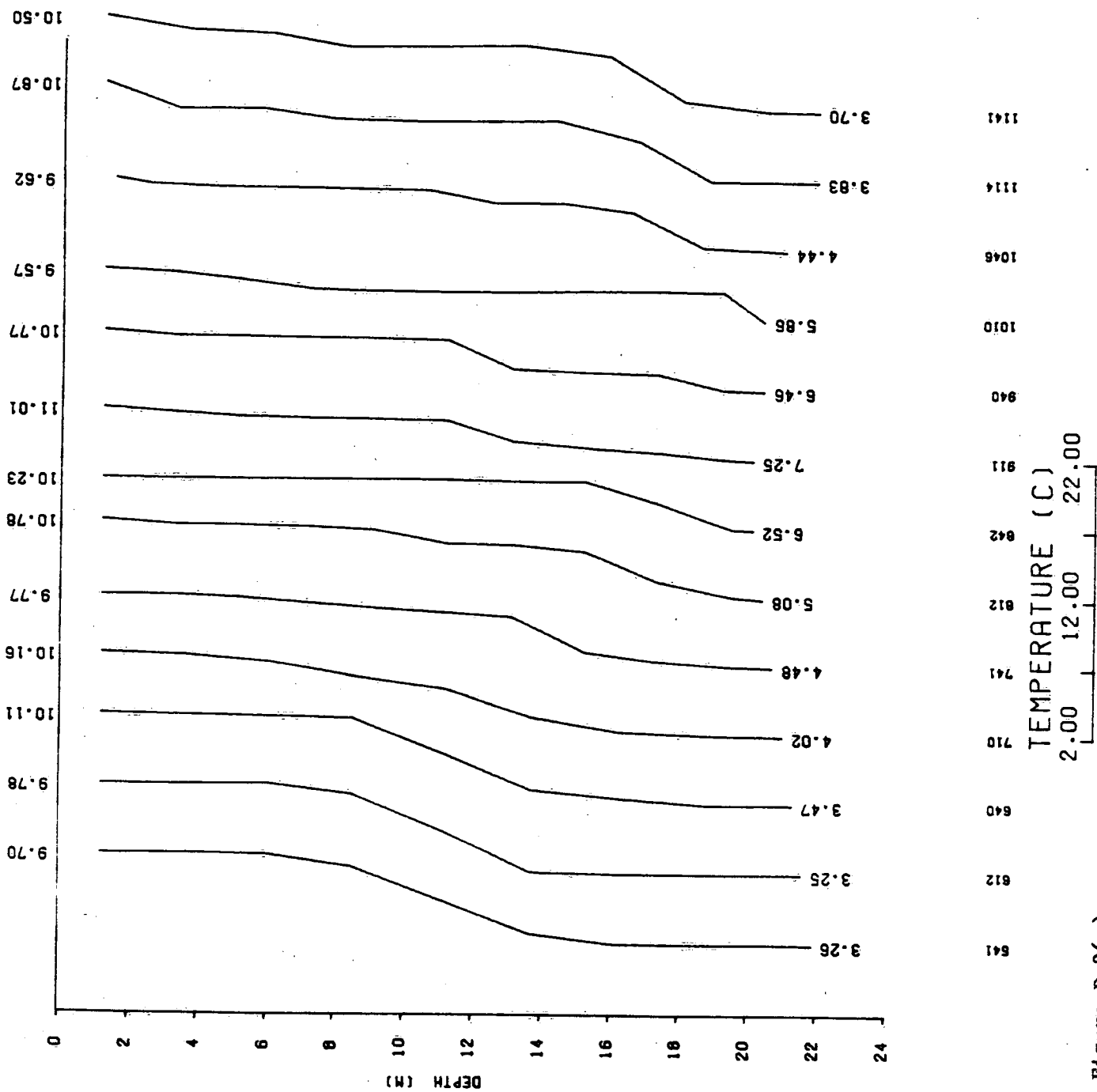


Figure D.2(a)

ST LAWRENCE STN 60 JUNE 29 1986

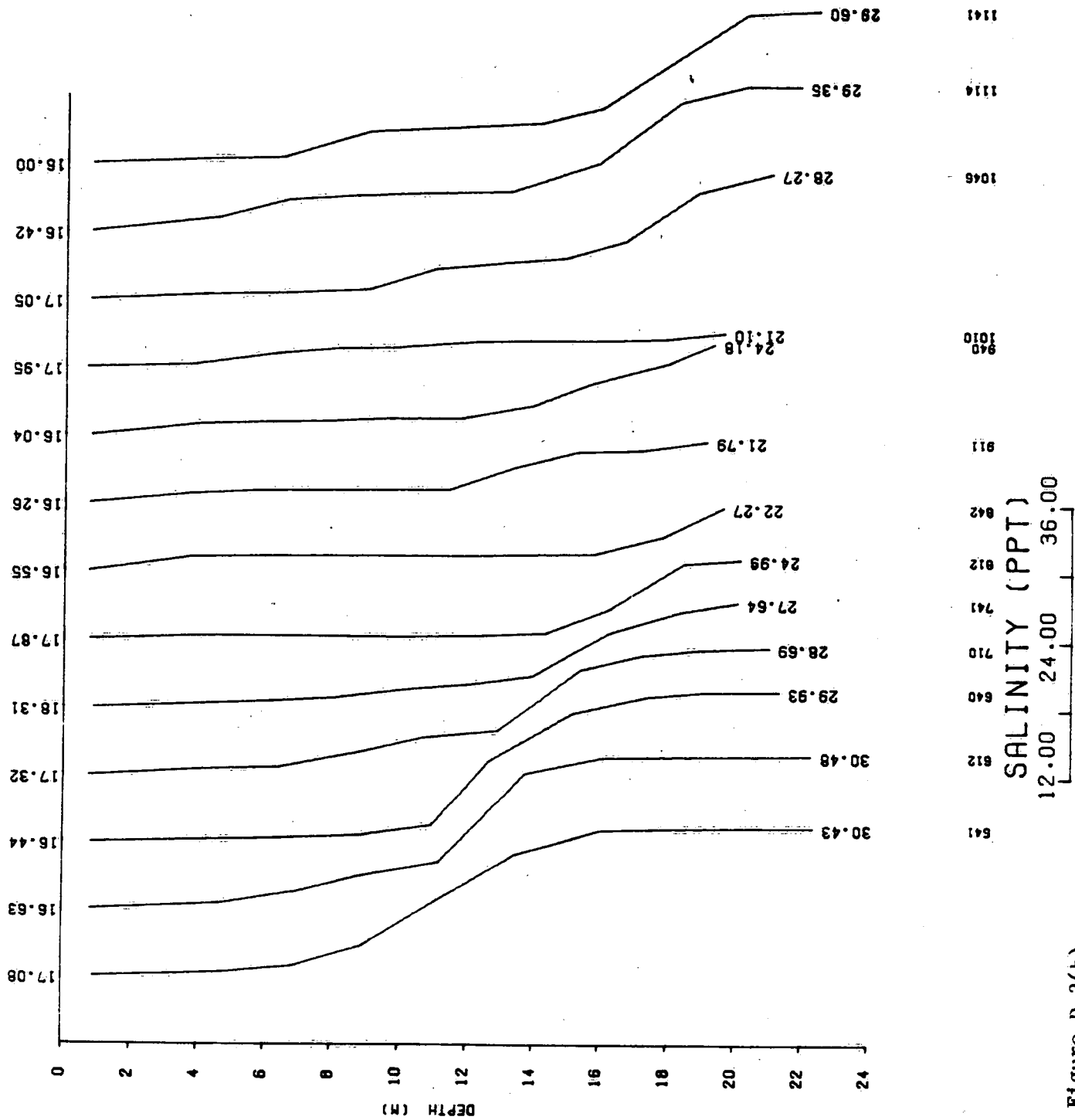


Figure D.2(b)

ST LAWRENCE STN 000 JUNE 29 1986

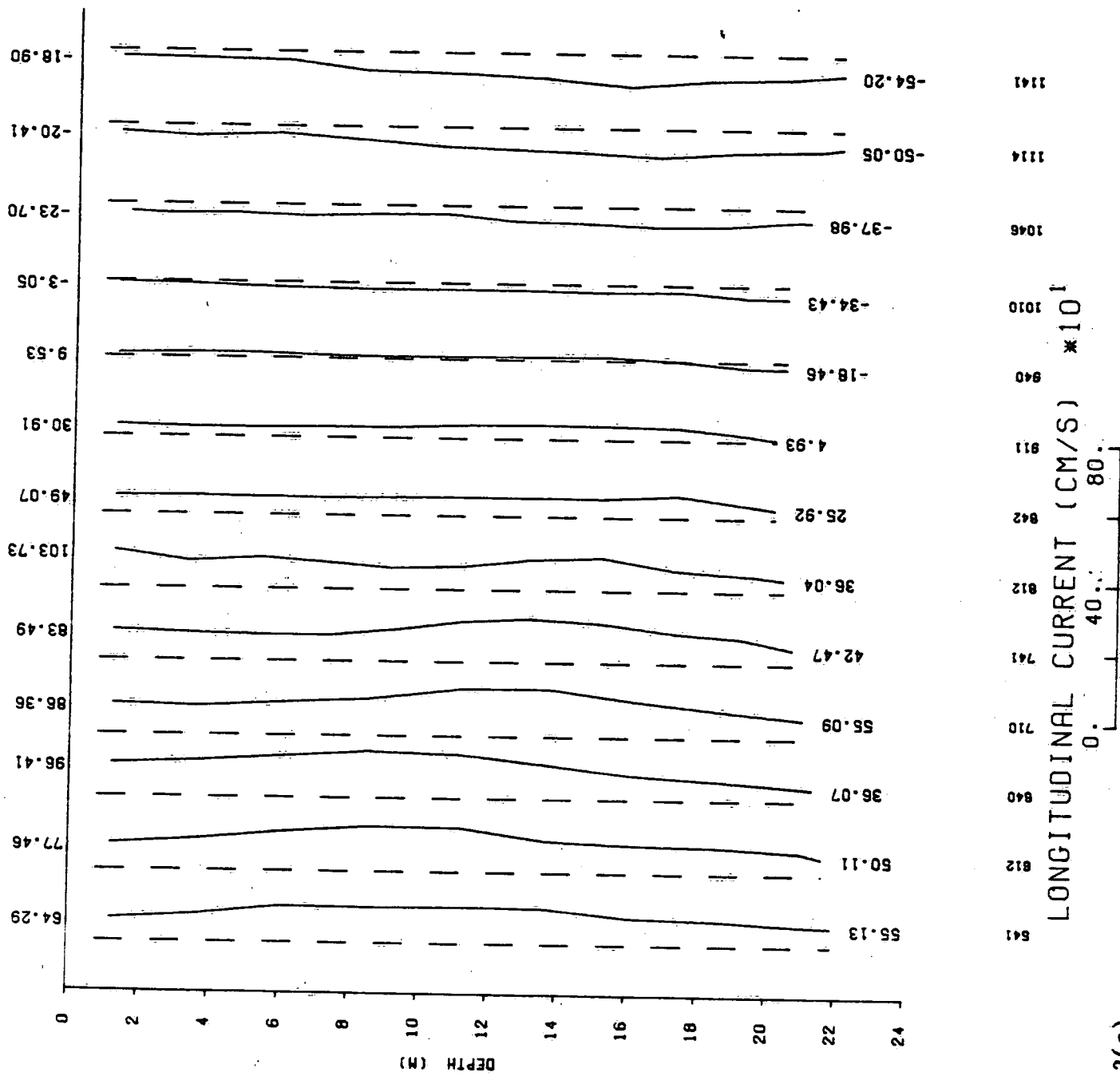


Figure D.2(c)

ST LAWRENCE 6E300 JUNE 29 1986

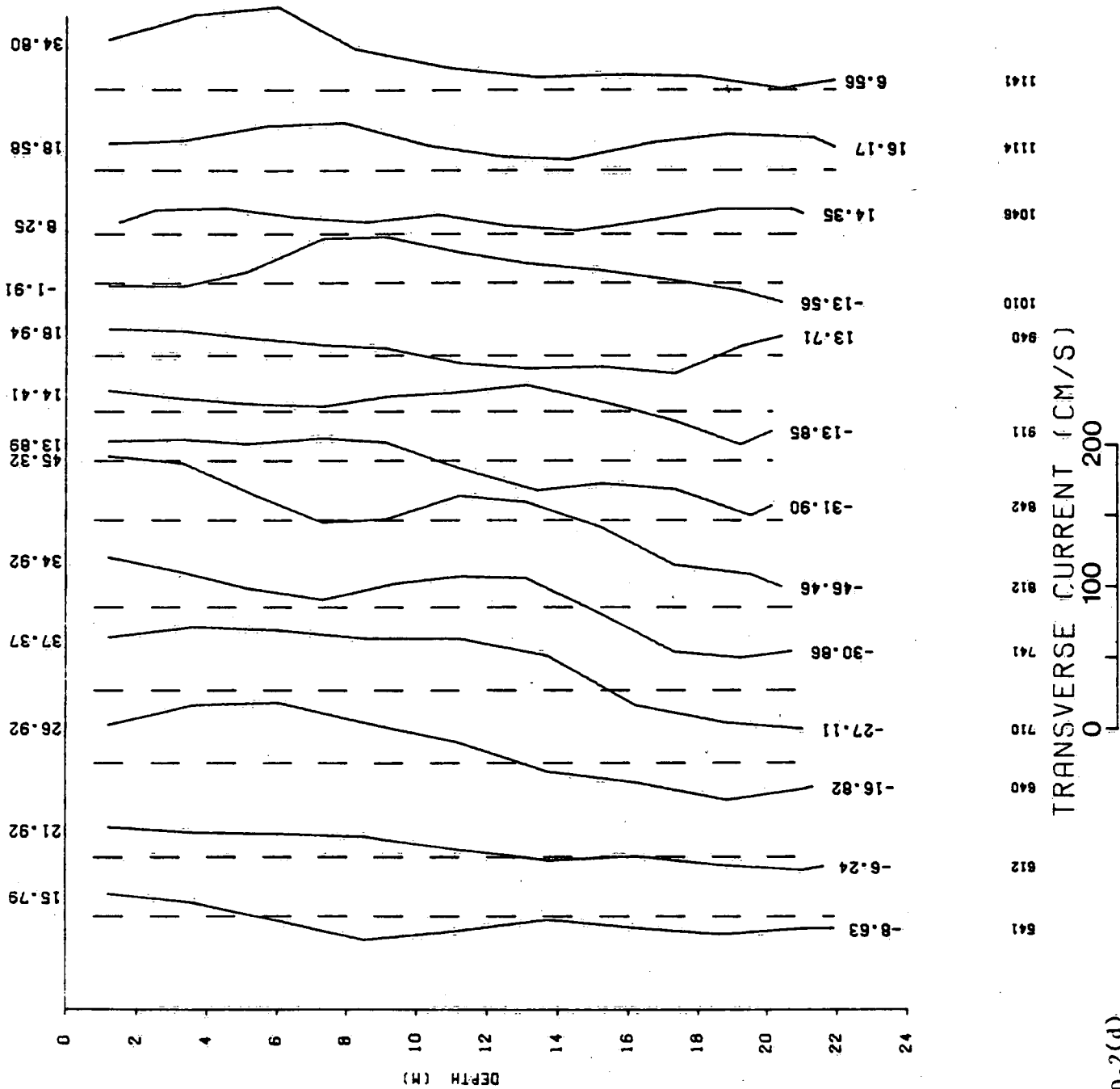


Figure D.2(d)

ST LAWRENCE STN 8 JUNE 29 1986

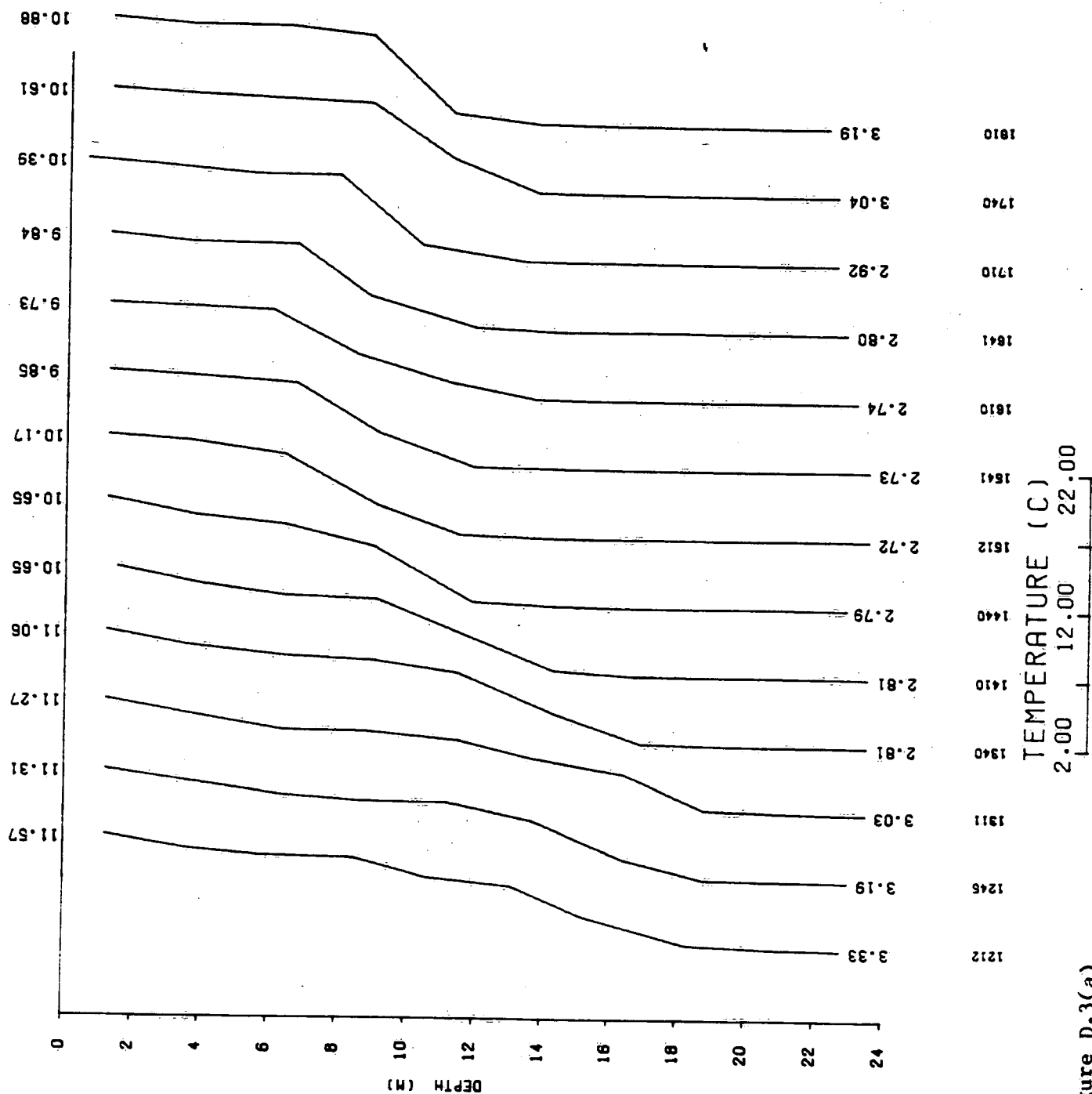


Figure D.3(a)

ST LAWRENCE STN 6E3 JUNE 29 1986

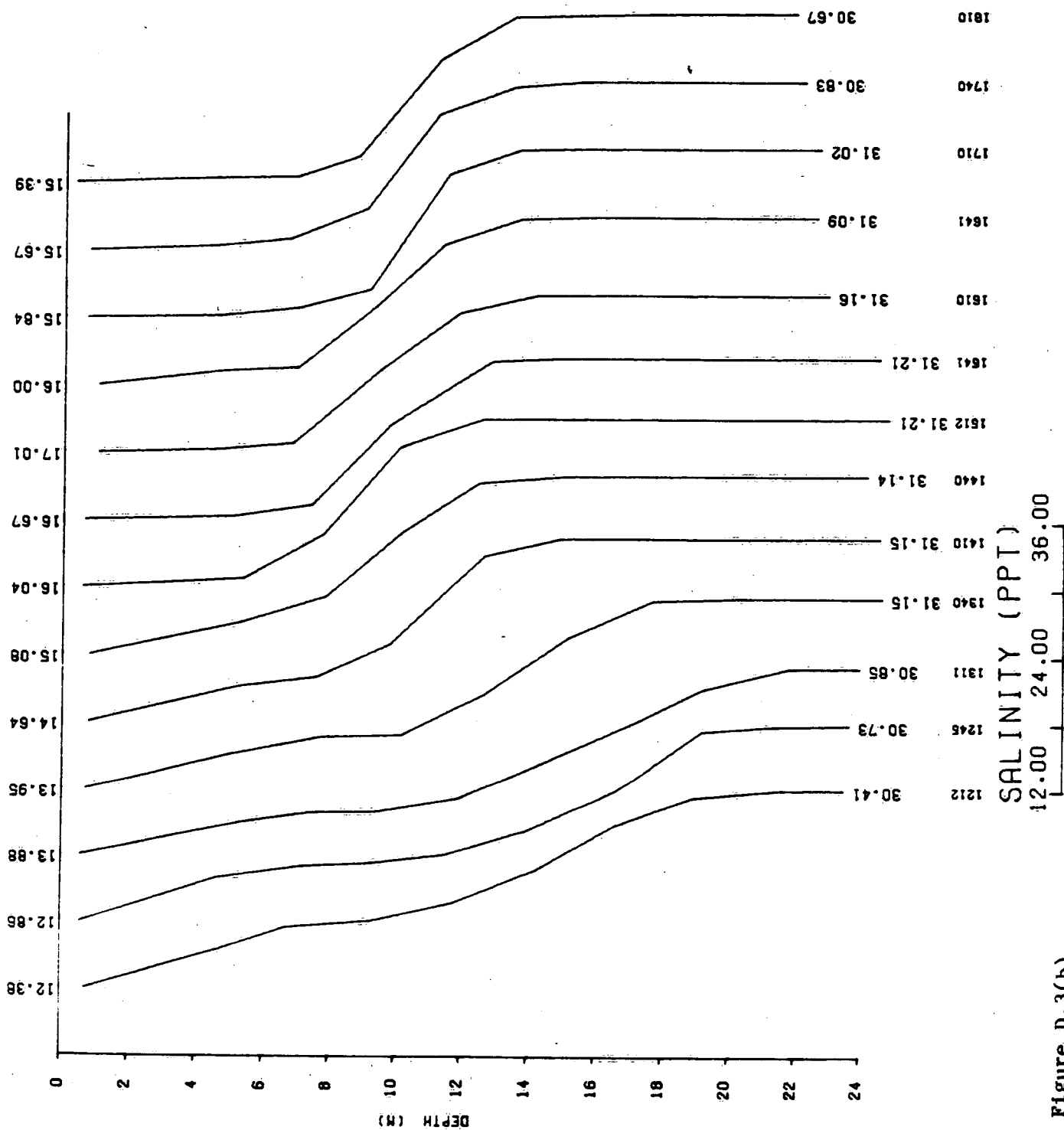


Figure D.3(b)



ST LAWRENCE STN 663 JUNE 29 1986

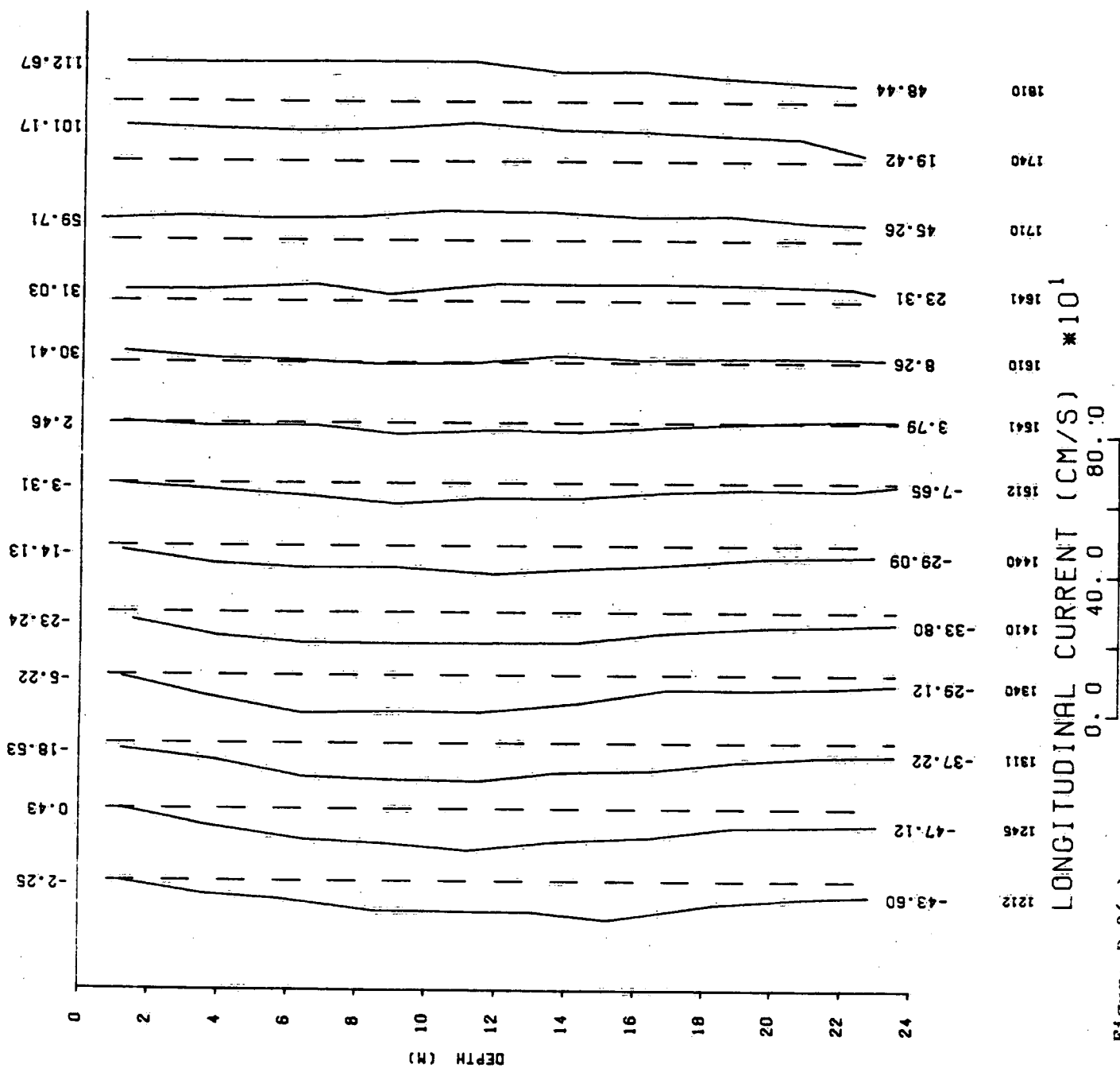


Figure D.3(c)

ST LAWRENCE 6E300 JUNE 29 1986

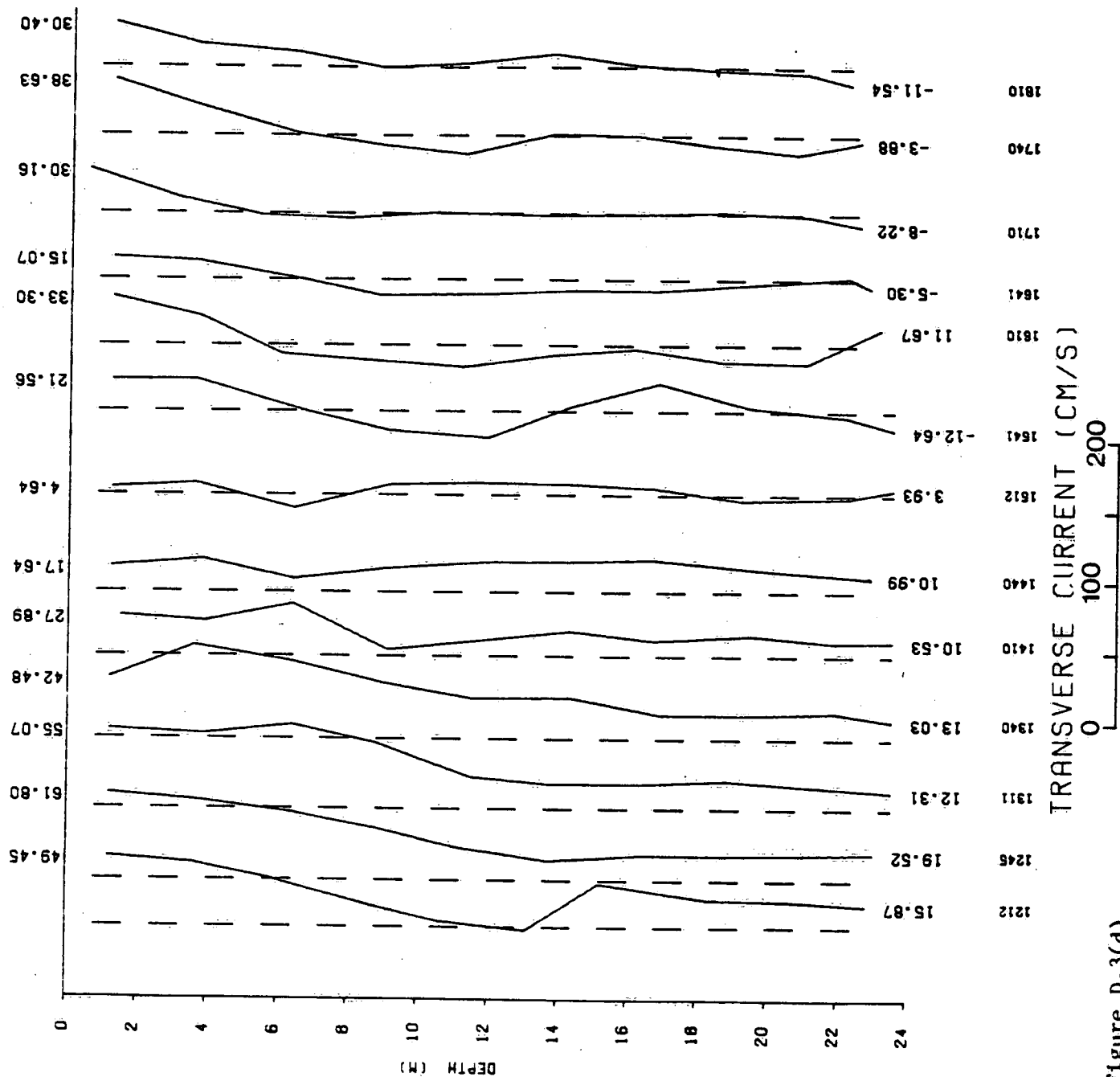


Figure D.3(d)

ST LAWRENCE 6E300 JUNE 29 1986

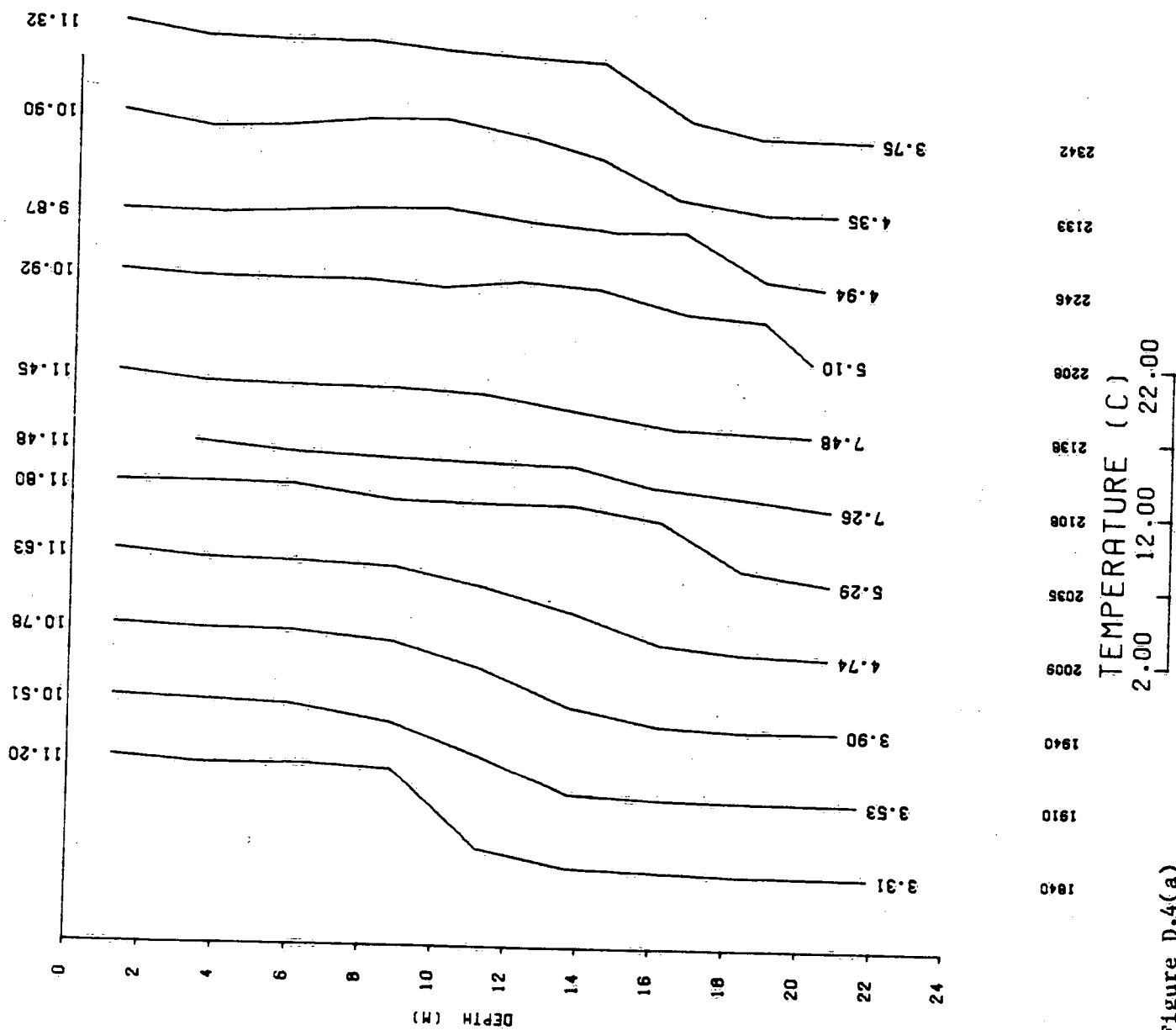


Figure D.4(a)

ST LAWRENCE 06300 JUNE 29 1986

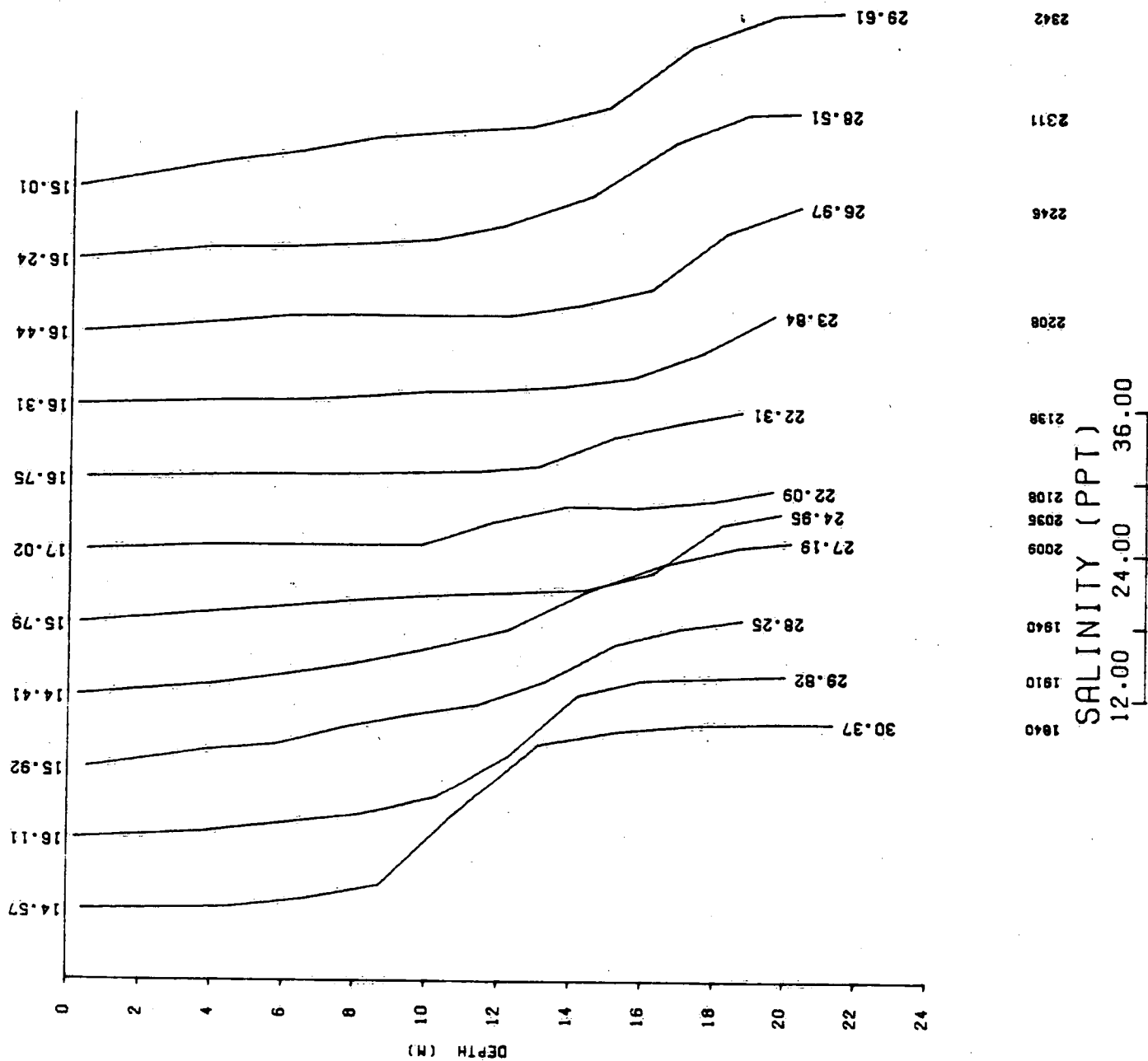


Figure D.4(b)

ST LAWRENCE STN 6E300 JUNE 29 1986

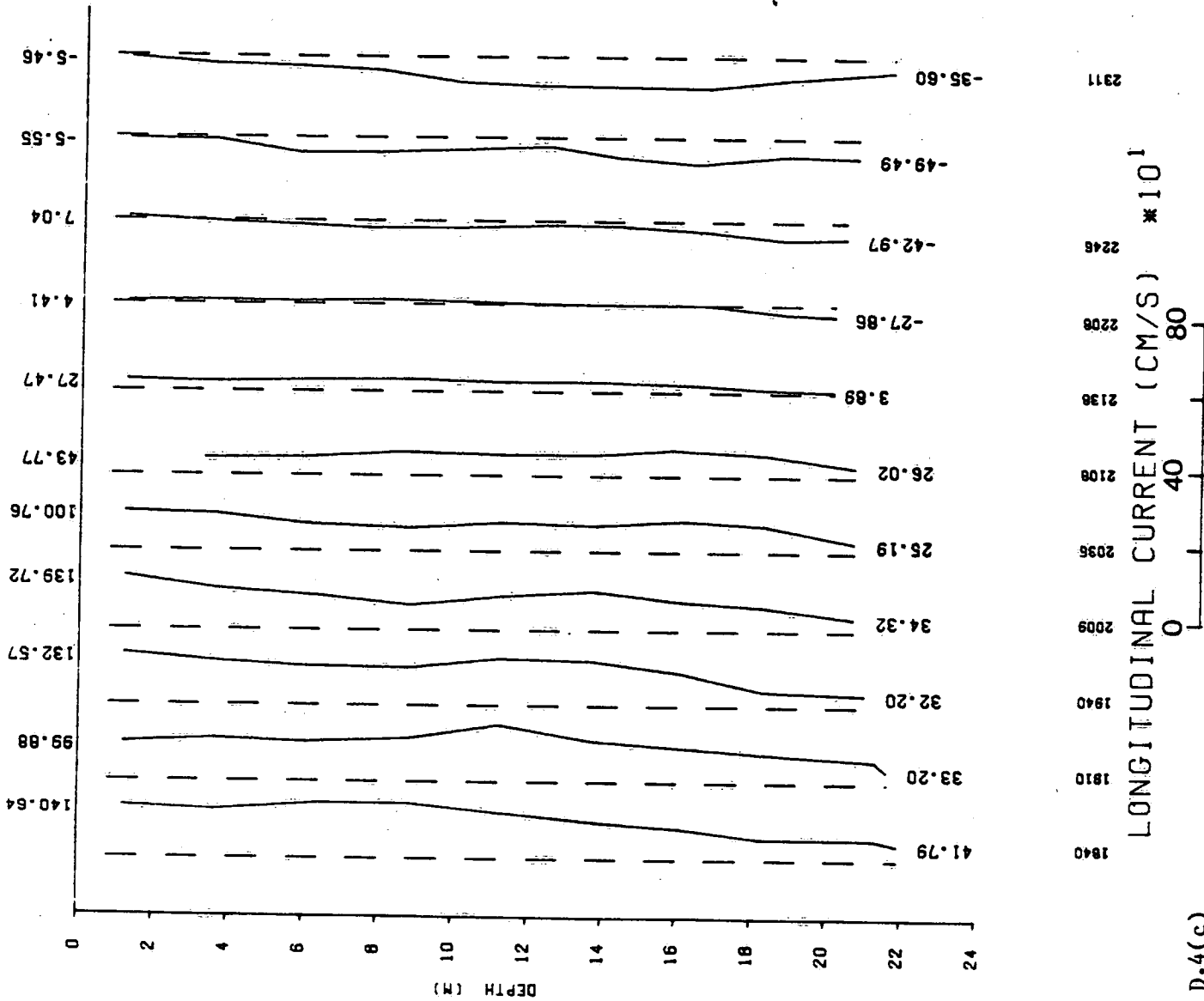


Figure D.4(c)

ST LAWRENCE 6E300 JUNE 29 1986

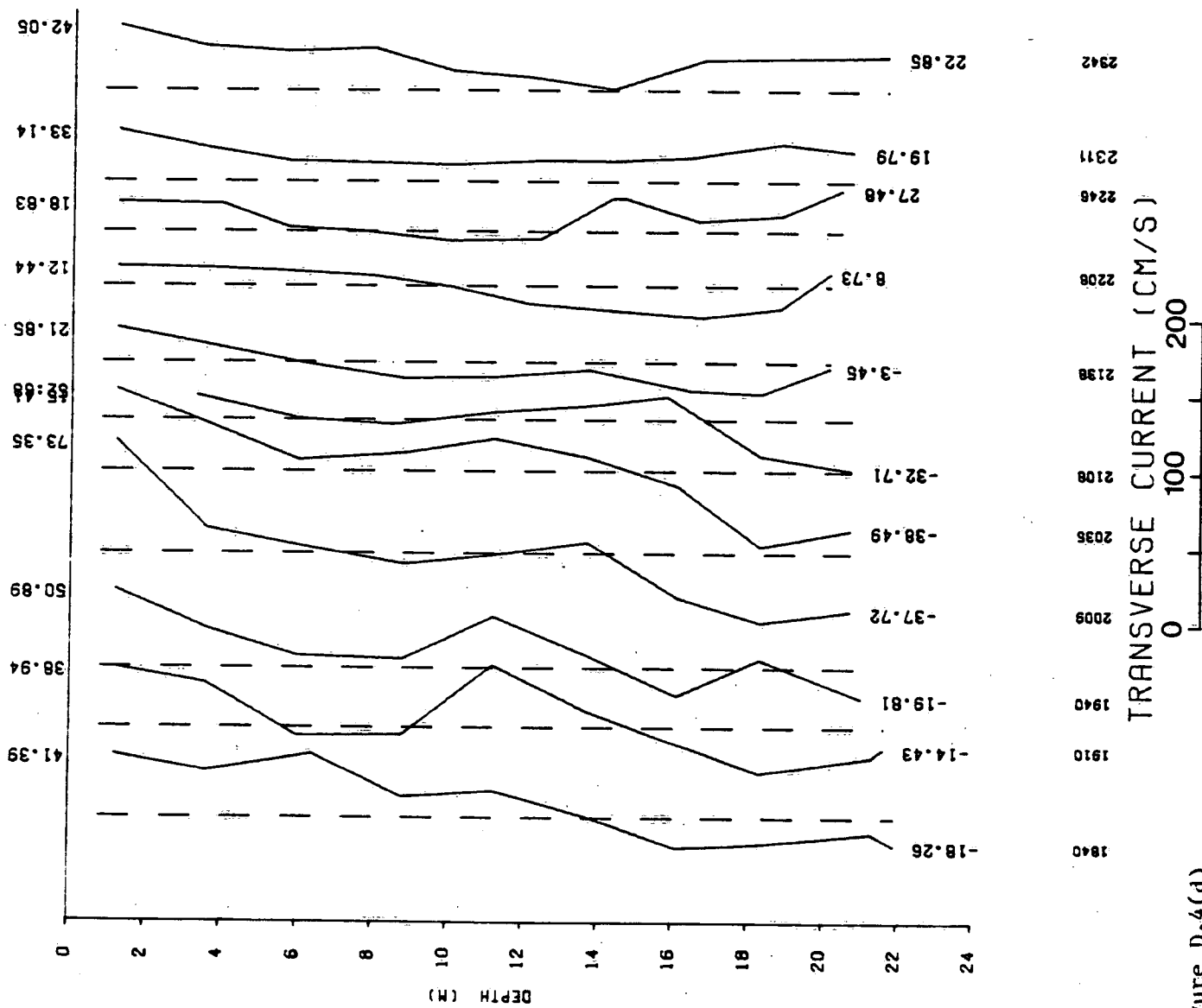


Figure D.4(d)

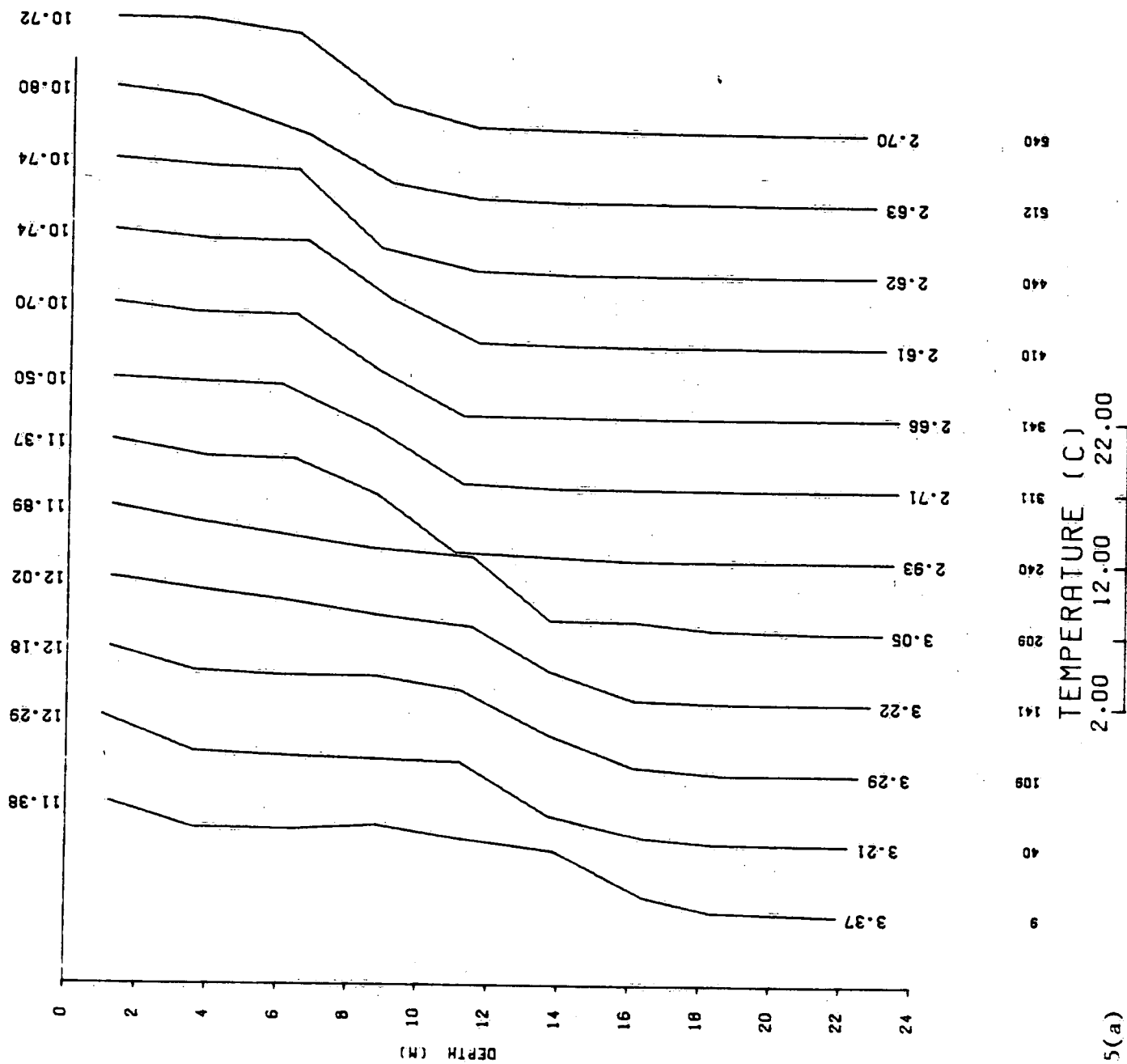


Figure D.5(a)

ST LAWRENCE STN 6E300 JUNE 30 1986

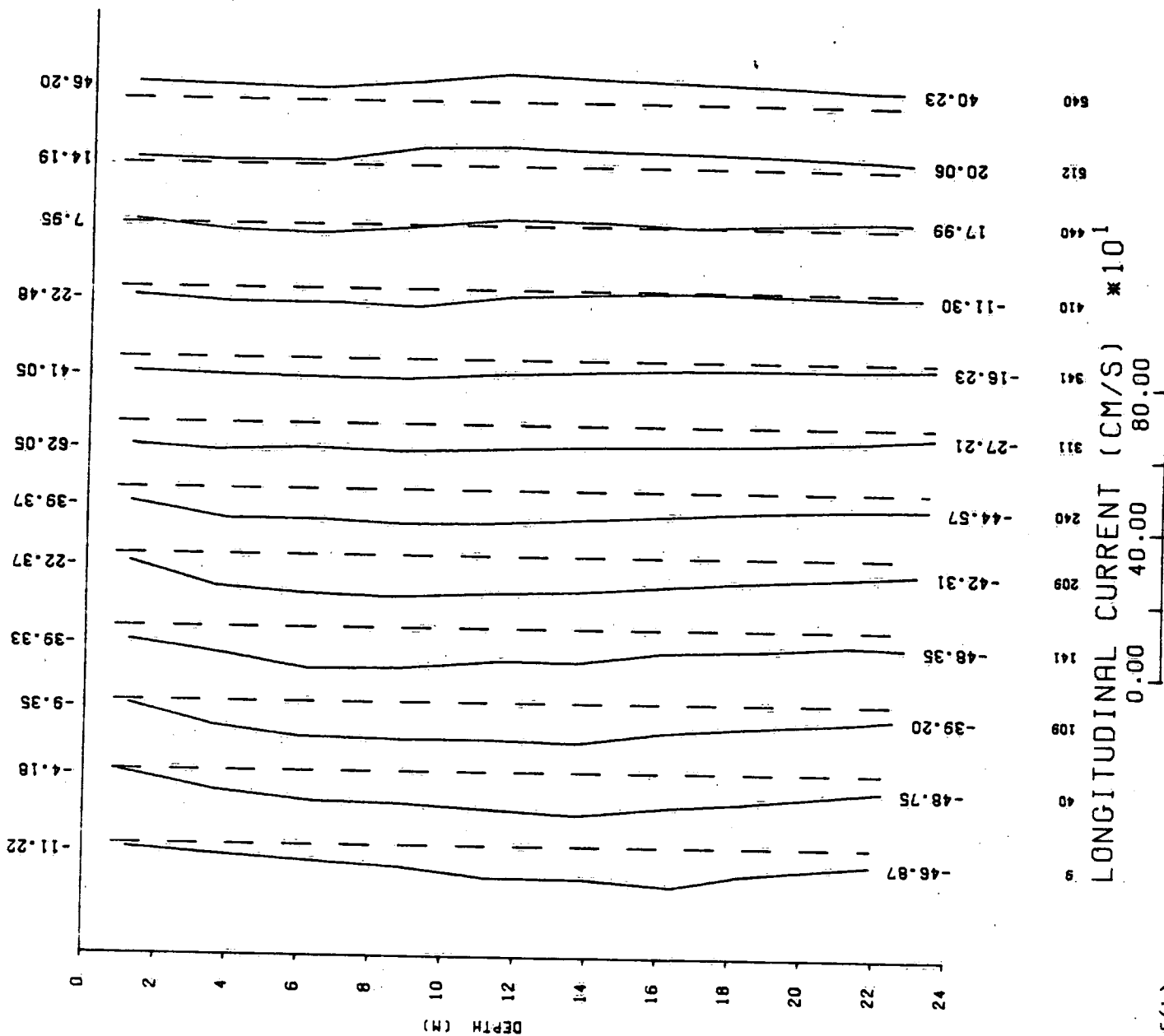


Figure D.5(b)



ST LAWRENCE STN 6 JUNE 30 1986

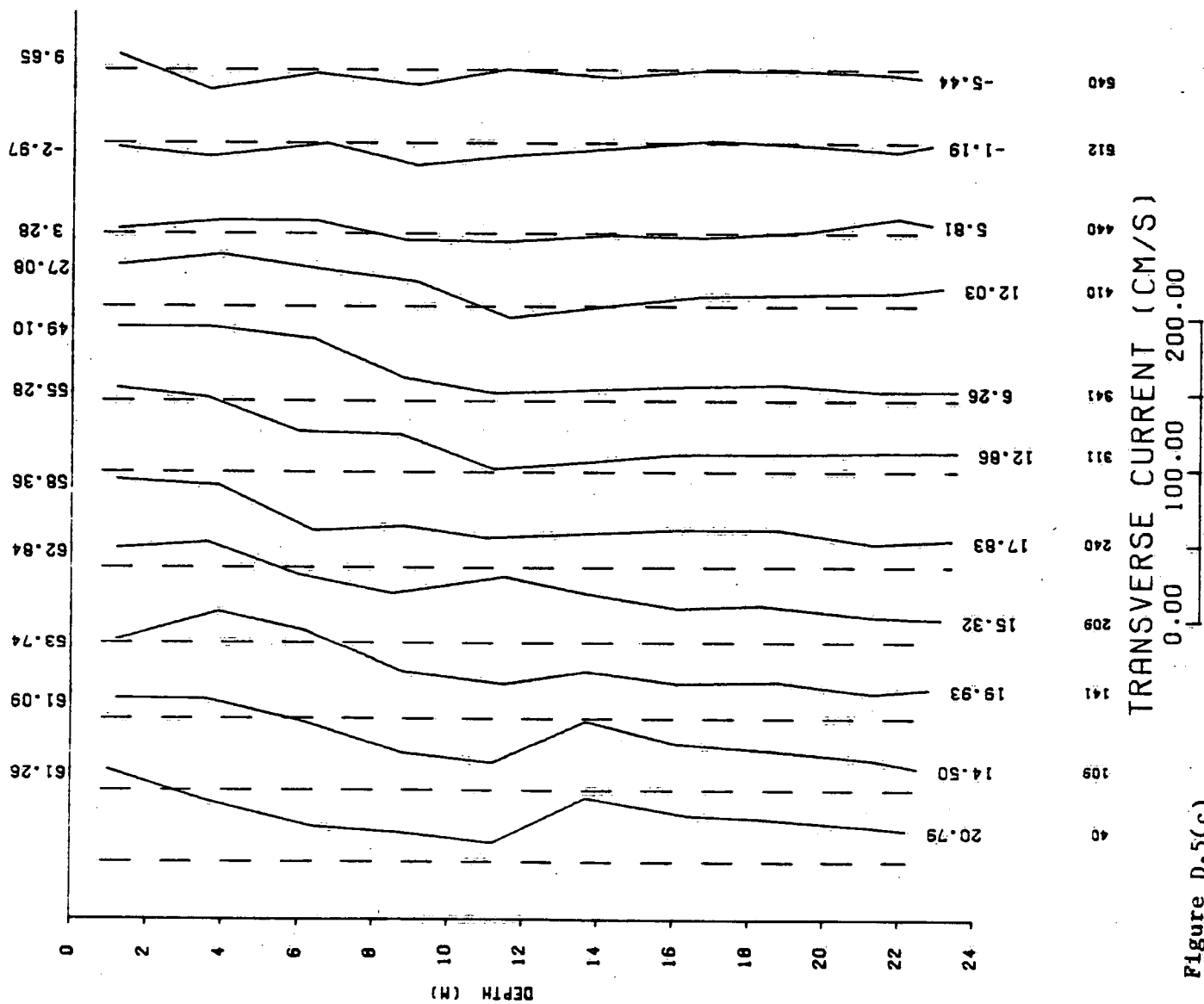


Figure D.5(c)

ST LAWRENCE STN 000 JUNE 1986

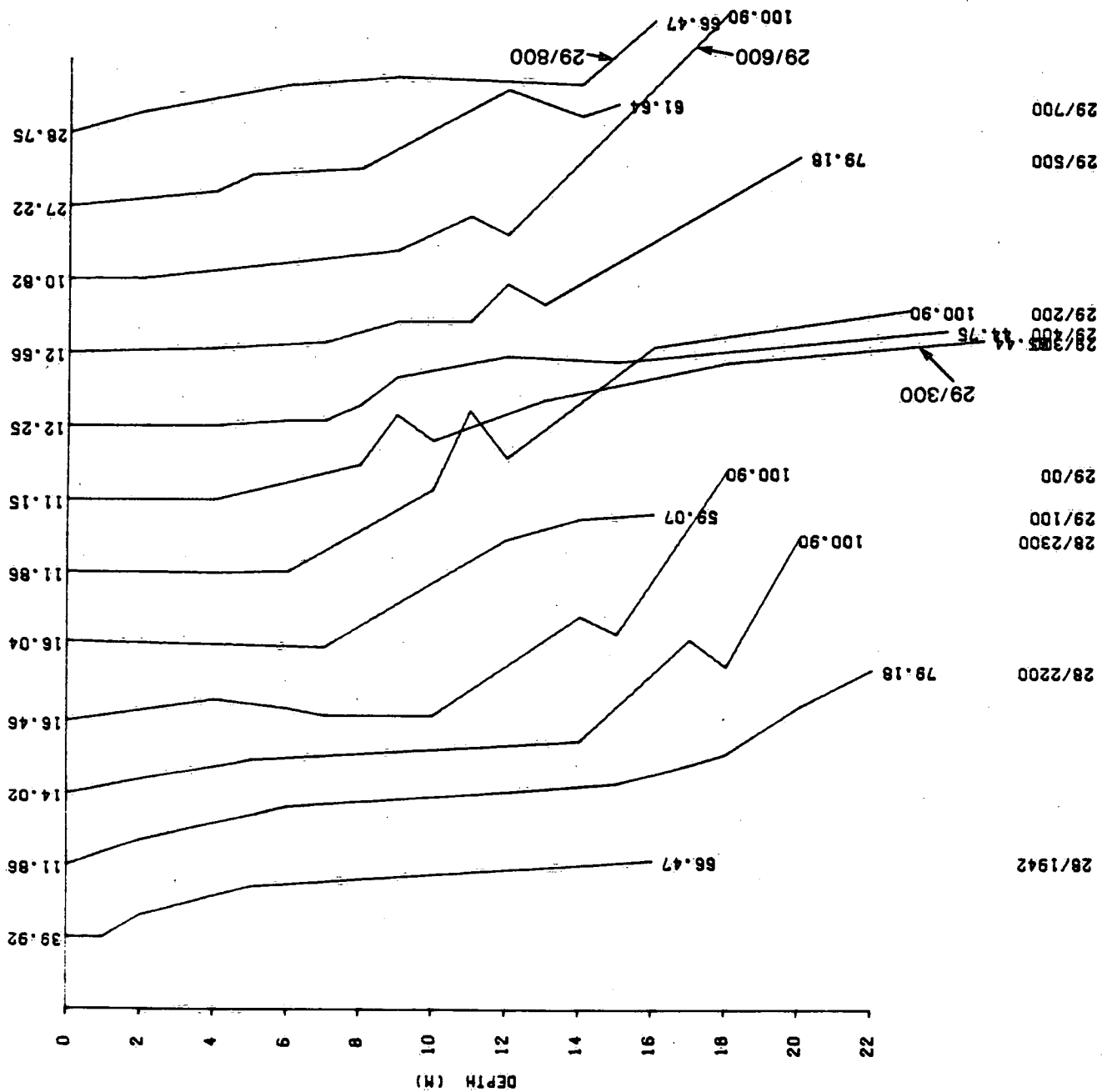


Figure D.6(a)

SUSPENDED SEDIMENT (MG/L)

0.00 50.00 100.00

ST LAWRENCE STN 6 JUNE 1986

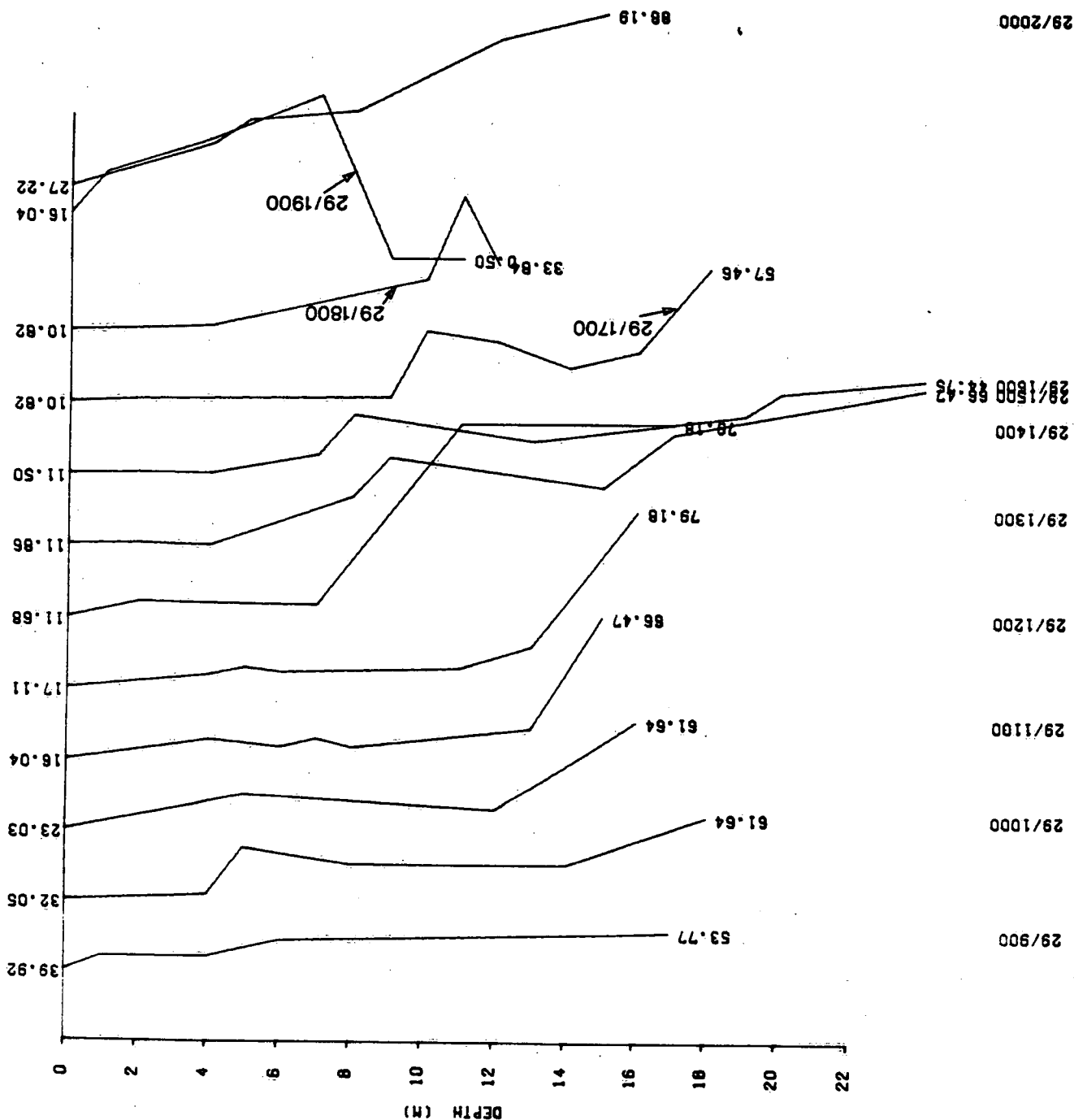


Figure D.6(b)

SUSPENDED SEDIMENT (MG/L)

0.00 50.00 100.00

ST LAWRENCE IN 6E300 JUNE 1986

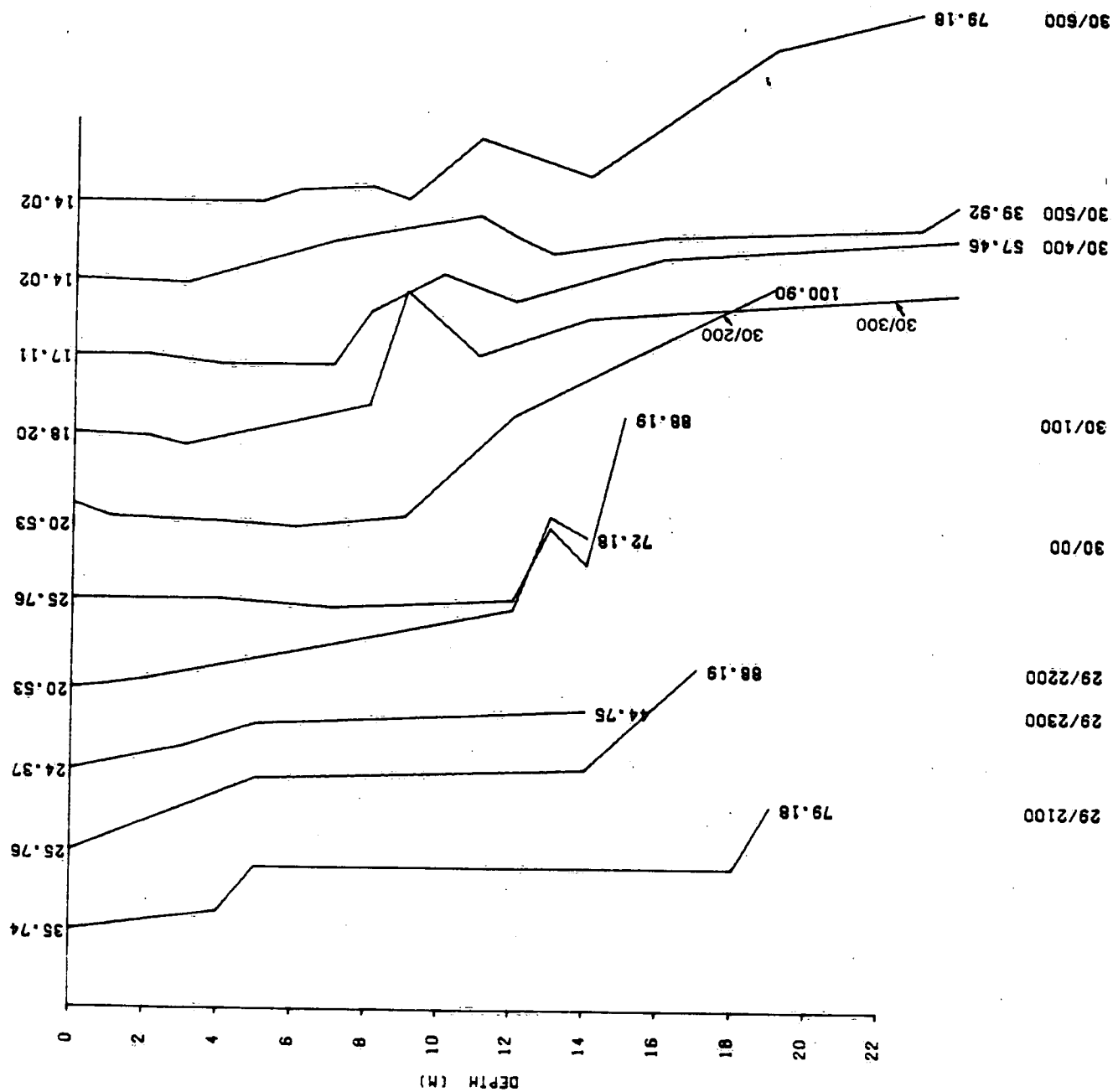


Figure D.6(c)

SUSPENDED SEDIMENT (MG/L)

0.00 50.00 100.00

**APPENDIX E**

Station 6E400 Latitude N 48° 08'37"

Longitude W 69° 36'16"

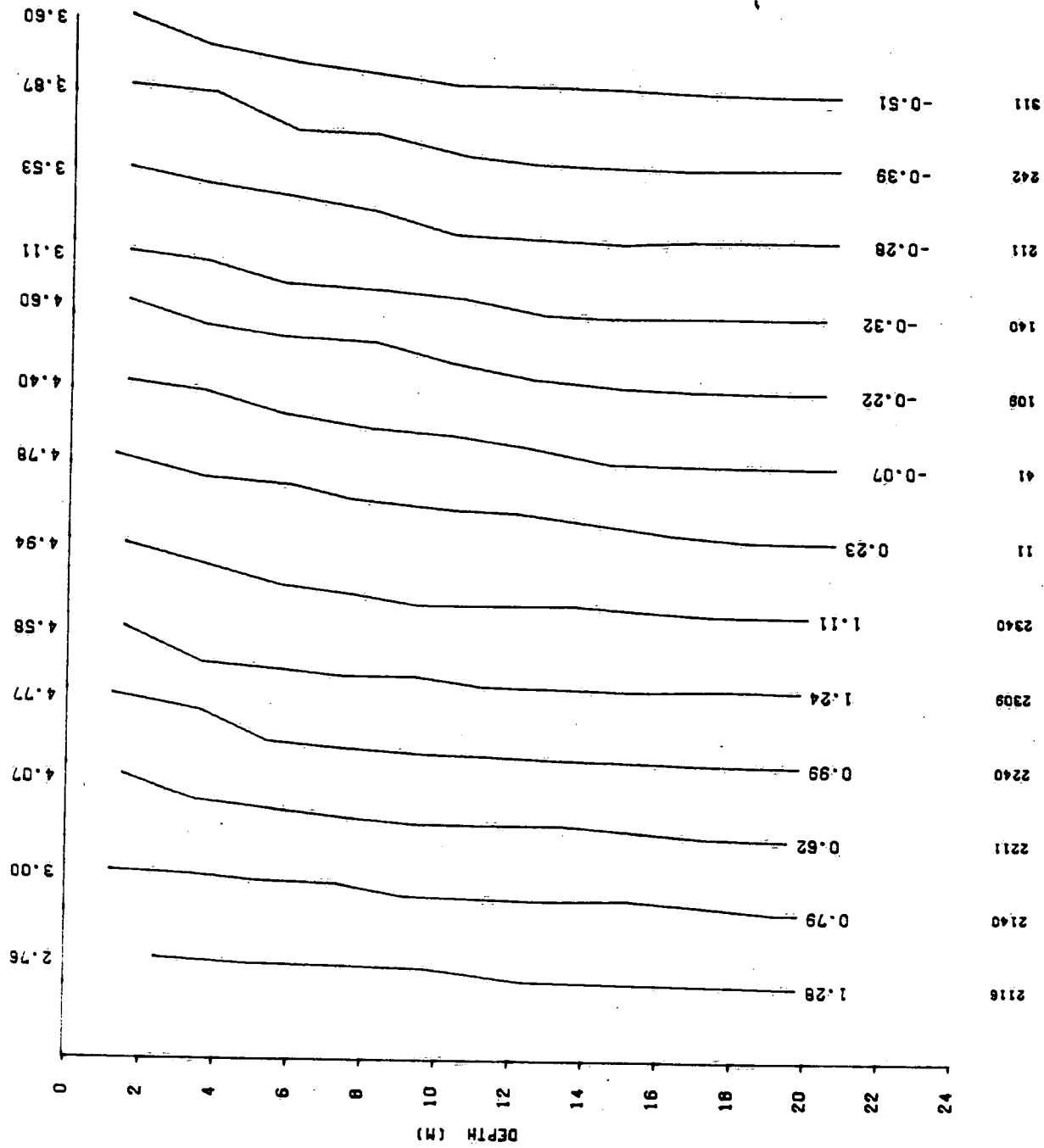
List of Figure Captions

- Figure E.1. Profiles from 21:16 to 03:11 July 1, 1986 (GMT) of (a) temperature, (b) salinity, (c) along-channel flow and (d) across-channel flow (positive to SE).
- Figure E.2. Profiles from 03:41 to 09:39 July 2, 1986 (GMT) of (a) temperature, (b) salinity, (c) along-channel flow and (d) across-channel flow (positive to SE).
- Figure E.3. Profiles from 10:09 to 16:16 July 2, 1986 (GMT) of (a) temperature, (b) salinity, (c) along-channel flow and (d) across-channel flow, (positive to SE).
- Figure E.4. Profiles from 16:49 to 21:44 (GMT) of (a) temperature, (b) salinity, (c) along-channel flow and (d) across-channel flow (positive to SE).

Figure E.5. Profiles from 22:10 July 3 to 3:42 July 3, 1986 (GMT) of (a) temperature, (b) along-channel flow and (c) across-channel flow (positive to SE).

Figure E.6. Profiles of suspended sediment (a) from 11:87 July 1 to 9:00 July 2, 1986, (b) from 11:00 July 2 to 5:00 July 3.

ST LAWRENCE STN 8 JULY 1 1986



TEMPERATURE (C)  
0.00 8.00 16.00

Figure E.1(a)

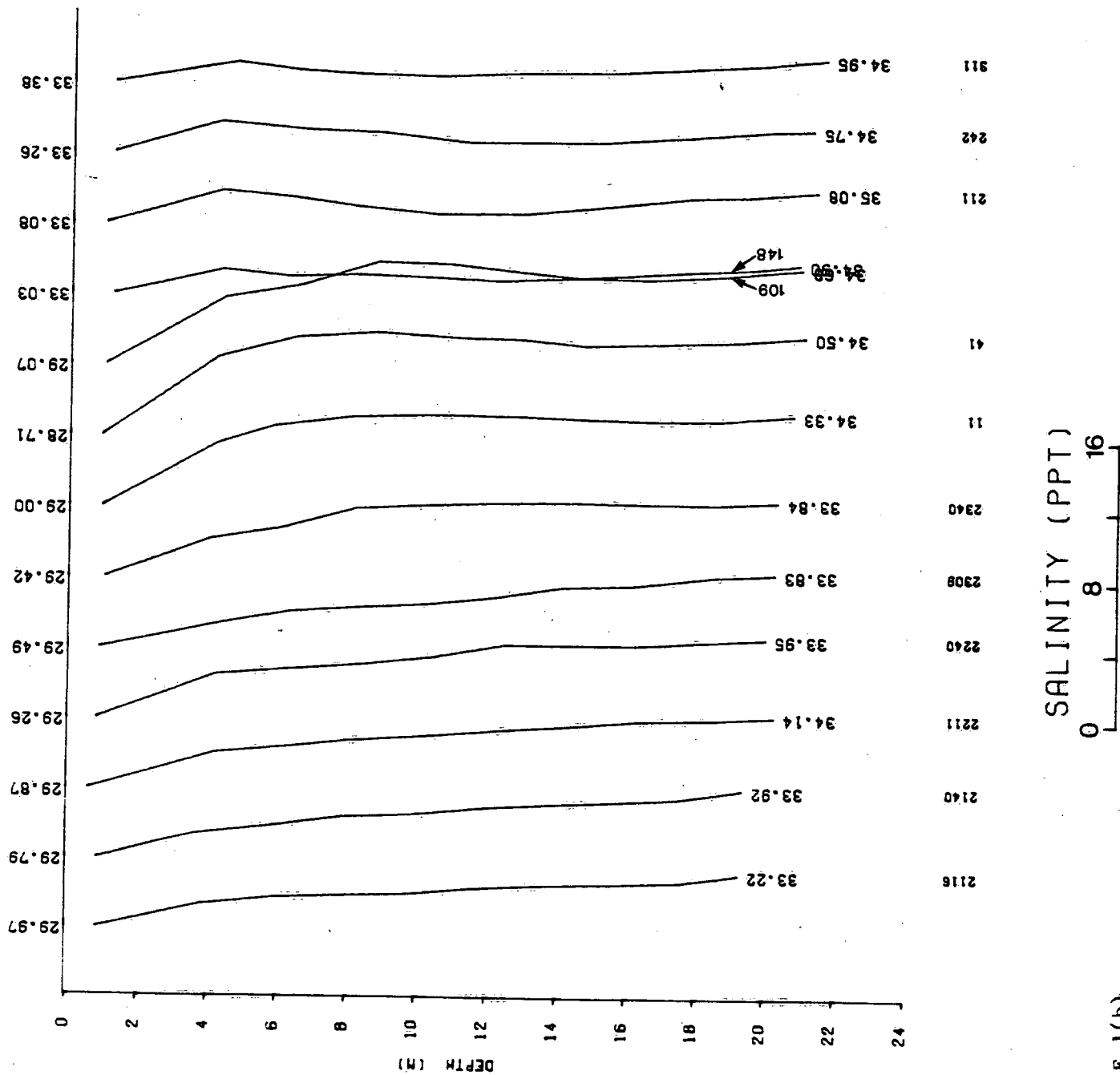


Figure E.1(b)



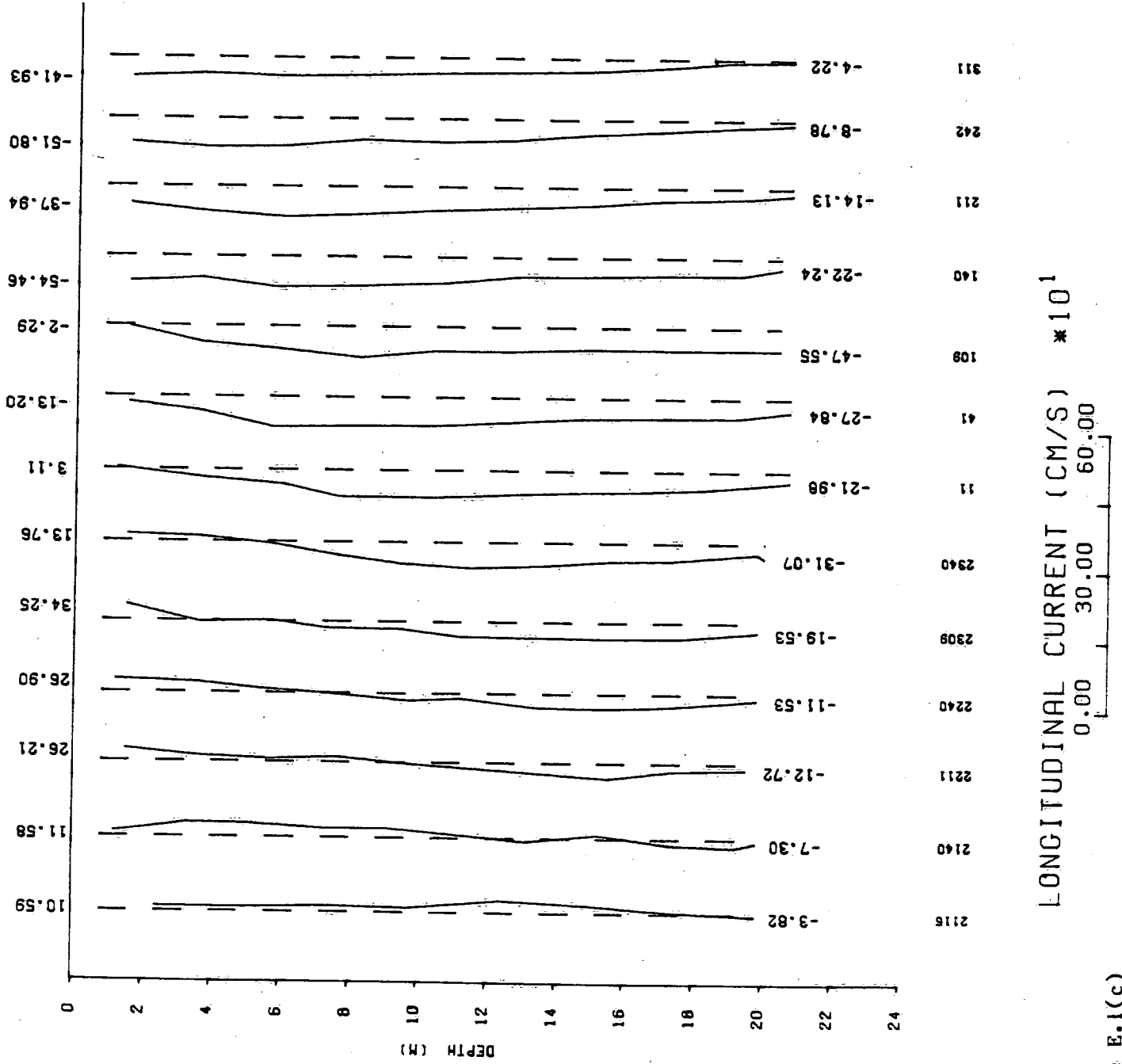


Figure E.1(c)

ST LAWRENCE STN 6 JULY 1 1986

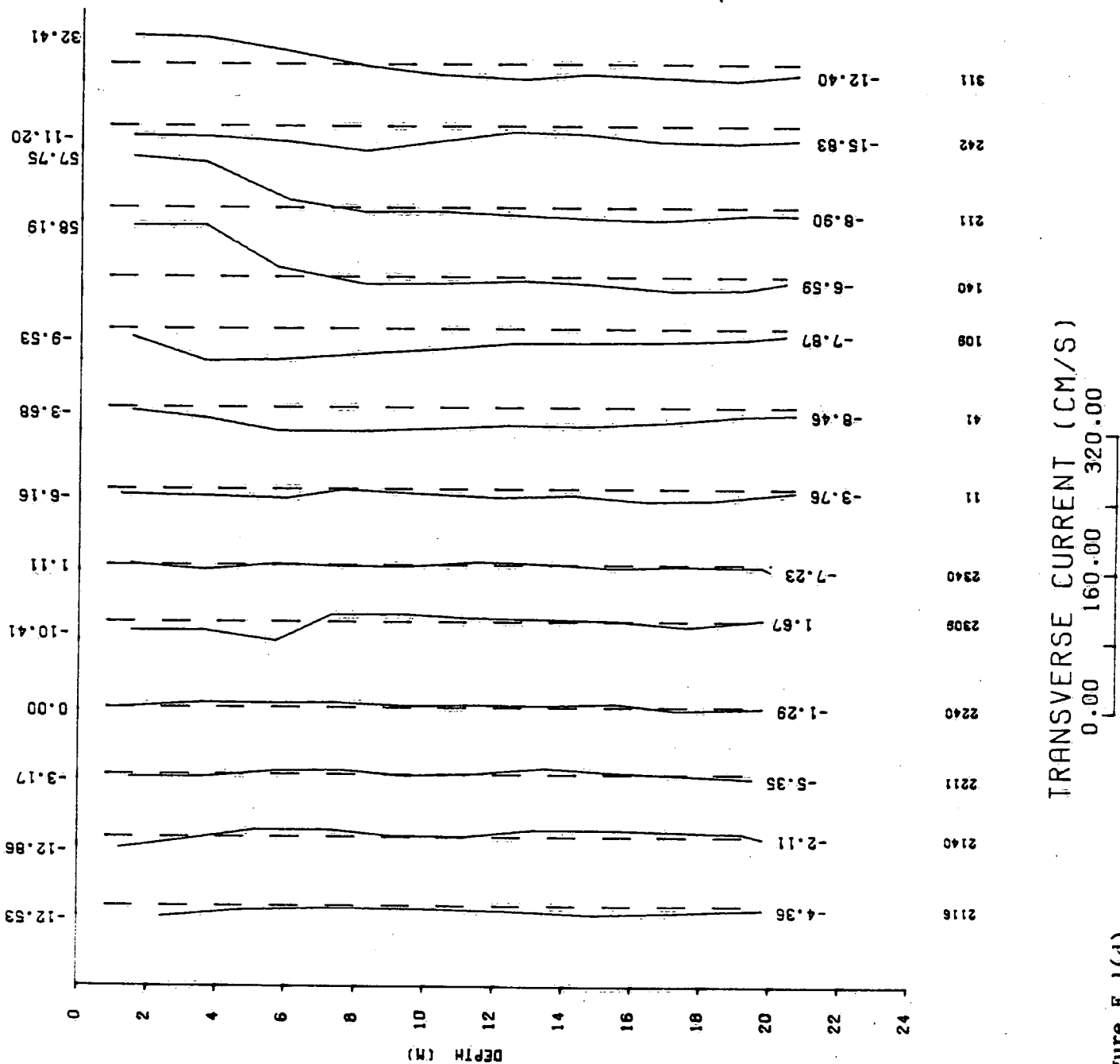


Figure E.1(d)

ST LAWRENCE 6E400 JULY 2 1986

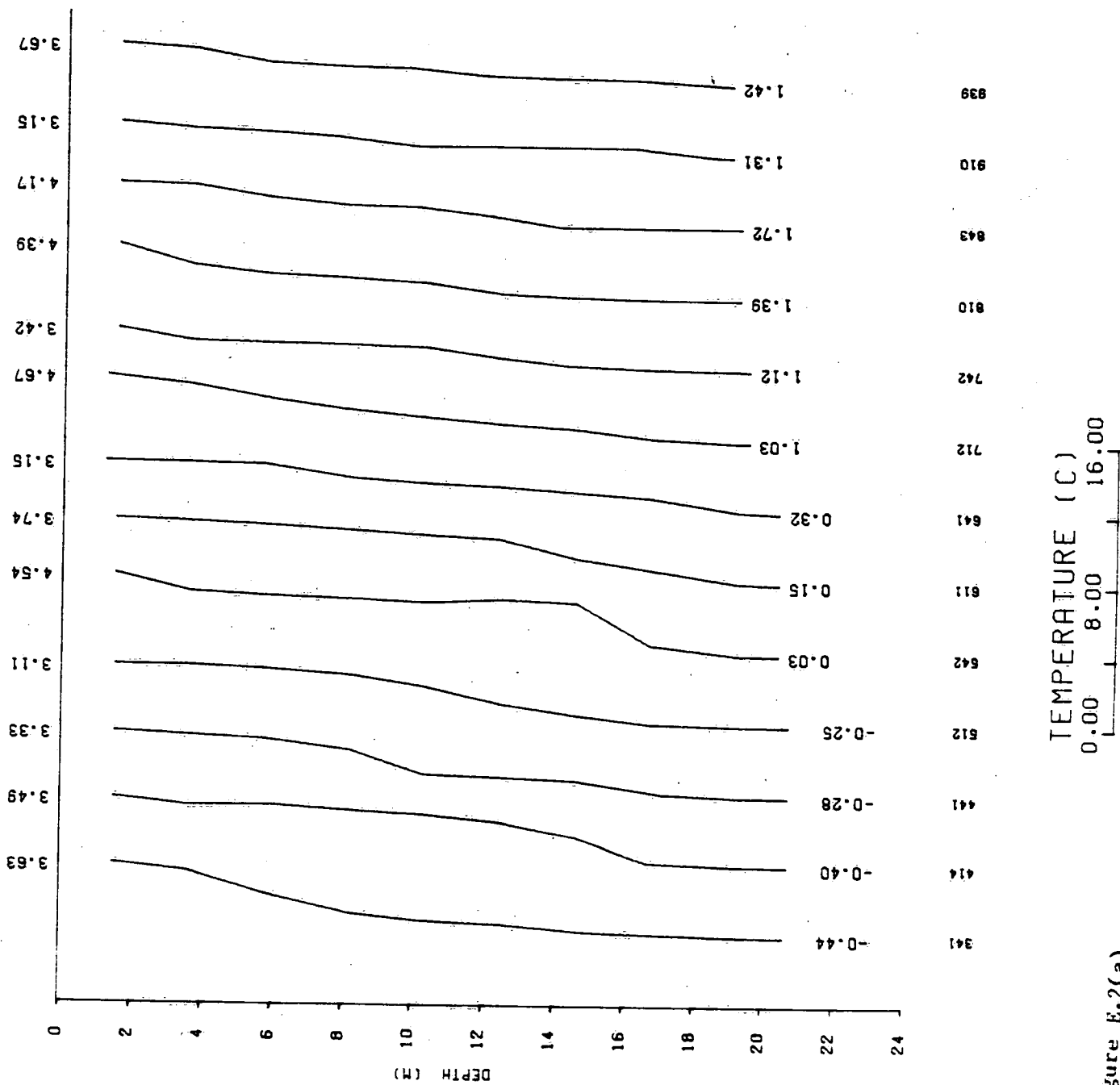


Figure E.2(a)

ST LAWRENCE STN 400 JULY 2 1986

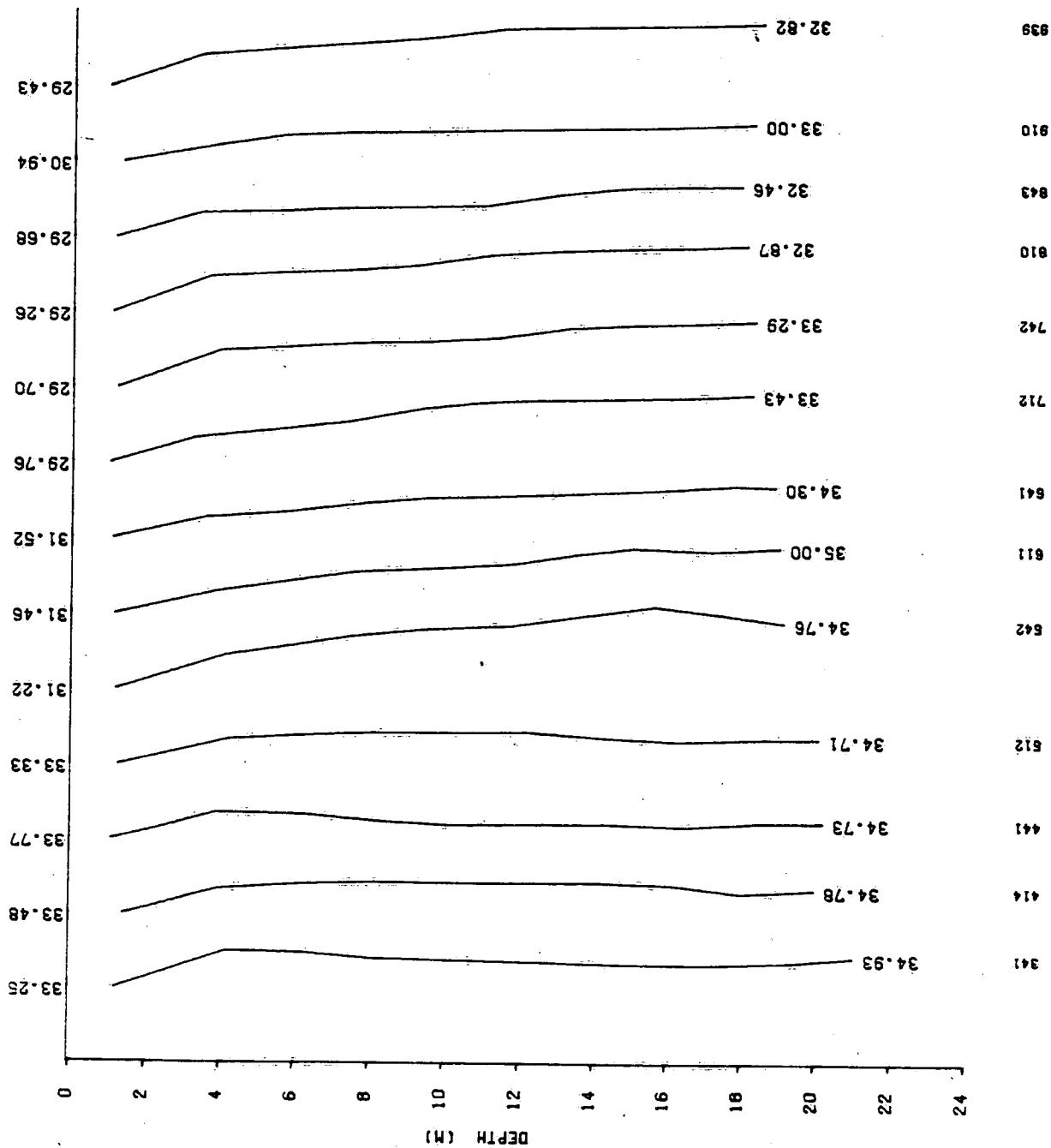


Figure E.2(b)

ST LAWRENCE N 6E400 JULY 2 1986

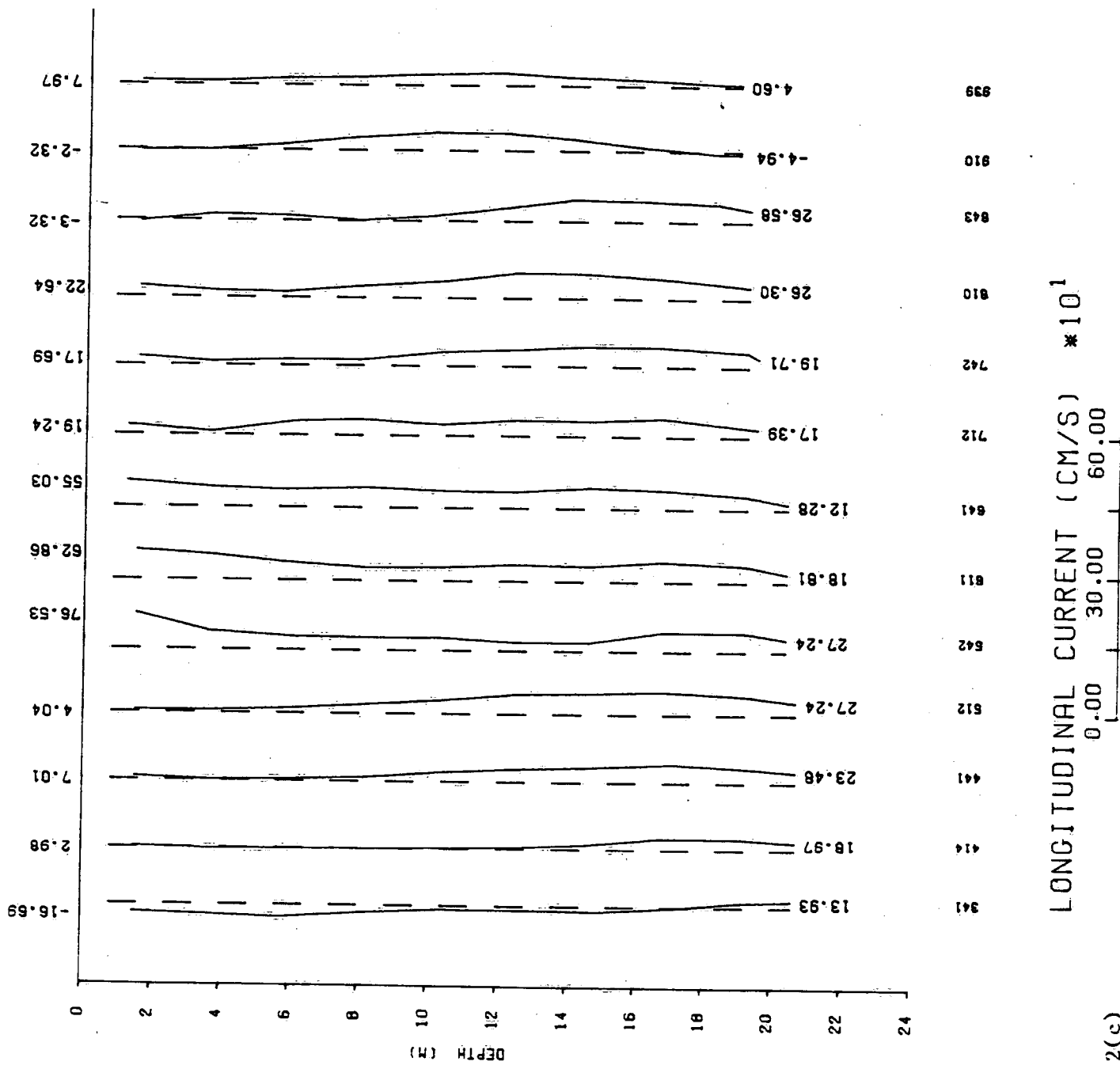


Figure E.2(c)

ST LAWRENCE STN 6E JULY 2 1986

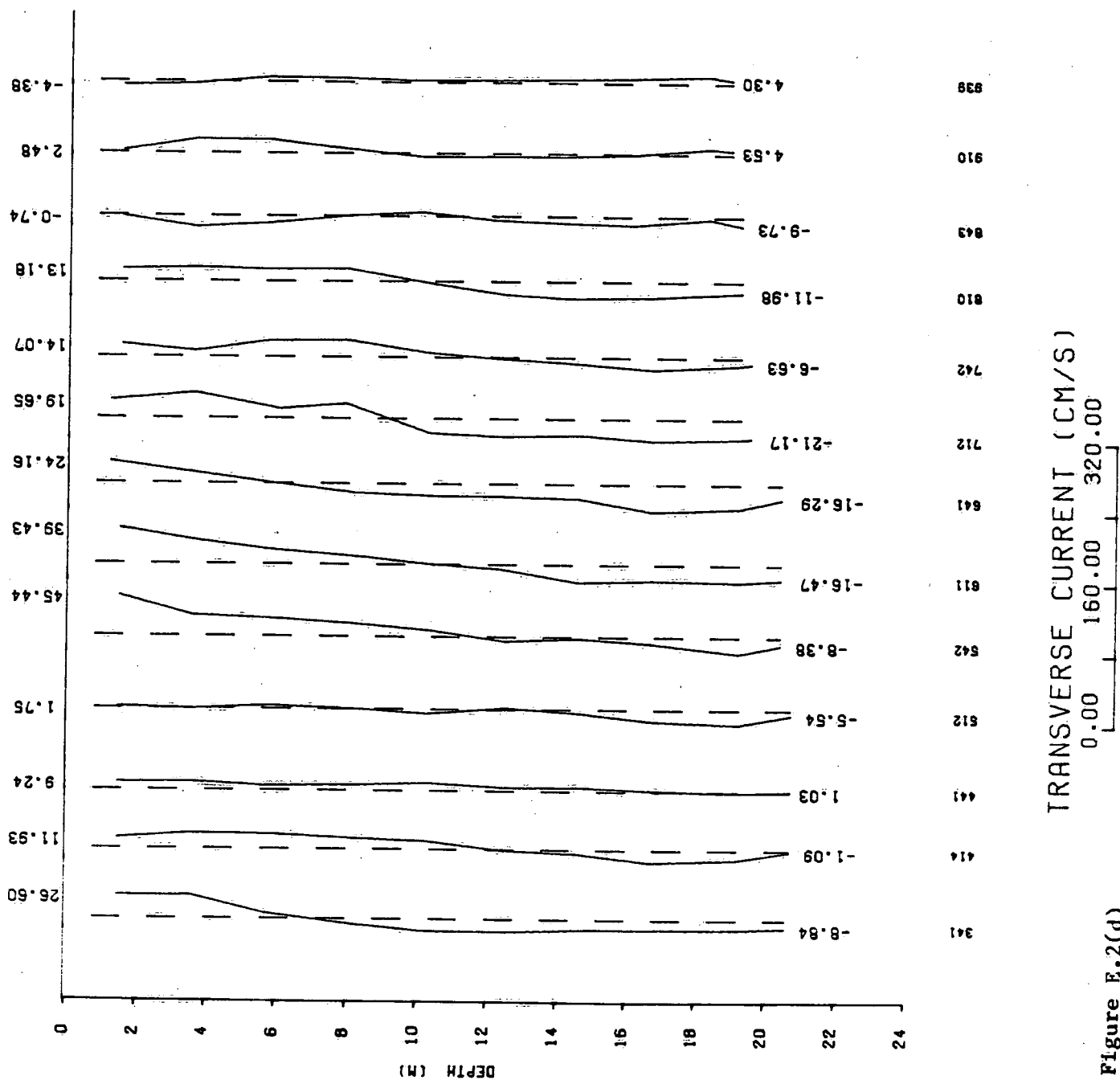
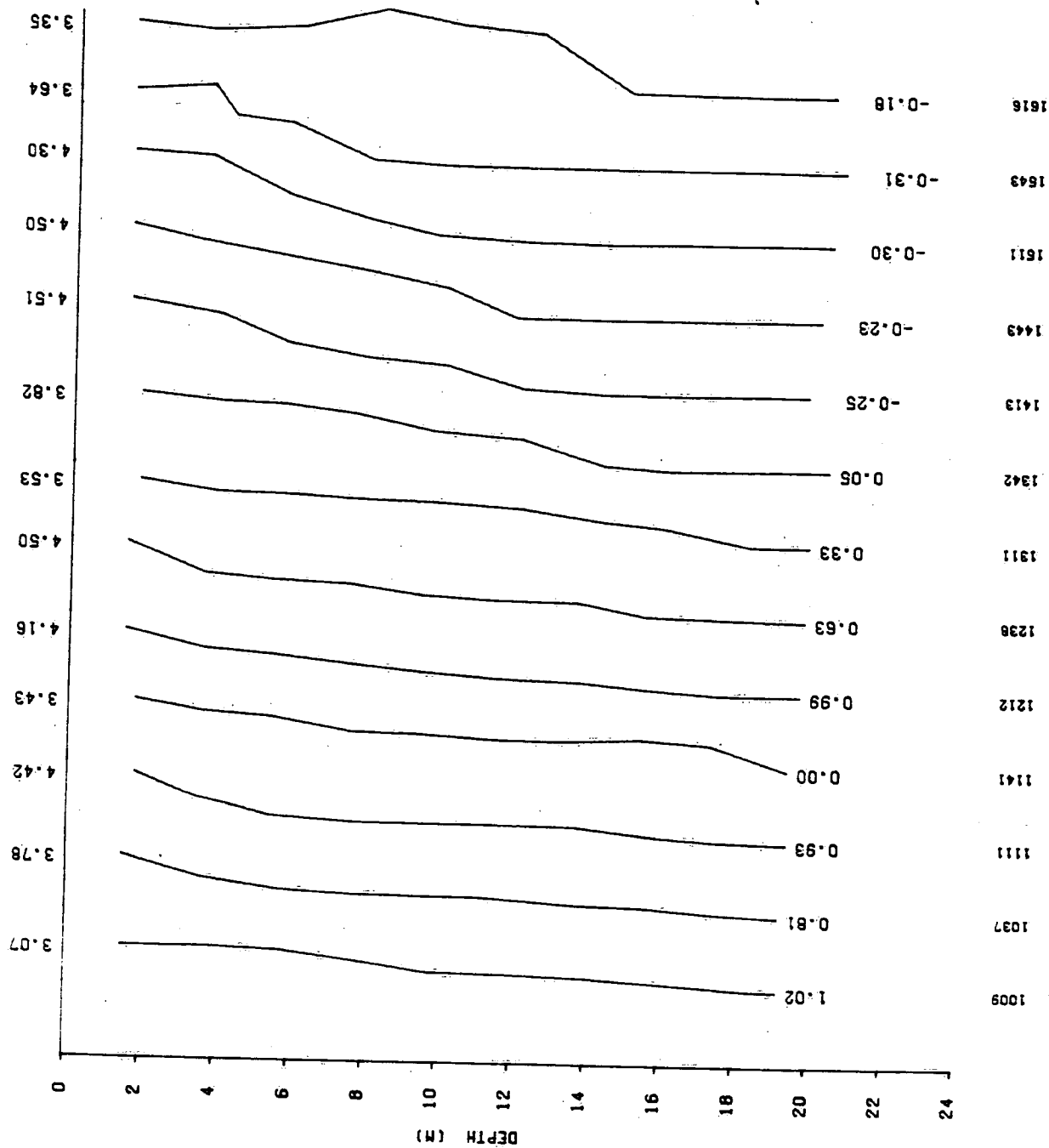


Figure E.2(d)

ST LAWRENCE STN 00 JULY 2 1986



TEMPERATURE (C)  
0.00 8.00 16.00

Figure E.3(a)

ST LAWRENCE STN 6E40 JULY 2 1986

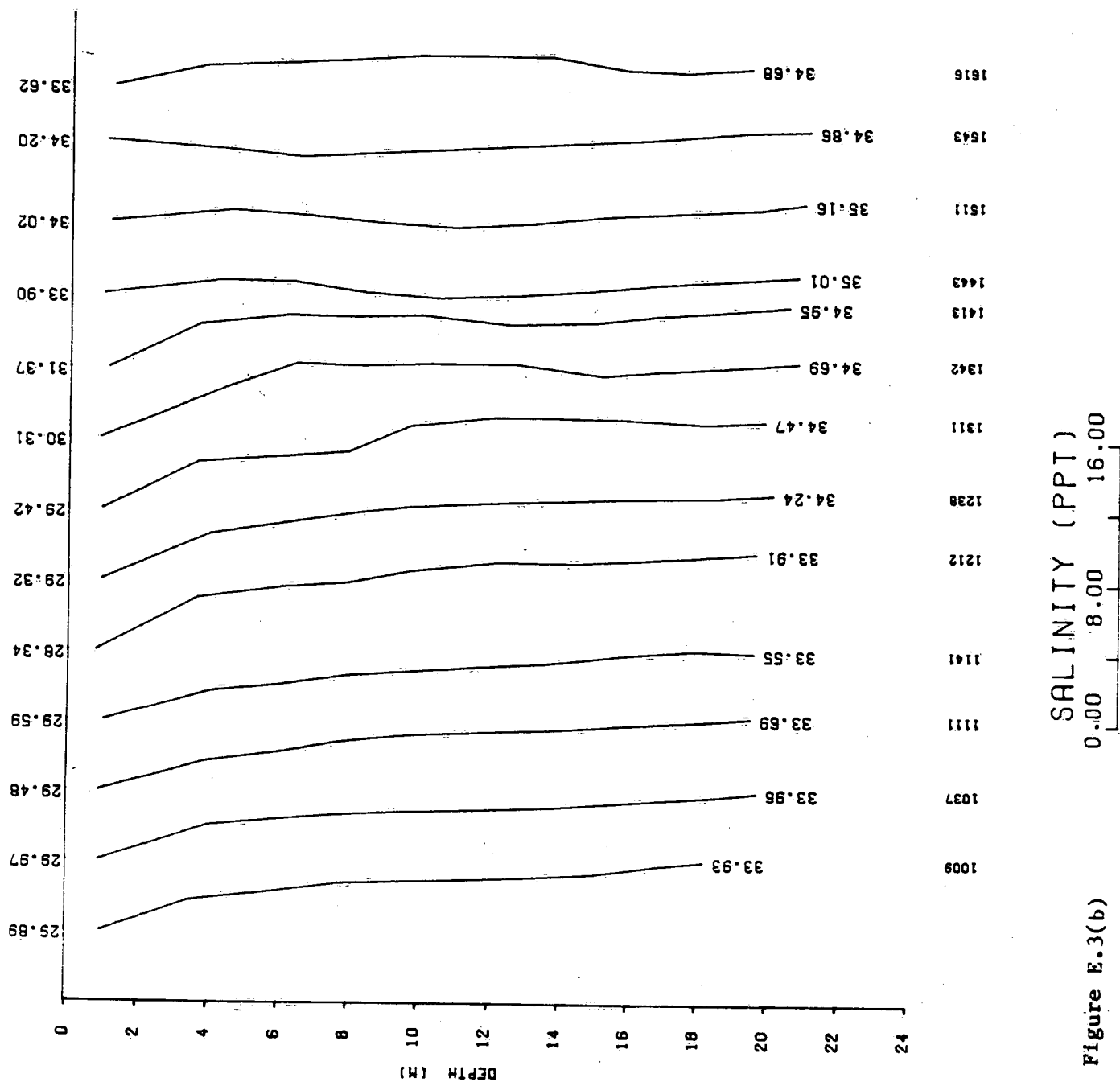


Figure E.3(b)



ST LAWRENCE STR 400 JULY 2 1986

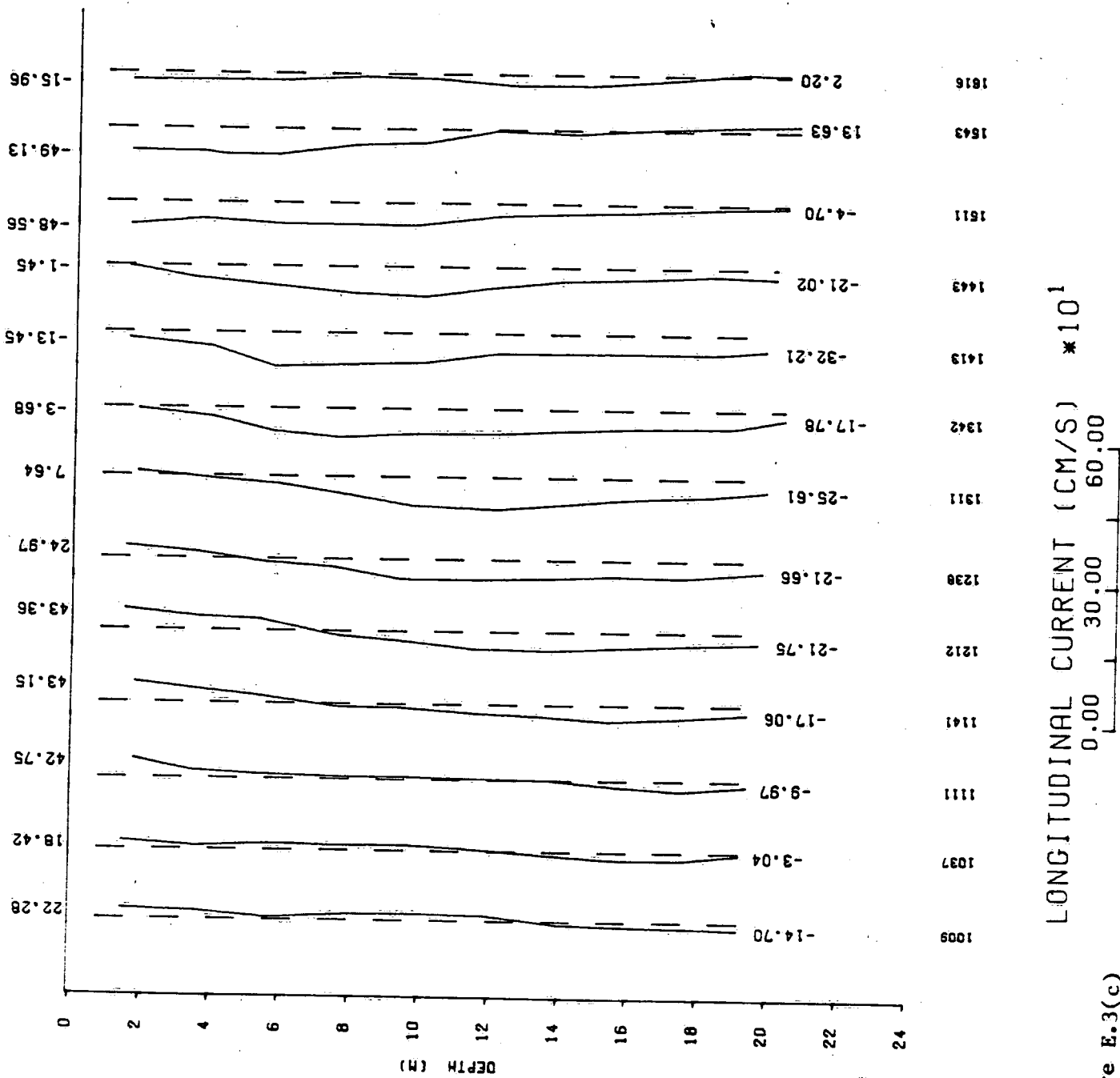


Figure E.3(c)

ST LAWRENCE STN 000 JULY 2 1986

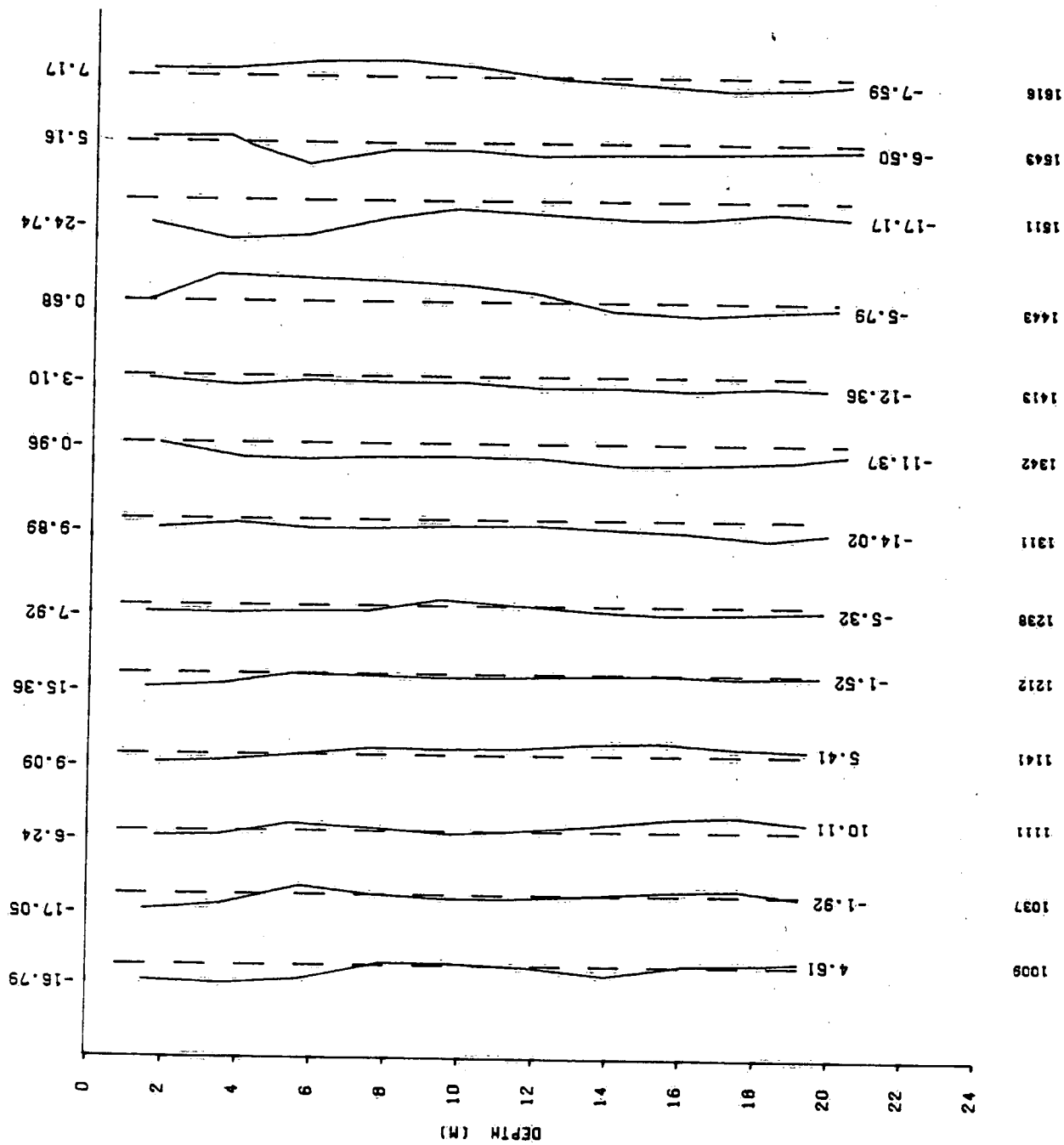


Figure E.3(d)

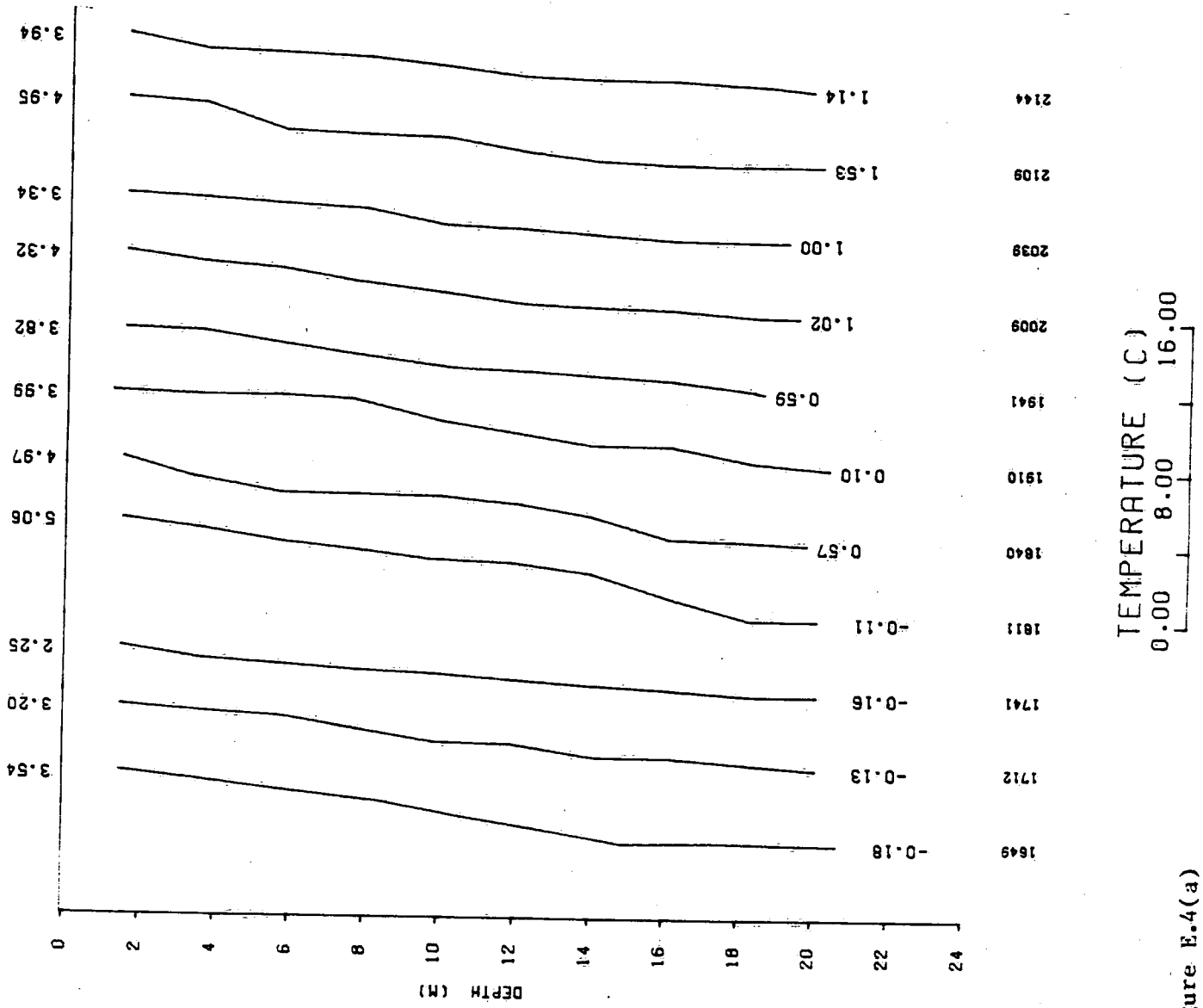


Figure E.4(a)

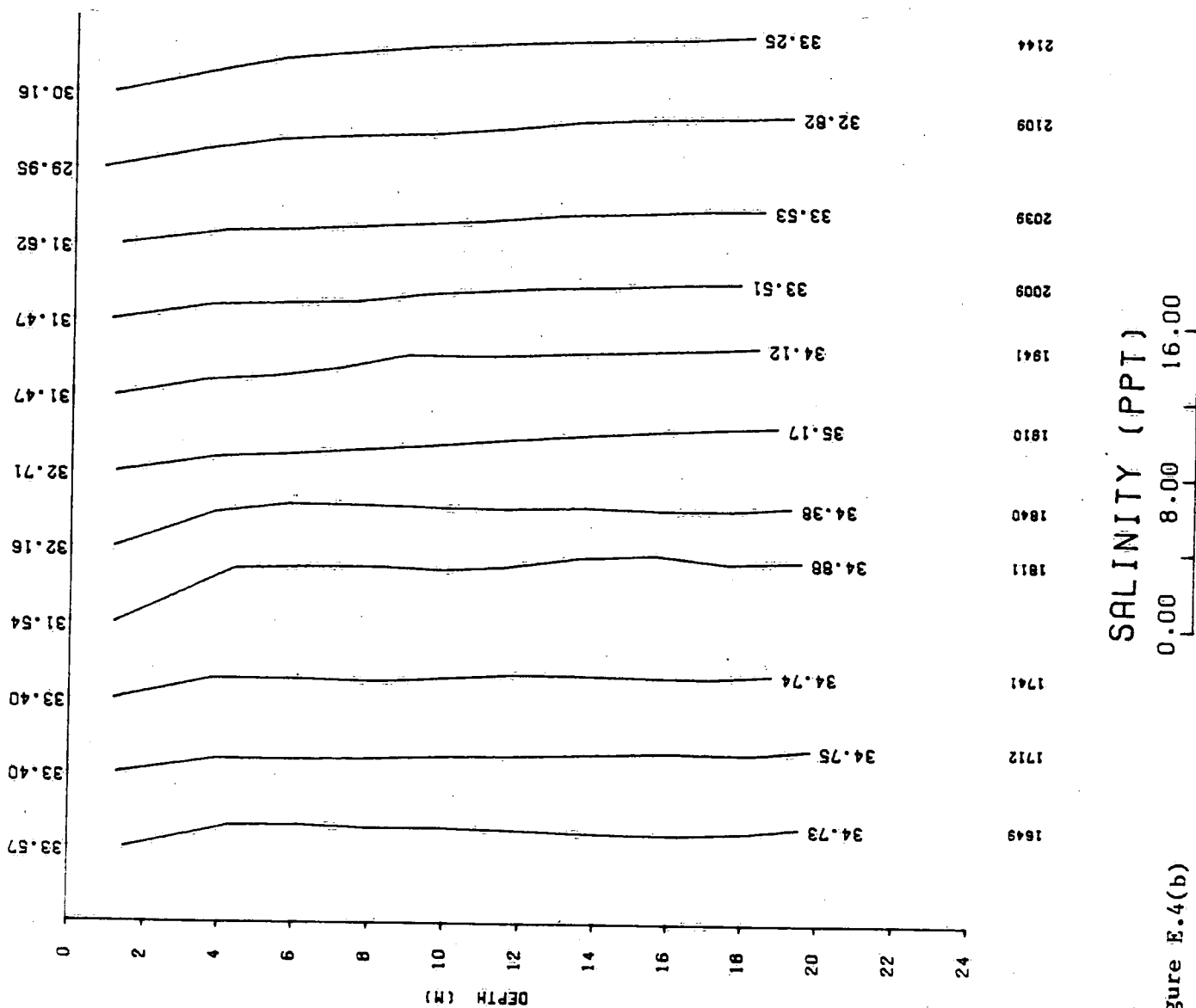
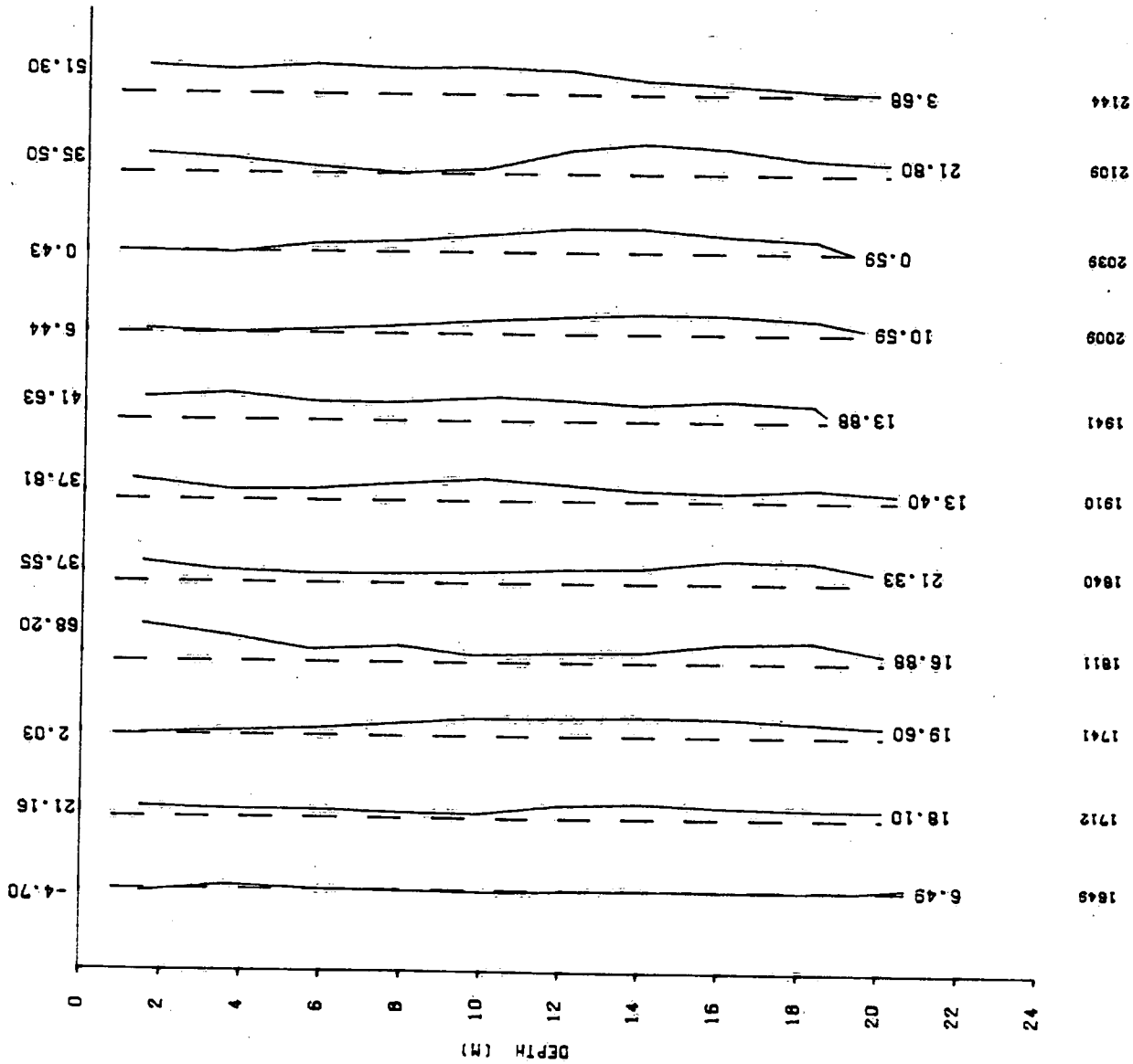


Figure E.4(b)

ST LAWRENCE 6E400 JULY 2 1986



LONGITUDINAL CURRENT (CM/S)  
0.00 160.00 320.00

Figure E.4(c)

ST LAWRENCE 6E400 JULY 2 1986

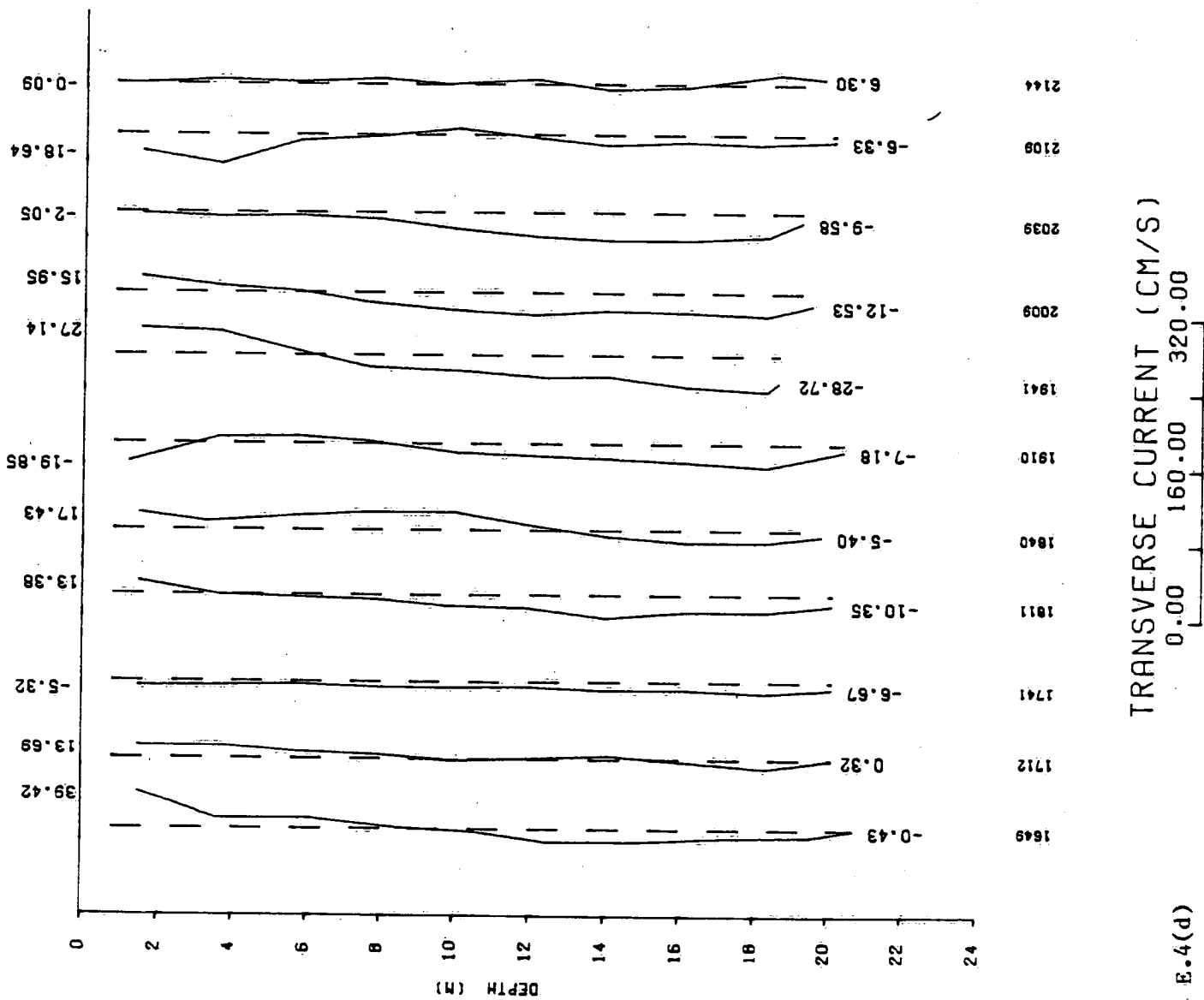


Figure E.4(d)

ST LAWRENCE STN 6E400 JULY 3 1986

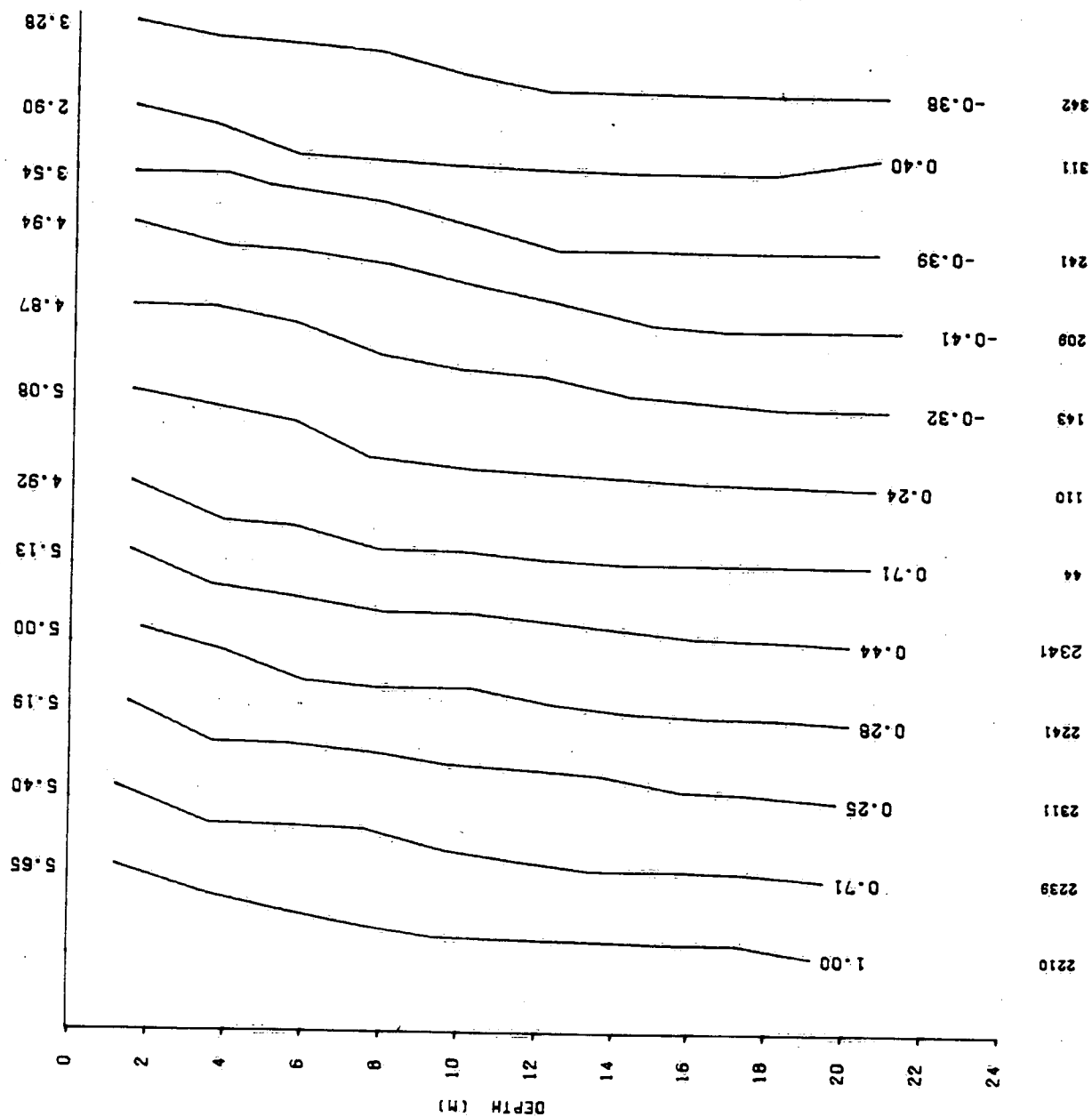


Figure E.5(a)

ST LAWRENCE SIN 0129 19 1975

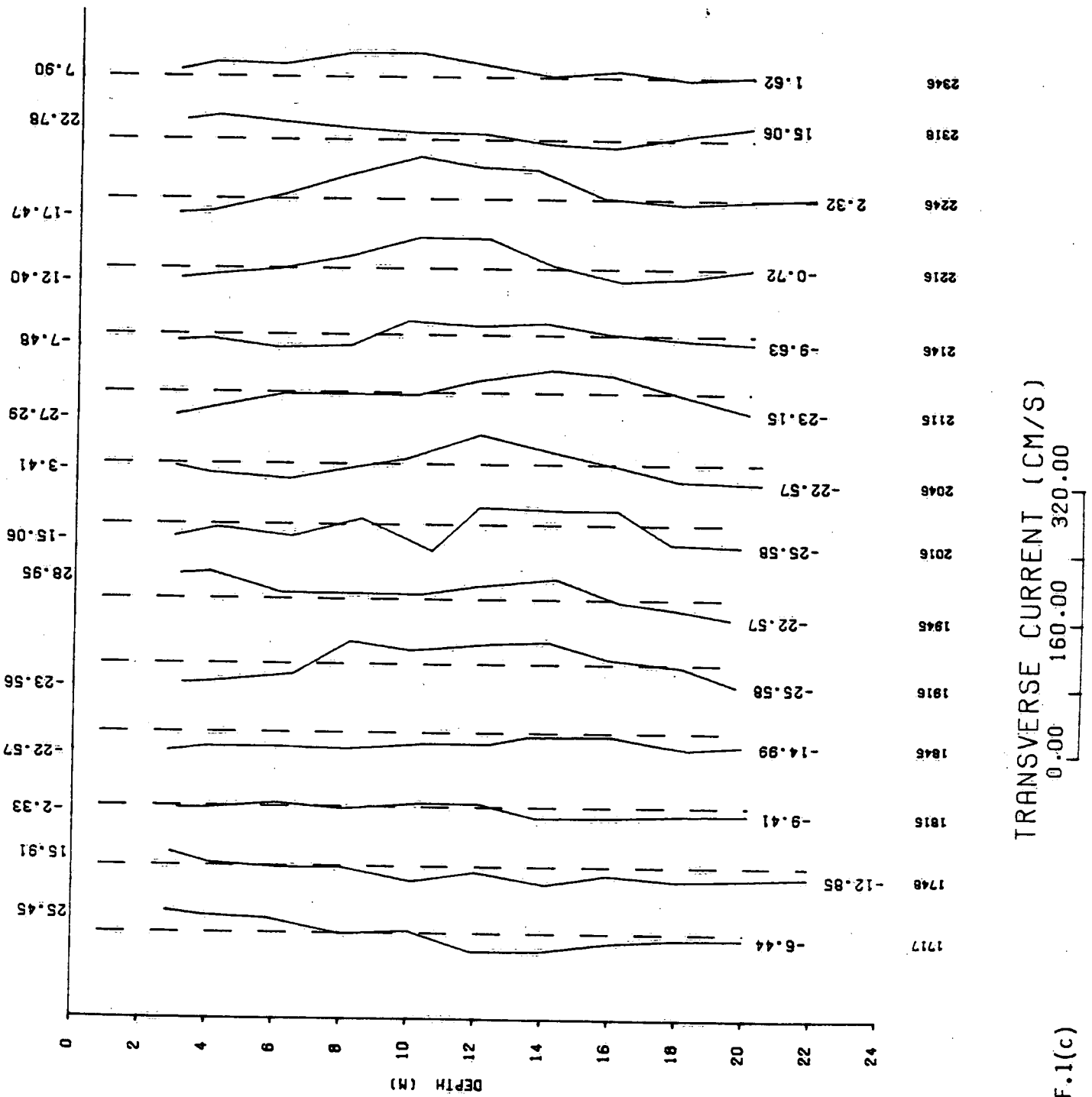
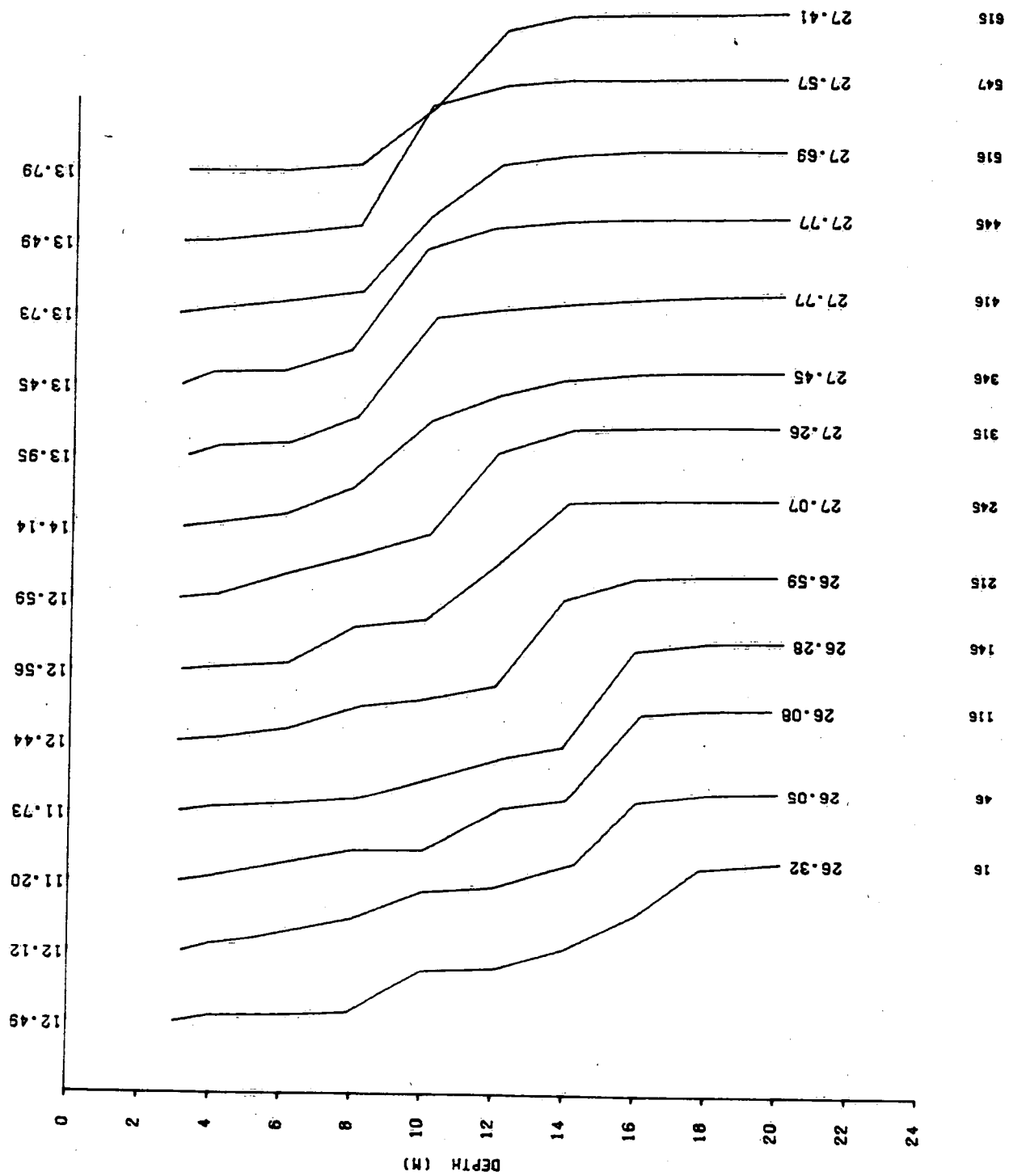


Figure F.1(c)



ST LAWRENCE STN 012A 20 1975



SALINITY (PPT)  
12.00 24.00 36.00

Figure F.2(a)

ST LAWRENCE STN 0 MAY 20 1975

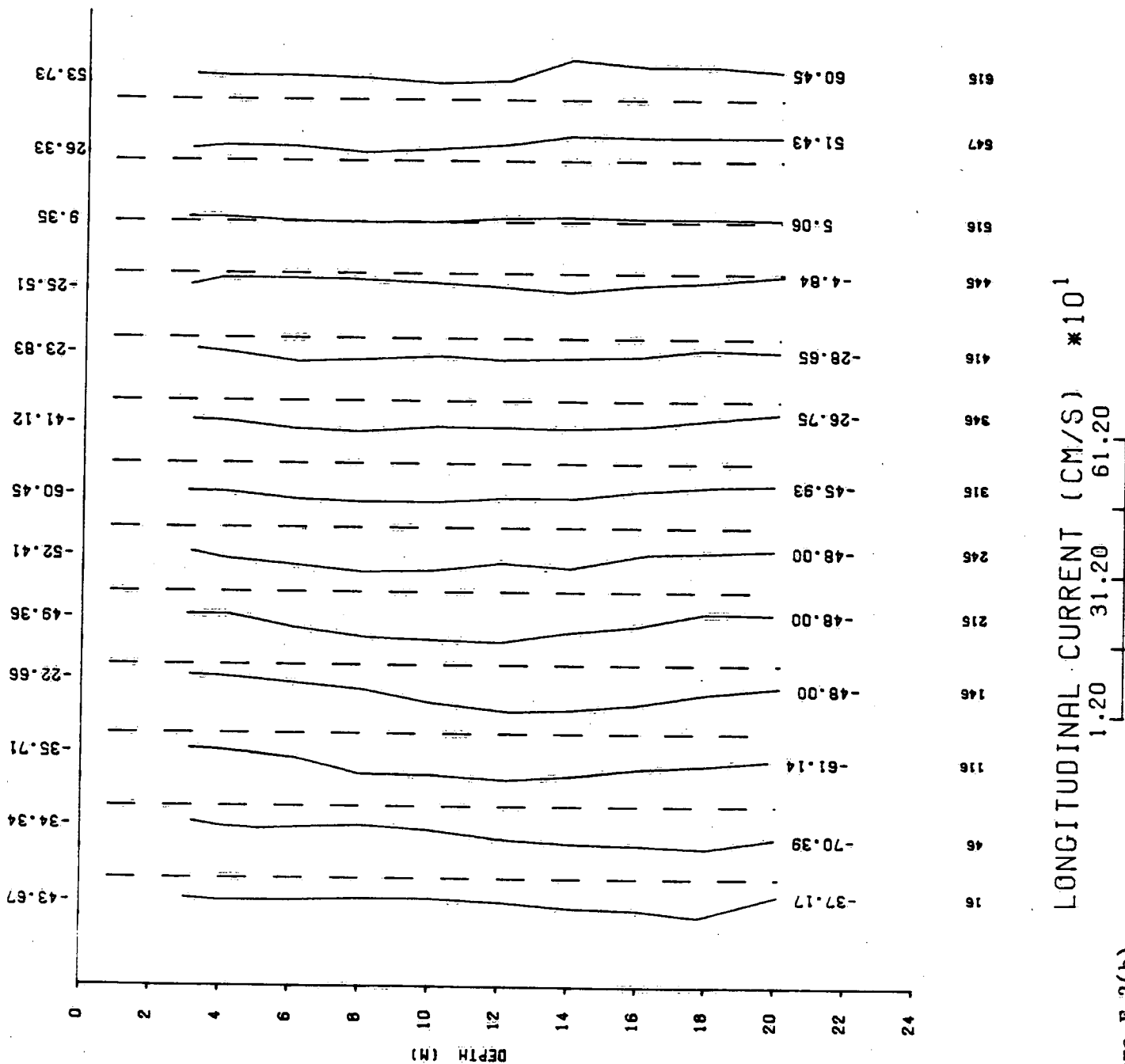
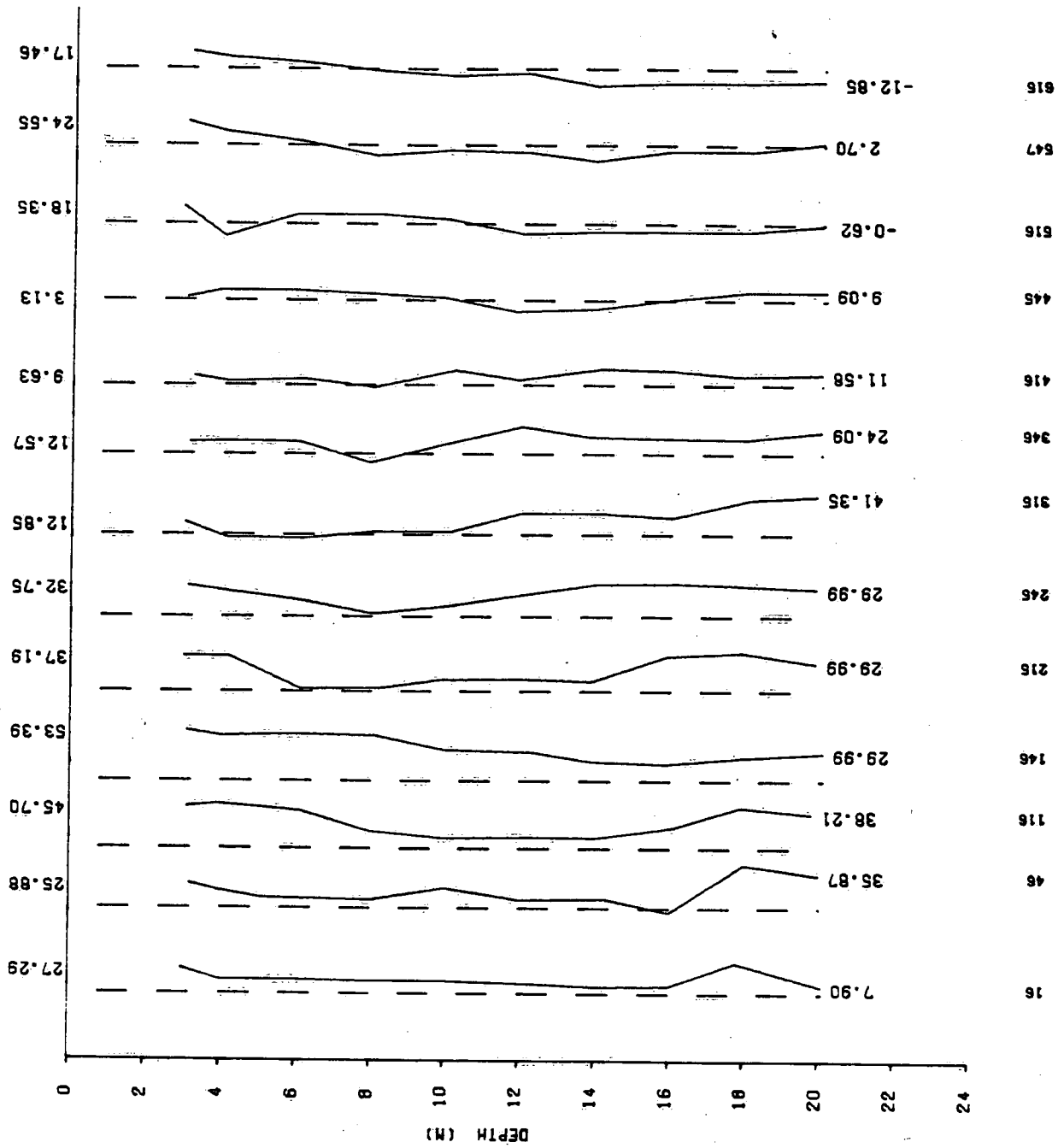


Figure F.2(b)



TRANSVERSE CURRENT (CM/S)  
12.00 172.00 332.00

Figure F.2(c)

ST LAWRENCE STN 6E400 JULY 3 1986

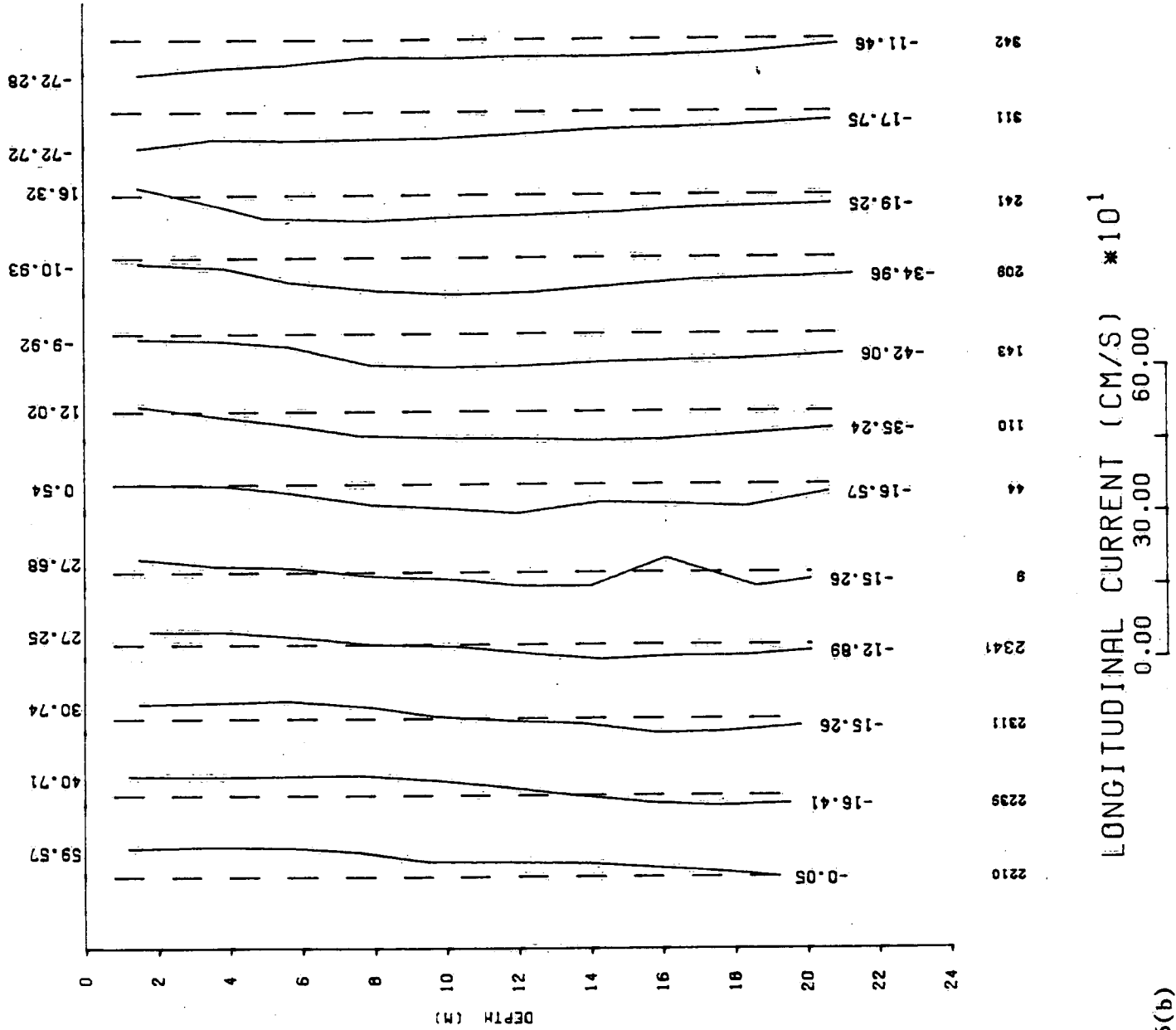


Figure E.5(b)

ST LAWRENCE 6E400 JULY 3 1986

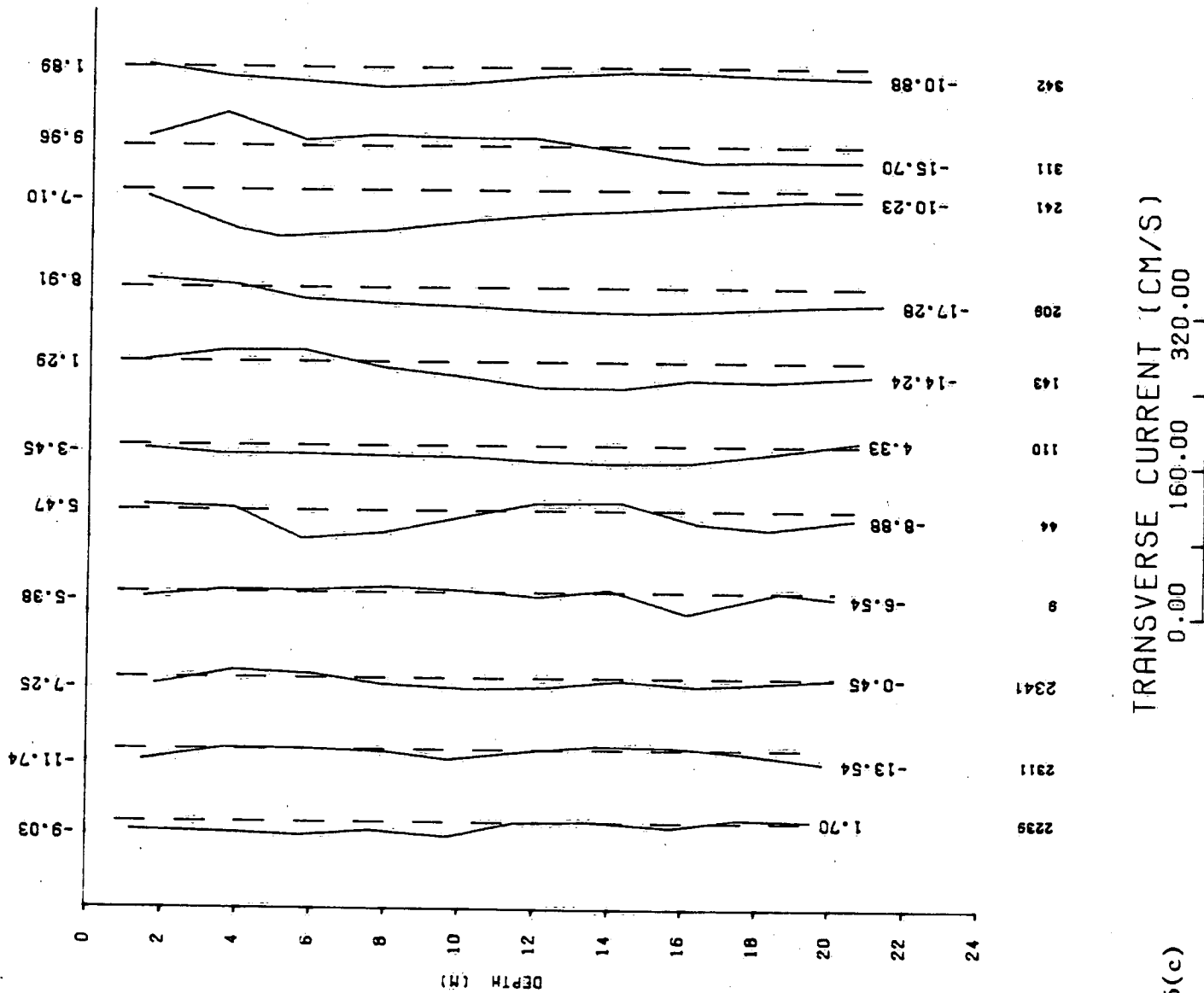


Figure E.5(c)

ST LAWRENCE 6E400 JULY 1986

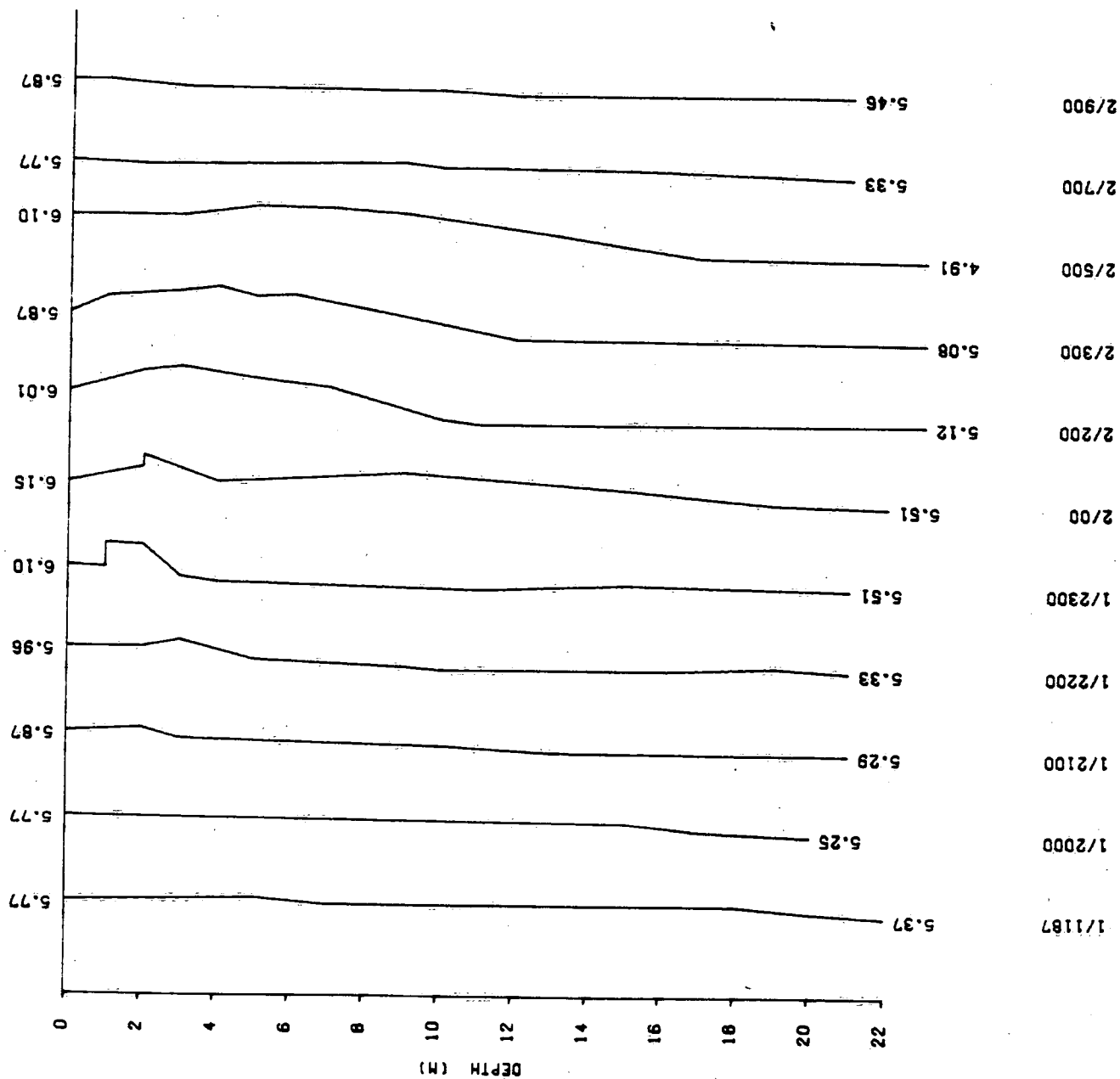


Figure E.6(a)

SUSPENDED SEDIMENT (MG/L)

0.00 4.00 8.00

**APPENDIX F**

Station 012      Latitude N 47°29'30"  
                         Longitude W 70°4'18"  
                         from Muir (1978).

List of Captions

- Figure F.1.      Profiles from 17:17 to 23:46 May 19, 1975 (GMT) of (a) salinity, (b) along-channel flow and (c) cross-channel component of flow (positive to SE).
- Figure F.2.      Profiles from 00:16 to 06:16 May 20, 1975 (GMT) of (a) salinity, (b) along-channel flow and (c) across-channel flow (positive to SE).
- Figure F.3.      Profiles from 09:01 to 14:00 May 29, 1975 (GMT) of (a) salinity, (b) along-channel flow and (c) across-channel flow (positive to SE).
- Figure F.4.      Profiles from 14:30 to 21:00, May 29, 1975 (GMT) of (a) salinity, (b) along-channel flow and (c) across-channel flow (positive to SE).

ST LAWRENCE STN 400 JULY 1986

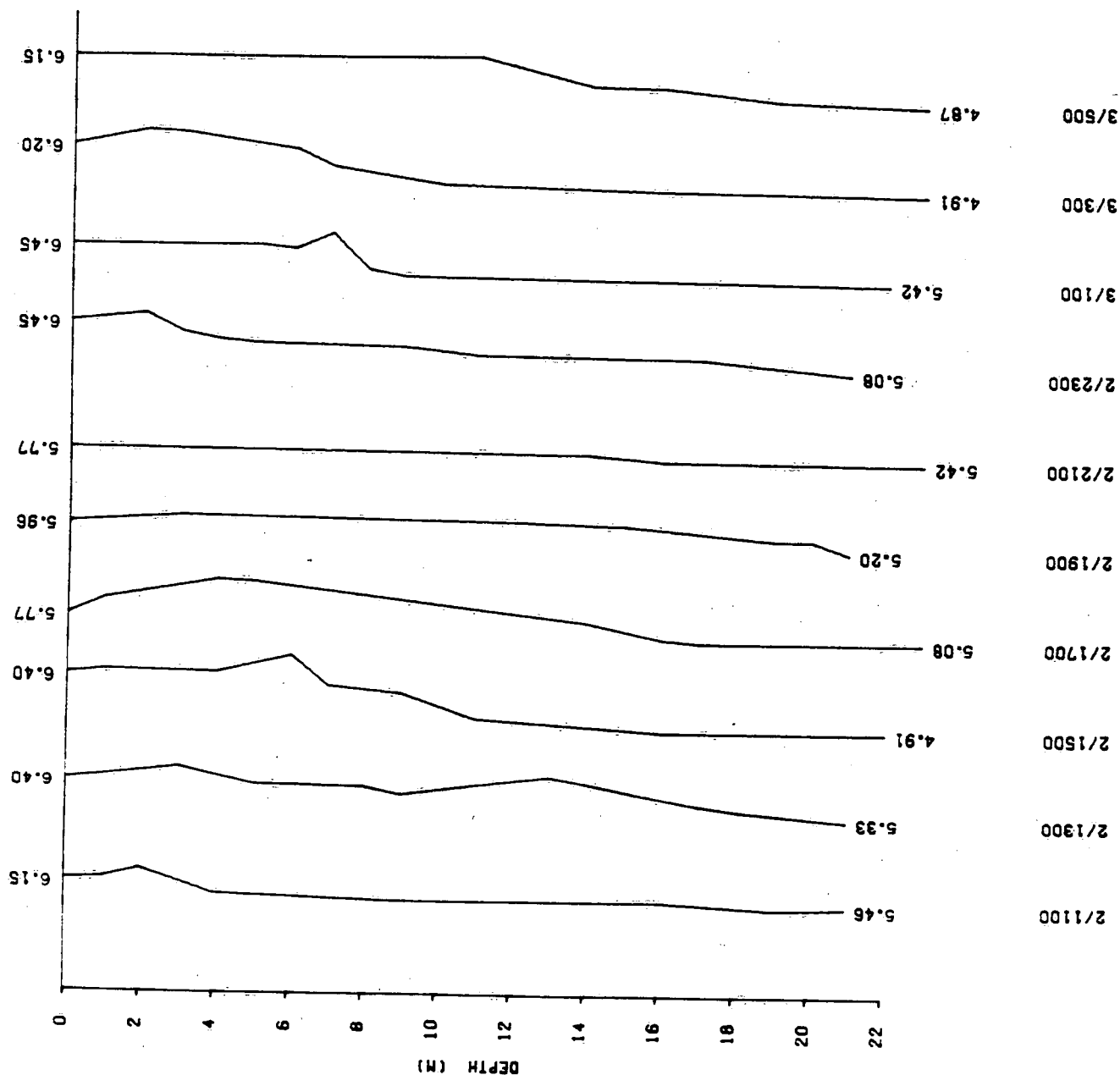


Figure E.6(b) SUSPENDED SEDIMENT (MG/L)



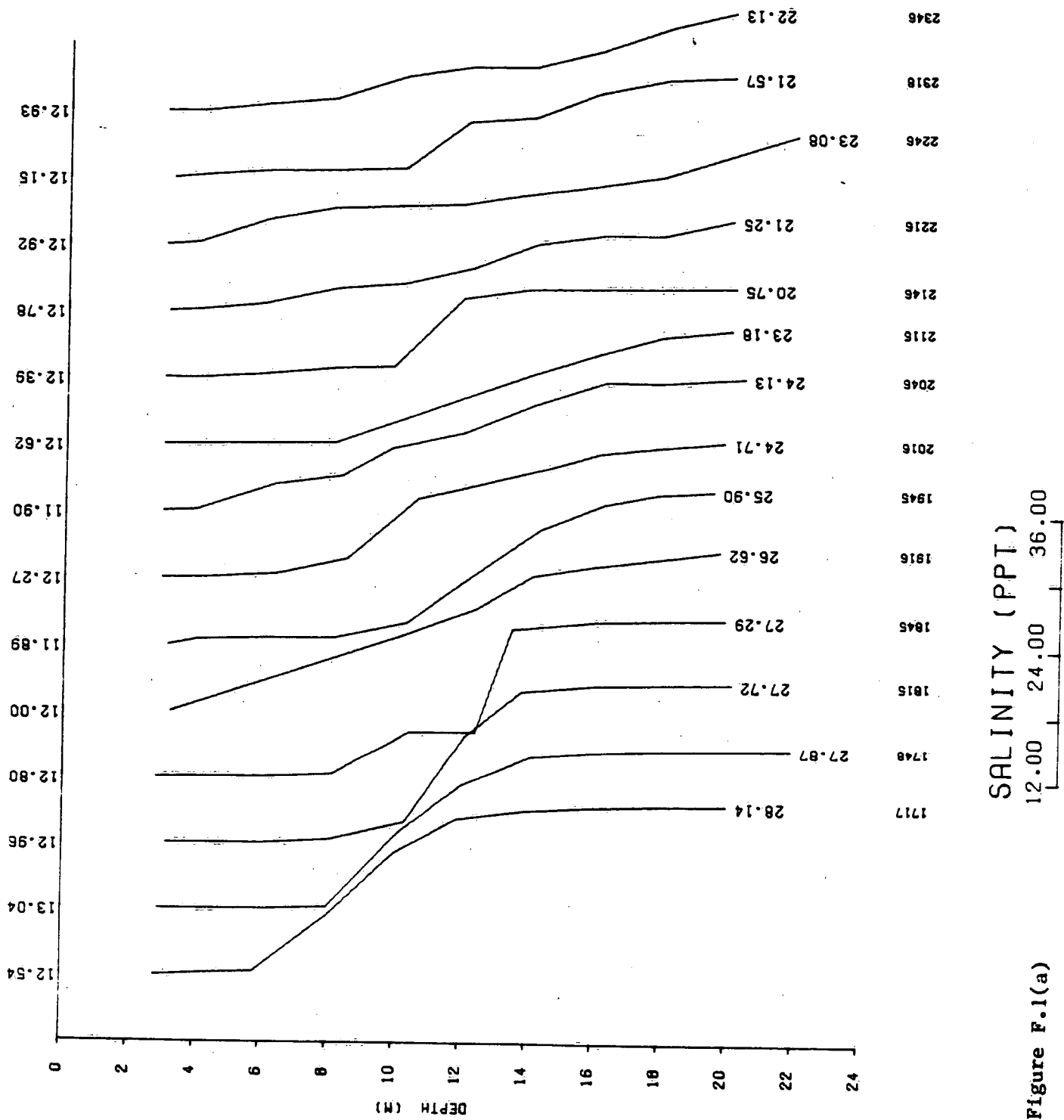


Figure F.1(a)

ST LAWRENCE ST. 28 MAY 19 1975

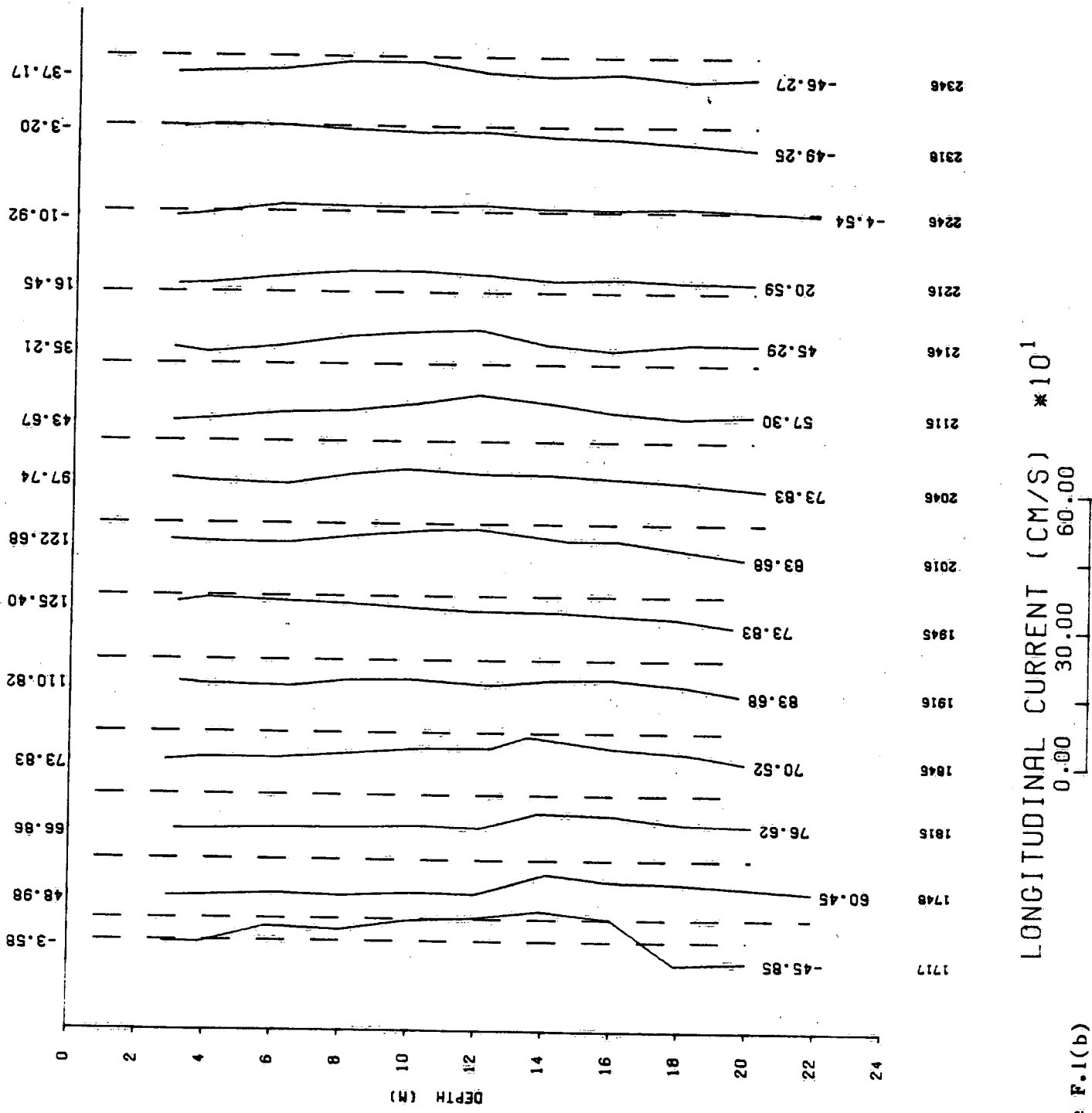


Figure F.1(b)

ST LAWRENCE SIN 0128 MAY 29 1975

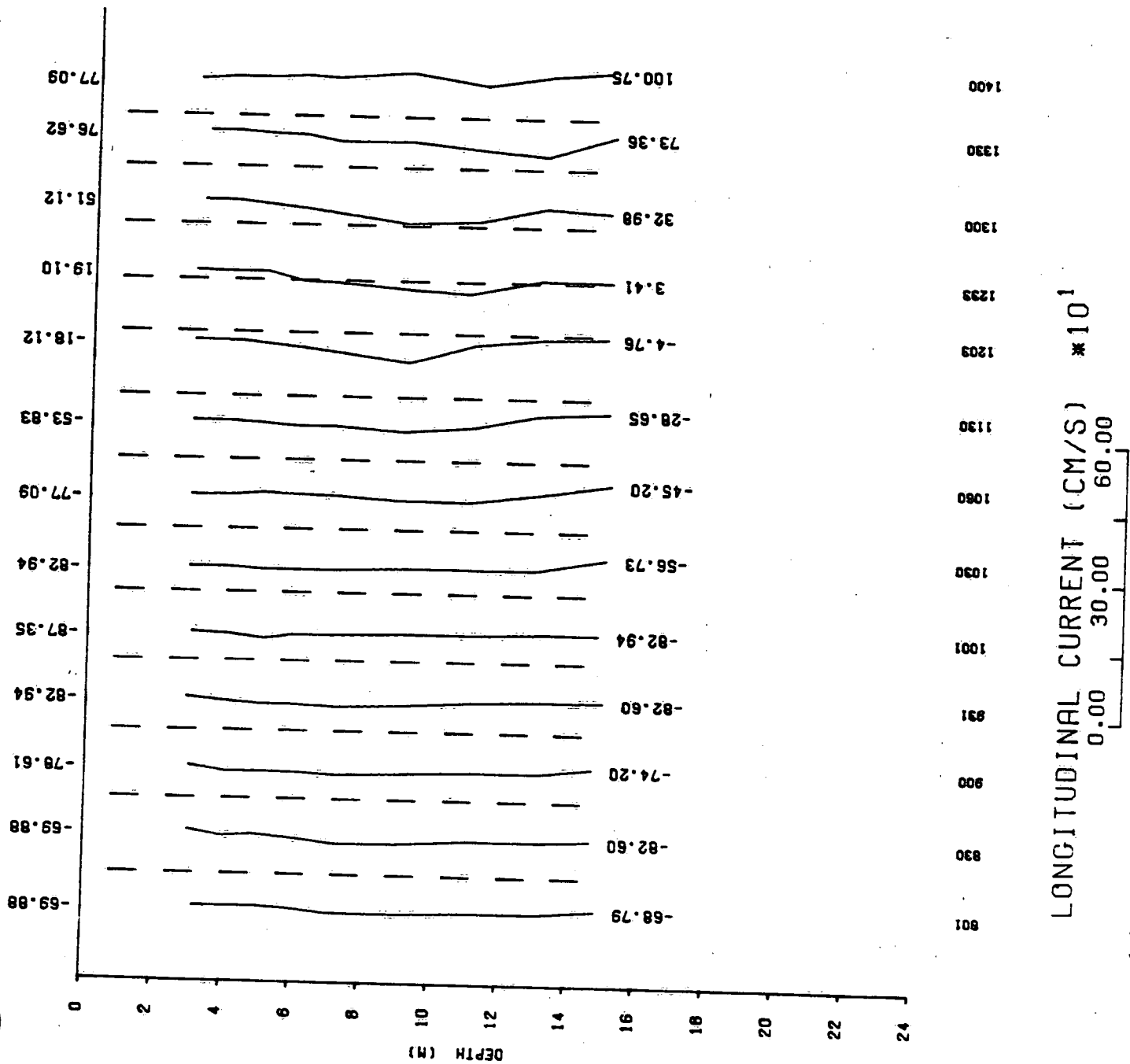


Figure F.3(b)

ST LAWRENCE STN 012B MAY 29 1975

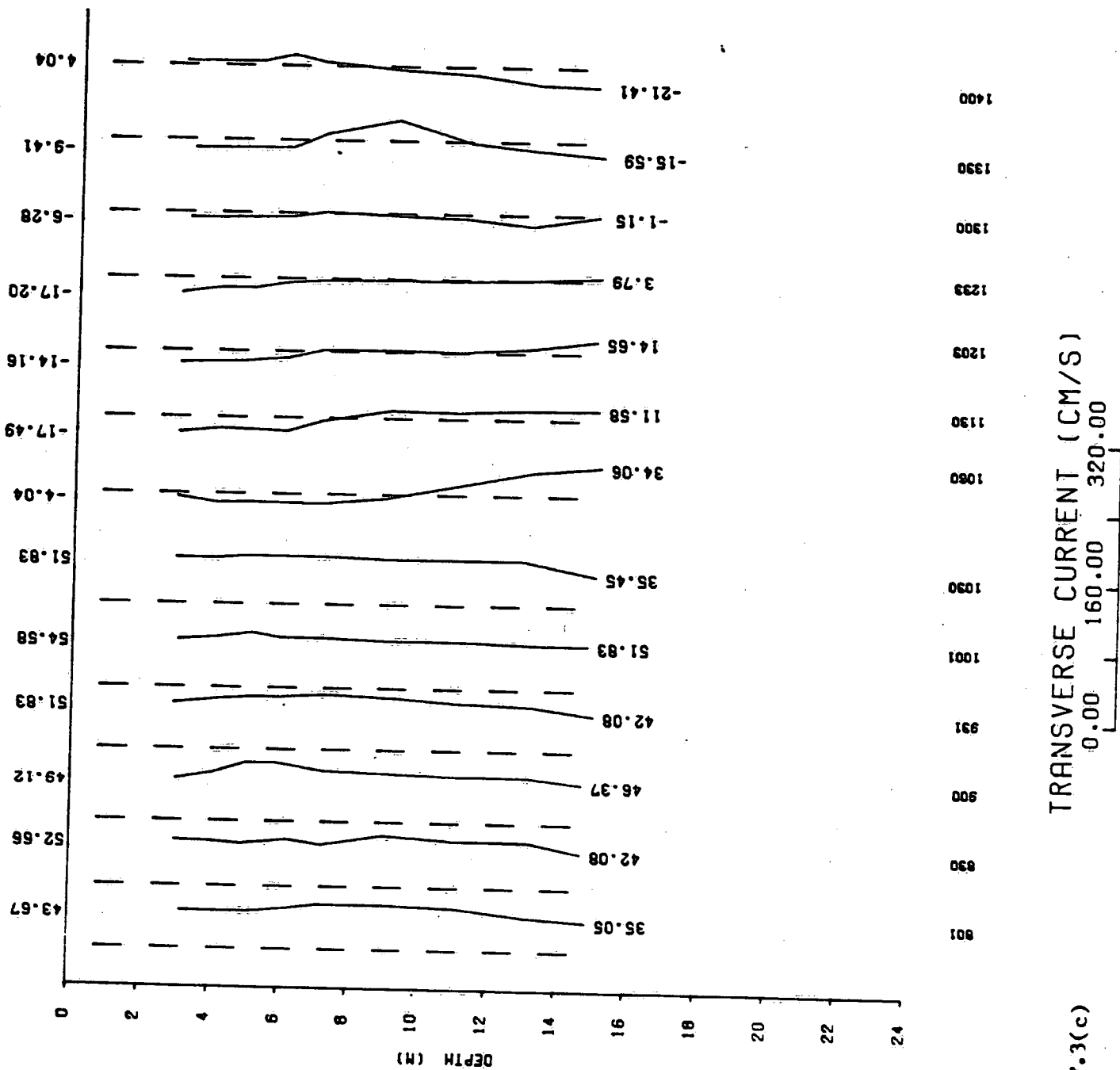


Figure F.3(c)

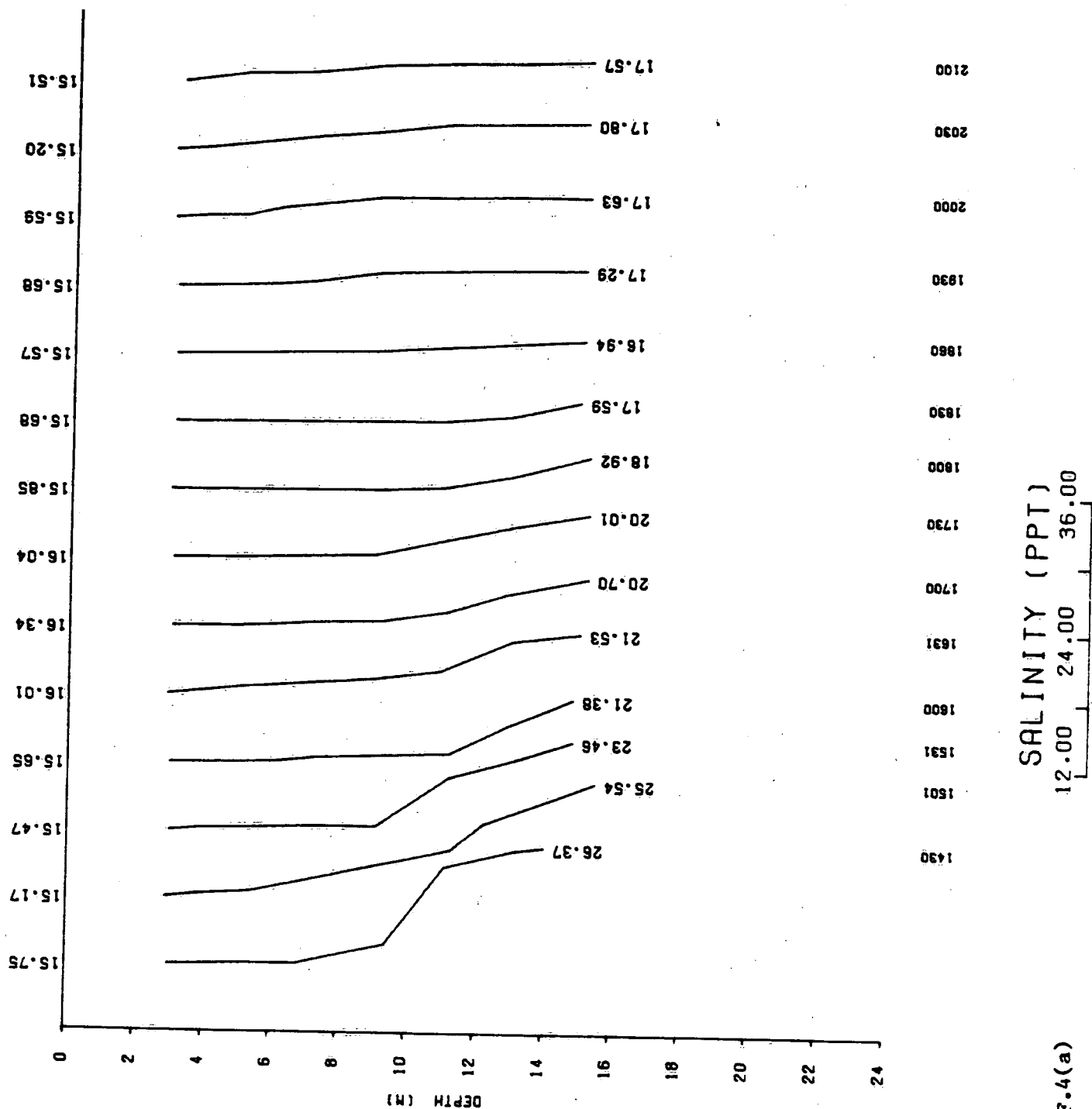


Figure F.4(a)

ST LAWRENCE SIN 01 MAY 29 1975

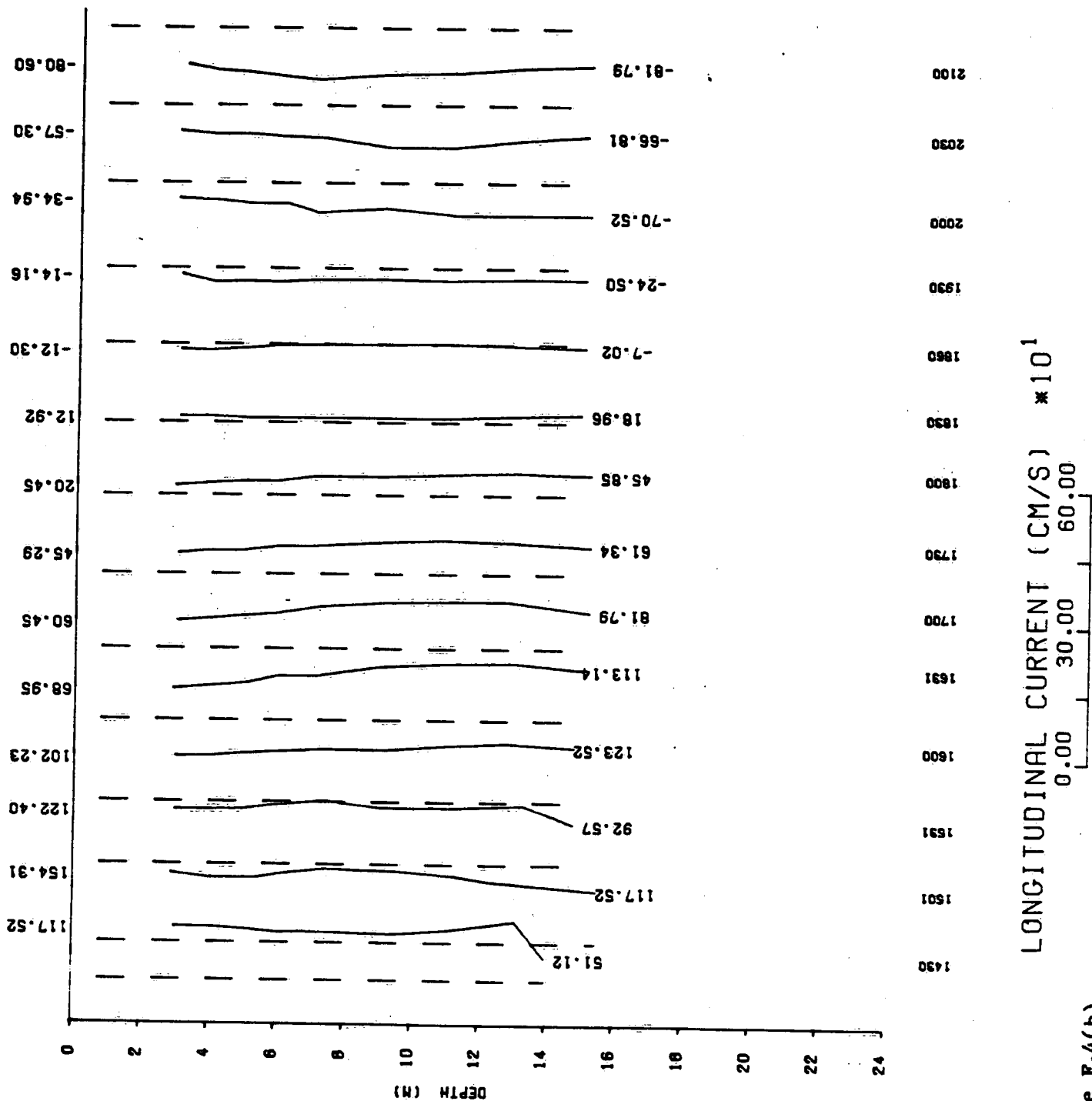


Figure P.4(b)

SI LAWRENCE SIN 0028 MAY 29 1975

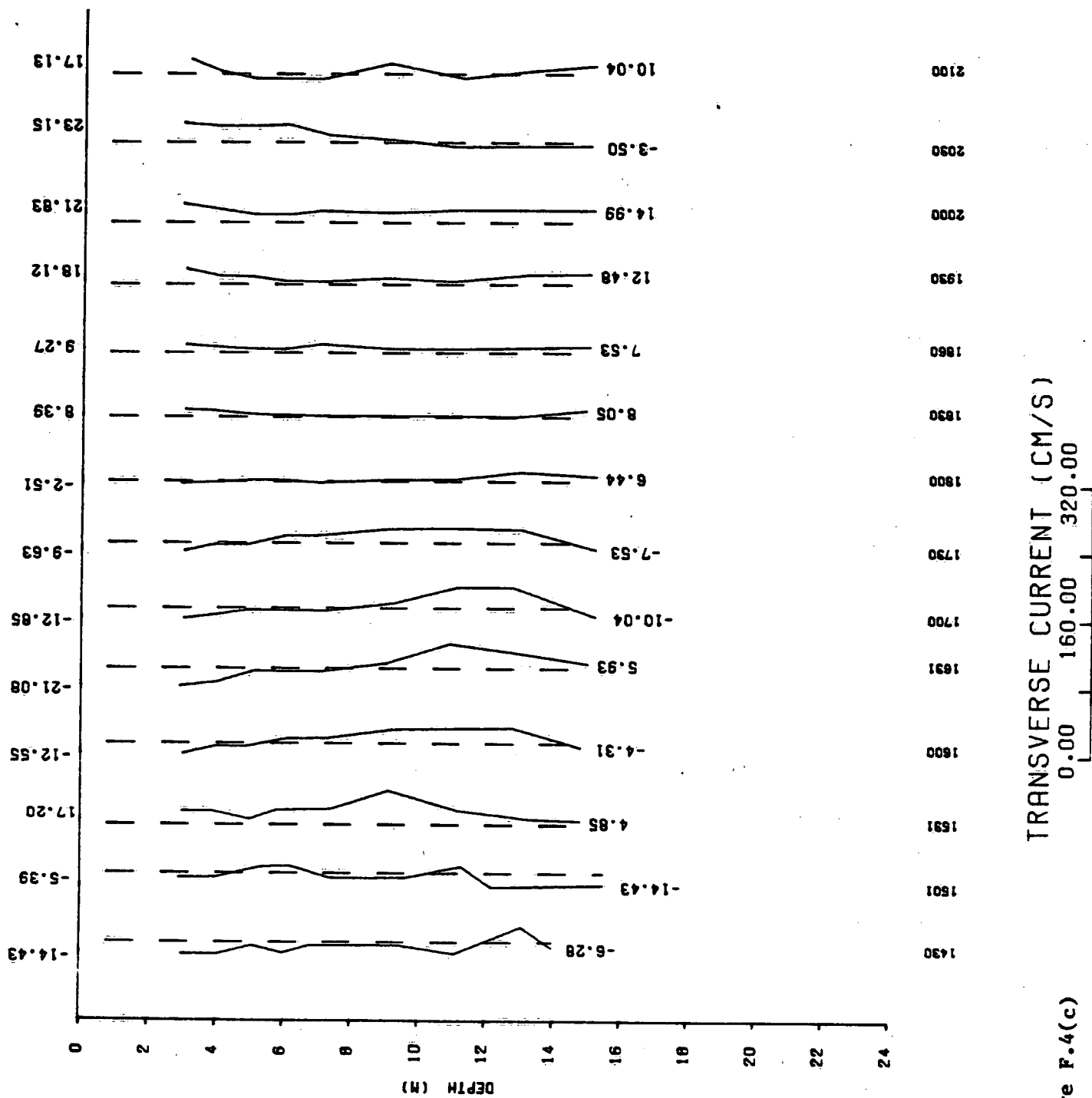


Figure F.4(c)

## APPENDIX G

In order to calculate the mean,  $\mu$ , of a quantity,  $u$ , in the presence of oscillation of dominant frequency,  $w$ , the method of Bloomfield (1976) results in

$$\mu = \frac{1}{N} \left( \sum_{i=1, N} u_i - A \times SS - B \times SC \right)$$

where  $N$  samples of the variable,  $u_i$ , are evenly spaced and

$$SS = \sum_{i=1, N} \sin w t_i;$$

$$SC = \sum_{i=1, N} \cos w t_i;$$

$$A = \frac{1}{\Delta} \left( \sum_{i=1, N} u_i \cos w t_i \times D3 - \sum_{i=1, N} u_i \sin w t_i \times D2 \right)$$

$$B = \frac{1}{\Delta} \left( \sum_{i=1, N} u_i \sin w t_i \times D1 - \sum_{i=1, N} u_i \cos w t_i \times D2 \right)$$

$$\Delta = D1 \times D3 - (D2)^2$$

$$D1 = \frac{N}{2} (1 + DN \cos (N-1) w)$$

$$D2 = \frac{N}{2} DN \sin (N-1) w$$

$$D3 = \frac{N}{2} (1 - DN \cos (N-1) w)$$

$$DN = \frac{\sin NW/2}{N \sin W/2}$$



**APPENDIX G**

The field observations plotted in the Appendices A to F as well as hourly meteorological data are available in edited form on the magnetic tape DM529 stored by the Data Management Section of the National Water Research Institute. The tape is nine track, EBCDIC code, 1600 bits per inch and unlabeled. The machine specifiers are NT, D = 1600, F = S, LB = KV, CV = EB; File RT = F, BT = K, FL = 137, RB = 10. The record length is 80 column.

This tape contains 26 files of data and associated plotting routines.

As well the data of Muir and Budgell have been obtained from the Bedford Institute on magnetic tapes DM108 for the 66 current meter moorings. In addition, all current and salinity profiles taken at anchor station from 1973 to 1977 by Dr. Muir are stored on DM154. A sample copy of the program required to read the data is given on the following page.

```

11.06.04.DISKTP(T12C0)
11.06.05./USER(088,)
11.06.05.ABSC, B.
11.06.05.CHARGE,NLR,046.
11.06.06.$PRCLOG,PROC1,,*.
11.06.07.$SETFS,PROC1/FS=AD.
11.06.07.PROC1.
11.06.10.NOTE,OUTPUT./
11.06.10.SYSNEWS.
11.06.11.IF,CT=IAO.RUN,QMSCAN.
11.06.12.$REVERT.CCL
11.06.13.$REVERT.* USER PROLCGUE NOT FOUND.
11.06.13.DEFINE,TAPE1=TURKEY1.
11.06.14.LABEL,TAPE2,NT,D=1600,F=S,LB=KL,PD=R,VSN=DM154,CV=AS.
11.1C.C2.NTO41, ASSIGNED TO TAPE2, VSN=DM154.
11.1C.C2.FTN,L=OUTPUT.
11.1C.C3. .107 CP SECONDS COMPILATION TIME
11.1C.C3.LGO.
11.1C.C5. CM LWA+1 = 13520B, LOADER USED 31200B
11.13.21. STOP NORMAL TERMINATION
11.13.21. 020200 MAXIMUM EXECUTION FL.
11.13.21. 10.663 CP SECONDS EXECUTION TIME.
11.13.21.UEAD, 0.003KUNS.
11.13.21.UEPF, 0.070KUNS.
11.13.21.UEFT, 11.446KUNS.
11.13.21.UEMS, 14.700KUNS.
11.13.21.UECP, 11.355SECS.
11.13.21.AESR, 18.434UNTS.
11.13.21.$CUT(* /OP=E)
11.13.23. NO FILES PROCESSED.
11.13.23.$DAYFILE(OUTPUT,JT=D)
11.13.33.UCLP, 70, C22, 0.255KLNS.

```

```

1          PROGRAM BUFCPY(INPUT,OUTPUT,TAPE1=0,TAPE2=0)
          C
          C COPY RECORDS FROM M/T T DISC USING BUFFER
          C WHERE SBUFCPY IS THE SUBMIT FILE.
          C NOTE - BUFFERING TO DISC WORKS TOO !
          C
          C DIMENSION IA(100)
          C DO 13 J=1,4
          C   100 BUFFER IN(2,0) (IA(1),IA(100))
          C   10 IF(UNIT(2)) 10,999,999
          C   CONTINUE
          C   LEN=LENGTH(2)
          C   600 WRITE(1,600)(IA(I),I=1,LEN)
          C   15 FORMAT(8A10)
          C   IF(UNIT(1)) 20,999,999
          C   20 CONTINUE
          C   GO TO 100
          C   999 ENDFILE 1
          C   13 CONTINUE
          C   20 STOP " NORMAL TERMINATION"
          C   900 STOP " E.C.F. ON INPUT"
          C   STOP " E.C.F. ON OUTPUT"
          C END

```

ST COMMENCE SIN 0128 HRT 29 1975

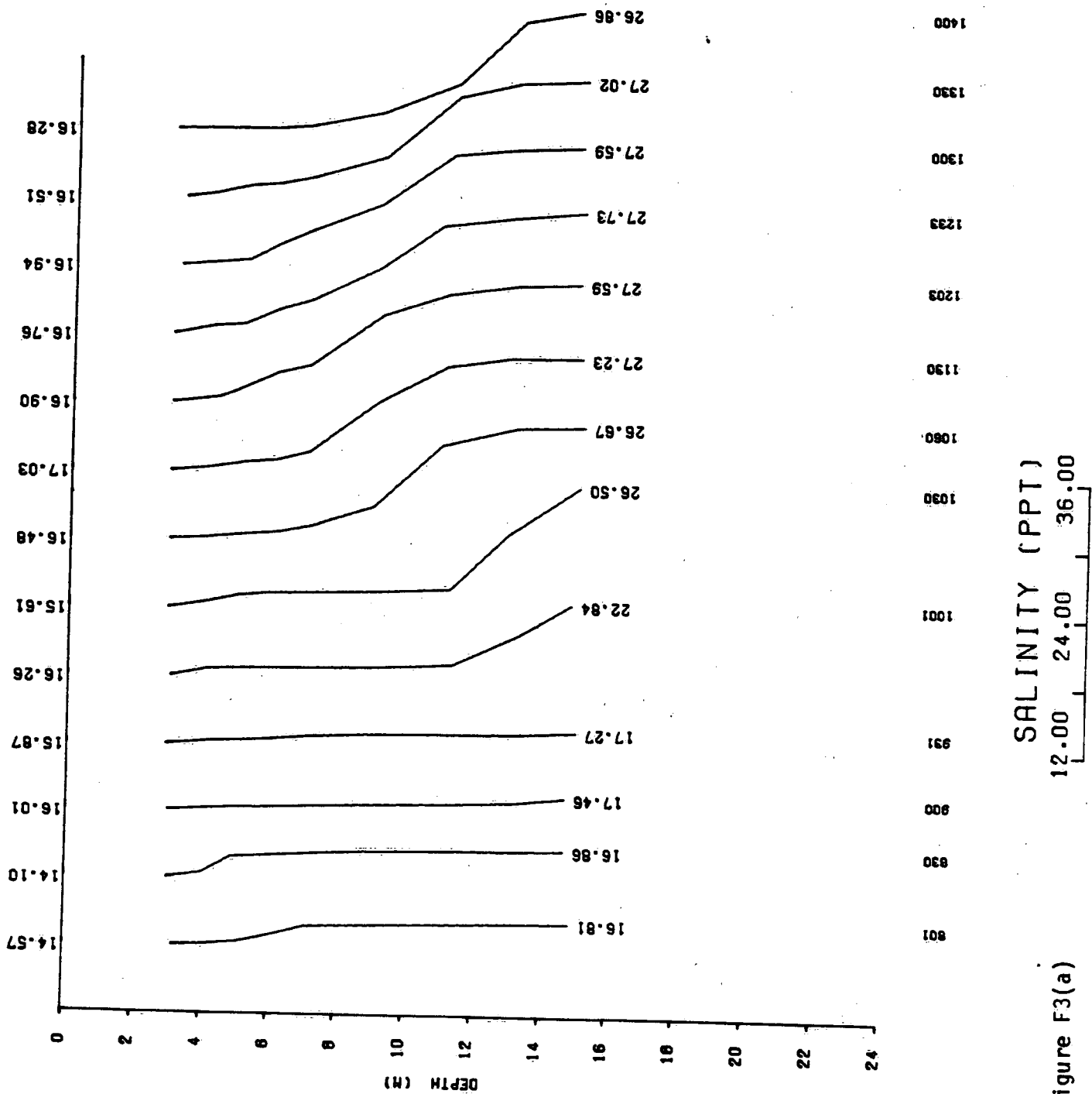


Figure F3(a)